NASA TECHNICAL NOTE

NASA TN D-5482

C. 1

NASA TN D-5482

EXTERNAL PROTON BEAM CHARACTERISTICS OF THE NASA SPACE RADIATION EFFECTS LABORATORY SYNCHROCYCLOTRON

by
Gerald F. Hill, William C. Honaker
Langley Research Center
and
Fred F. Hubble III
Florida State University

NATIONAL AERONAUTICS AND SPACE ADMINISTRATION • WASHINGTON, D. C. • FEBRUARY 1970

1. Report No. NASA TN D-5482	2. Government Accession No.	3. Recipient's Catalog No.
4. Title and Subtitle EXTERNAL PROTON BEAM CHARACTERISTICS OF THE NASA SPACE RADIATION EFFECTS LABORATORY SYNCHROCYCLOTRON		5. Report Date February 1970 6. Performing Organization Code
7. Author(s) Gerald F. Hill, William C. Honaker (Langley Research Center) and Fred F. Hubble III (Florida State University)		8. Performing Organization Report No. L-6482 10. Work Unit No. 124-09-29-02-23
9. Performing Organization Name and Address NASA Langley Research Center Hampton, Va. 23365		11. Contract or Grant No. 13. Type of Report and Period Covered Technical Note
12. Sponsoring Agency Name and Address National Aeronautics and Space Administration Washington, D.C. 20546		14. Sponsoring Agency Code

15. Supplementary Notes

16. Abstract

The proton beam transport system for the 600-MeV synchrocyclotron at the NASA Space Radiation Effects Laboratory (SREL) was set up to deliver a series of proton beams covering an energy range of 40 MeV to 595 MeV. The energies of these beams were measured at 10 points with a range-energy spectrometer and found to be 595, 480, 380, 325, 225, 155, 95, 75, 50, and 40 MeV. An energy spread of ±4.9 MeV was found for the high-energy (595-MeV) primary-beam extraction system and ±1.13 MeV for the low-energy (325-MeV) primary-beam extraction system.

Proton beam intensities of the 595-MeV and 325-MeV beams were measured and found to be 5.3×10^{10} and 3.0×10^{10} protons/sec, respectively.

Relative beam intensity profiles were determined for each beam configuration.

Appropriate magnet settings, copper degrader thicknesses, main magnet current, and other relevant data are presented for each beam configuration.

17. Key Words Suggested by Author(s)	18. Distribution Statement
Space radiation Proton beam intensities Synchrocyclotron	Unclassified – Unlimited

19. Security Classif. (of this report)	20. Security Classif. (of this page)	21. No. of Pages	22. Price*
Unclassified	Unclassified	78	$3.00

*For sale by the Clearinghouse for Federal Scientific and Technical Information Springfield, Virginia 22151

EXTERNAL PROTON BEAM CHARACTERISTICS OF THE NASA SPACE RADIATION EFFECTS LABORATORY SYNCHROCYCLOTRON

By Gerald F. Hill, William C. Honaker
Langley Research Center

and

Fred F. Hubble III
Florida State University

SUMMARY

The proton beam transport system for the 600-MeV synchrocyclotron at the NASA Space Radiation Effects Laboratory (SREL) was set up to deliver a series of proton beams covering an energy range of 40 MeV to 595 MeV. The energies of these beams were measured at 10 points with a range-energy spectrometer and found to be 595, 480, 380, 325, 225, 155, 95, 75, 50, and 40 MeV. Proton beam energy spread was also determined from analysis of the Bragg curves obtained with high-purity copper absorbers. An energy spread of ±4.9 MeV was found for the high-energy (595-MeV) primary-beam extraction system and ±1.13 MeV was found for the low-energy (325-MeV) primary-beam extraction system. As expected, the lower energy beams, obtained by degrading through copper, were found to be less monoenergetic than the two primary extracted beams (595 MeV and 325 MeV).

Proton beam intensities were also determined from both activation analysis of polystyrene samples and a secondary emission chamber. The maximum beam intensity measured at 595 MeV was 5.3×10^{10} protons/sec and that measured at 325 MeV was 3.0×10^{10} protons/sec.

Relative beam intensity profiles were determined for each beam configuration. Profiles of the proton beams at 595, 480, 380, and 325 MeV were obtained with a scanning solid-state ionization chamber (diode). Small disks of polystyrene were used to determine the relative intensity profiles of the proton beams at 225, 155, 95, 75, 50, and 40 MeV.

Appropriate magnet settings, copper degrader thicknesses, main magnet current, and other relevant data are presented so that interested experimenters may either make reproductions of these beam configurations or use the data as a starting point in setting up new beams.

INTRODUCTION

The National Aeronautics and Space Administration has in operation a Space Radiation Effects Laboratory (SREL) designed for simulating the space radiation environment. The SREL is a NASA Langley Research Center facility operated under contract by the College of William and Mary. This facility, shown in plan view in figure 1, consists of a 600-MeV proton synchrocyclotron (figs. 2 and 3), a 3-MeV electron Dynamitron, and a 10-MeV electron linac. By combining beams from these machines, simultaneous irradiation with protons and electrons is possible.

Variation of the proton energies from the synchrocyclotron is achieved by degrading either of the two primary extracted beams which have nominal energies of 600 MeV and 300 MeV. This degrading is accomplished by use of copper absorbers located in the magnet hall of the facility. (See figs. 4 and 5.) By this means, proton beams having energies from 600 MeV to approximately 40 MeV can be obtained at the target position in either one of the two target areas – namely, the combined target area (CTA) or the proton target area (PTA). Either small- or large-area proton beams are available in the two target areas, with the final proton beam configuration being dependent upon the adjustment of 21 or more magnets located in the proton beam transport system (PBTS) indicated in figure 6.

Although the proton beam characterization study was initially undertaken to determine the versatility of the synchrocyclotron and the transport system, it also provided the necessary data for obtaining a variety of beams covering a wide energy spectrum. The beam energies were chosen to cover part of the energy range expected in space. Many other beam configurations may be obtained quite easily by using the data presented herein as a starting point. An extensive proton beam characterization study has been performed, and the purpose of this paper is to summarize the part of the study which involves 10 small-area beams delivered to the combined target area.

DESCRIPTION OF EXPERIMENTAL APPARATUS

Range-Energy Spectrometer

A range-energy spectrometer, consisting of variable-thickness absorbers and two ionization chambers, was designed for use in determining the range of (up to approximately 600 MeV) protons in copper. (See fig. 7.) The proton beam entering the combined target area is directed toward the range-energy spectrometer as shown in figure 8. The beam in passing through the range-energy spectrometer passes in turn through ionization chamber 1, the variable-thickness absorber wheels, the thick stationary absorbers, and finally through ionization chamber 2. The outputs of the two ionization chambers are

fed into two identical channels of electronics, each consisting of a filter, current integrator, voltage divider, and voltage-to-frequency converter; and then the outputs are fed into a scaler. (See figs. 9 and 10.)

The range-energy spectrometer was constructed to provide selection of thicknesses of copper ranging from zero to 12 inches (30.48 cm) in increments of 0.002 inch (0.051 mm). This feature was accomplished by using a combination of thick stationary disks of copper (8 inches (20.3 cm) in diameter) and the selected thicknesses mounted in the three wheels, as shown in figure 7. There are five thin absorbers and one open position on each wheel with each position bearing an assigned number. A closed-circuit TV camera is set up so that an experimenter can monitor the wheel positions. (See fig. 9.) The wheels are driven by remotely controlled motors which are energized through pushbutton controls by the experimenter. A total of 216 possible absorber-thickness combinations are available with the wheels.

Ionization Chambers

Two identical 10-inch-diameter (25.4-cm), large-area, parallel-plate, ionization chambers, which are part of the range-energy spectrometer, were used to monitor proton beam intensities. (See fig. 11.) The ionization chambers contained seven 0.002-inch-thick (0.051-mm) aluminized mylar plates, each spaced 0.25 inch (6.35 mm) apart with insulation rings. The plates were as thin as practical to minimize the proton beam transmission energy loss. Mylar sheets, 0.01 inch (0.254 mm) thick, were used for the ionization-chamber windows.

Gas inlet and outlet valves were placed on opposite sides of each chamber to allow purging. Chamber pressure was maintained at 790 torrs (1 torr = 133.322 N/m^2) throughout each phase of an experiment. Medical-grade helium gas was used in both ionization chambers. Prior to their use at SREL, the ionization chambers were calibrated at the cyclotron at Harvard University at three energies by using an evacuated Faraday cup as a standard.

Secondary Emission Chamber

A large-area, parallel-plate, secondary emission chamber was designed and used to monitor proton beam intensity of several (225-, 155-, 95-, 75-, 50-, and 40-MeV) beams at SREL. (See fig. 12.) The secondary emission chamber contained 20 aluminum plates, 0.0005 inch (0.013 mm) thick by 12 inches (30.48 cm) in diameter and spaced 0.25 inch (6.35 mm) apart. These plates were also made as thin as practical to minimize proton beam energy loss in the chamber. Insulation rings were used between the plate assembly and the chamber wall. The 20 plates were alternately connected to a positive 1000-volt source and to the collector terminal. Chamber pressure was

maintained between 10^{-5} and 10^{-6} torr during each run, since the chamber sensitivity was found to remain constant with pressure below 10^{-4} torr. The secondary emission chamber was calibrated by using the activation technique of the $C^{12}(p,pn)C^{11}$ reaction in polystyrene as shown in figure 13.

Solid-State Ionization-Chamber Scanner System

An X-Y scanning system was designed to scan over an area of approximately 144 inches^2 (930 cm^2) using a solid-state ionization chamber (fig. 14) as a sensor for relative spatial intensity studies of the proton beams. The scanning system was remotely controlled and sensor position was indicated within ±0.01 inch (0.25 mm).

The commercially available silicon diodes (ref. 1) used in these investigations were chosen because of their small size, high reverse-leakage resistance, and minimum encapsulation. The p-n junction is contained within a silicon wafer approximately 0.02 by 0.02 by 0.01 inch (0.5 by 0.5 by 0.2 mm). Ribbons of gold-flashed copper 0.004 inch (0.1 mm) thick by 0.02 inch (0.5 mm) wide, are welded to the large faces of the wafer for leads. The silicon wafer and a small portion of the leads are encapsulated in epoxy resin, with the detector having an overall diameter of 0.059 inch (1.5 mm) or less. Since these diodes are sensitive to light, they were coated with a black lacquer to shield from light.

As diodes of this type are exposed to radiation, the sensitivity, defined as the number of coulombs collected per rad of delivered dose, decreases until a plateau is reached at approximately 10^6 rads. Any additional exposure does not appreciably change the sensitivity. Therefore, the diodes were pre-exposed to approximately 10^6 rads of gamma rays. A typical sensitivity for the diodes used is 10^{-9} coulomb/rad. The total amount of charge collected is proportional to the integrated flux. (See ref. 1.) These diodes are essentially independent of dose rate up to 2500 rads/min. (See ref. 2.)

DESCRIPTION OF EXPERIMENTAL PROCEDURES

Setup of Proton Beam Transport System

An initial survey of anticipated users of the synchrocyclotron indicated a need for proton beams covering an energy range from 30 MeV to 600 MeV. On the basis of these requests, it was decided that 10 different beam energies covering the energy range of interest would be set up and analyzed. The energies chosen were 595, 480, 380, 325, 225, 155, 95, 75, 50, and 40 MeV. Proton beams with less than 40 MeV can be obtained but were found to have intensities which were too low for most of the proposed experiments.

Since the combined target area is the most versatile target area, it was decided to define the 10 different energy beams in the CTA. The two primary extracted beams

were initially assumed to have energies of 600 MeV and 300 MeV. Other proton beam energies were then obtained by inserting the proper thickness of copper in the beam degrader. (See BD1 in fig. 6.)

The first step in setting up a desired beam configuration was to adjust the first two quadrupole magnets (Q1 and Q2) and first bending magnet (M1) so that the current output of beam monitor 1 (BM1) was maximum. It was often found that maximization of the current output of a given beam monitor did not insure the desired beam shape; therefore, it was necessary to readjust magnet settings. This process was continued until the desired beam shape was obtained at the target position in the combined target area which is 10 feet (3.05 m) from the exit window of beam monitor 4 (BM4). The intensity at the target position was then maximized by fine tuning of the magnets.

Each magnet has a regulated power supply delivering the necessary current to produce the desired field strength. In some cases, two magnets are energized by a common power supply. The current to each power supply is measured by a precision potentiometer connected across a series resistor. Tables 1 to 10 list 10 different proton beams available and the conditions under which those beams may be obtained. Each beam setup has been repeated several times to assure the repeatability of the system. Graphs of magnet settings for each power supply as a function of proton energy are plotted in figure 15 so that an experimenter can determine the necessary magnet settings for any beam energy other than those measured.

Range-Energy Measurements

Prior to making a measurement, the range-energy spectrometer was properly alined with the exit window of the proton beam transport system, and the beam was established as indicated in tables 1 to 10.

Polaroid photographs of the beam spot size and position were taken at several locations to assure that the beam was traversing the entire system on its proper path. These photographs indicated very little scattering of the beam through the ionization chambers and air.

A precision current source was used to calibrate and balance the two identical channels of electronics before each range-energy measurement, as shown in the block diagram of figure 10.

After calibration of the electronics, the proton beam was passed through the open ports of the range-energy spectrometer. The ratio of counts accumulated on the scaler for ionization chamber 2 and the preset counts on the scaler for ionization chamber 1 constituted the data point corresponding to zero absorber thickness. A ratio of approximate unity was obtained, since the electronics had been matched and there was very little

energy loss in ionization chamber 1 and the intervening air. Current ratios (designated IC2/IC1 herein) were then taken as a function of copper absorber thickness, and the results of the calculations for the 325-MeV beam are shown in figure 16. This curve was obtained with ionization chamber 2 at a position corresponding to a solid angle of $\Omega_1 = 2.59$ steradians. (See fig. 17.) All the range-energy measurements were made with ionization chamber 2 at three positions in order to correct for Coulomb scattering effects on the shape of the Bragg curve.

Throughout the course of the experiments, data points were repeated to assure that the electronics were stable with time. Each data point repeated was found to agree very well with the first point taken. Each data point represents the average of three independent runs at the same absorber thickness.

Beam Intensity Measurements

The proton beam intensities of the smaller area beams at energies of 595, 480, 380, and 325 MeV were measured by using the $C^{12}(p,pn)C^{11}$ reaction. A secondary emission chamber was used for the energies of 225, 155, 95, 75, 50, and 40 MeV. The intensity of the small-area beams was determined by using a matrix of polystyrene samples close to the secondary emission chamber as shown in figure 13; a typical result is shown in figure 18. This method also served as a calibration of the secondary emission chamber. When the size of the beams became too large to use a matrix of a practical size, the secondary emission chamber was moved to the position shown in figure 19, and was used to determine the intensity of the beam. A horizontal and vertical array of polystyrene samples were activated to determine the beam profile.

Foil activation is considered one of the best techniques for determining high-energy proton beam intensities. The $C^{12}(p,pn)C^{11}$ reaction is widely used, since the cross section is known within ±5 percent over an energy range of 50 MeV to the GeV region. (See ref. 3.) The induced C^{11} atoms decay to B^{11} by positron emission with a half-life of 20.5 minutes and a maximum energy of 0.968 MeV.

To determine the absolute C^{11} activity induced in a polystyrene target, a gamma counting system was chosen for this experiment. The emitted positrons were stopped in a 0.04-inch-thick (1-mm) aluminum capsule surrounding the polystyrene target, and the gamma rays produced by positron annihilation were counted with a NaI(Tl) crystal and stored in the memory of a 400-channel pulse-height analyzer.

The polystyrene targets were 0.5 by 0.5 by 0.125 inch (1.27 by 1.27 by 0.318 cm) in size and were spaced next to each other in a matrix form as shown schematically in figure 18. This figure shows the percentage of the beam (595-MeV) which hit each polystyrene target. A Polaroid photograph was taken to assure that the proton beam was well contained within the matrix of targets as is evident from figure 18. The matrix of targets

was placed after the secondary emission chamber. As the targets were being irradiated for a half-life (20.5 minutes), the current from the secondary emission chamber was integrated for calibration purposes. Each target of the matrix was then counted for 1 minute live time on the 400-channel pulse-height analyzer. Clock time was kept for all sequences so that the necessary decay corrections could be made. Spectra from each sample were made and later analyzed on a computer to determine the number of incident protons.

Several precision gamma standard sources with accuracies within ±2 percent were used for calibration of the 3- by 3-inch (7.6- by 7.6-cm) NaI(Tl) crystal detector system. Nominal source-to-detector distances of 0, 2, and 4 inches (0, 5, and 10 cm) were chosen depending on the source strength of each irradiated polystyrene target. Crystal efficiency was determined for each target size and each source-to-detector distance. Since the targets were square and therefore not point sources, corrections were made in the calibrated efficiencies and were found to be 1.5 percent at 4 inches (10 cm). From the above calculations, the number of gamma rays being emitted from a source at a distance, 0, 2, or 4 inches (0, 5, or 10 cm), could be determined.

The secondary emission chamber was used to determine beam stability and was calibrated over an energy range of 595 MeV to 75 MeV. The $C^{12}(p,pn)C^{11}$ reaction was used to determine the total beam intensity of the 225-, 155-, 95-, 75-, 50-, and 40-MeV beams.

Relative Intensity Profile Measurements

Two techniques were used in determining the relative intensity of profiles. The solid-state ionization chamber (diode) was used successfully when beam intensities were sufficiently high; however, the $C^{12}(p,pn)C^{11}$ reaction technique was required when low beam intensities were being measured. All beams with energies of 595, 480, 380, and 325 MeV were scanned with a diode (fig. 14), and profiles of beams with energies of 225, 155, 95, 75, 50, and 40 MeV were determined from the $C^{12}(p,pn)C^{11}$ reaction.

The diode scanning system and sensor were mounted directly after the ionization chamber located at the target position in the combined target area. The scanning system was calibrated for position before each run. Data points were taken, and the output of the diode was compared with the preset counts for the ionization chamber. Therefore, any change in total beam intensity was indicated by a change in this ratio. A sufficient number of points were taken in both the horizontal and vertical directions to draw smooth curves representing the beam profile. Data points were repeated to assure stability of electronics, magnets, and so forth.

DISCUSSION OF EXPERIMENTAL RESULTS

Range-Energy Measurements

Several investigators have discussed the range-energy method of obtaining proton beam energies. (See refs. 4 to 6.) Mather and Segrè have investigated range-energy relations for high-energy protons in several materials, including copper. (See ref. 4.) Bakker and Segrè have also used the range-energy method for determining stopping power and energy loss for ion-pair production for 340-MeV protons in several materials, including copper. (See ref. 5.) Mather and Segrè have found that the mean range of a proton in a material corresponds to the thickness of material which causes the Bragg peak to decrease to 82 percent of its maximum height. Accordingly, complete range-energy curves, normalized to unity at the Bragg peak, were made for each of the 10 proton beams and are shown in figures 20 to 29. The thickness of copper corresponding to the 0.82 point was determined for each Bragg curve by computer fitting a least-square line through the data points which were in the vicinity of the 0.82 point. Correlation coefficients were found to be very close to unity if a total of six data points were fitted. By using these data and range-energy tables (ref. 7), the computer was used to obtain the proton beam energy. The computer then extrapolated these data to arrive at the proton range. This range was compared with range-energy tables (ref. 7) to determine the beam energy.

Coulomb scattering of the proton beam gives rise to a modified Bragg peak depending upon the position of ionization chamber 2. It was, therefore, decided to correct for this scattering by making a Bragg curve with ionization chamber 2 at several positions for each beam energy. (See fig. 17.) Figure 30 shows these modified Bragg peaks obtained with ionization chamber 2 located at four different positions. It can be seen from figure 30 that as the solid angle is decreased the peak height not only decreases but also indicates decreased transmissions and moves toward a smaller thickness of copper. This tendency is more apparent when the normalized data are plotted as in figure 31. By using this technique, the mean range of protons in copper can be determined by extrapolating the data to a solid angle of 2π steradians. This angle corresponds to having the first plate of ionization chamber 2 flush with the exit side of the copper absorbers. It is then possible for ionization chamber 2 to record all the protons leaving the copper absorbers in the forward direction. This condition gives rise to the true range curve, and, therefore, the energy can be determined. This method is indeed how the data were analyzed, and some data are illustrated in figures 32 and 33. Figure 32 illustrates the Coulomb scattering corrections used for the 595-MeV proton beam. An energy of 593.0 MeV was determined by extrapolating the data to an angle of 2π steradians. The 593.0-MeV energy indicated is referred to as a nominal 595-MeV beam throughout the report. Figure 33 shows a similar graph for the 325-MeV beam. It is seen from

this graph that the energy of the low-energy extraction system is 325 MeV, which is also referred to as a nominal 325-MeV beam.

The range-energy data obtained are estimated to be accurate within ±2 percent. Figure 34 shows a comparison of the experimental data (for the high-energy extraction system) and a calculated curve in which the initial beam energy is assumed to be 590 MeV. Range values of reference 7 were used in the calculations. It is seen that the experimental data points fit the calculated curve to within ±2 percent. A similar curve was obtained for the low-energy extraction system.

Charles F. Perdrisat and L. McMasters of the College of William and Mary have made an independent energy measurement of the high-energy proton beam using a Cerenkov detector. They found the beam to be 594.8 ± 1.5 MeV, which agrees very well with the 593-MeV result found in this experiment.

Blake, Boles, Nelson, and Parker (ref. 8) have recently activated a stack of polyethylene foils by using the low-energy extracted proton beam and they found the energy to be 325.7 MeV. This value also agrees very well with the 325.6-MeV result found in this experiment. The mean range and energy spread according to the procedure described by Mather and Segrè (ref. 4) was obtained from the curve of the observed relative ionization plotted against the absorber thickness. This procedure enables one to allow for the multiple scattering effects by comparing the experimental relative ionization curves with the corresponding curves calculated by using theoretical standard deviation of the range distribution.

Figure 35 shows a graph of percent energy spread as a function of proton energy for three higher energy beams. At 595 MeV the percent energy spread is ±0.84 and increases to ±1.5 at 380 MeV. Figure 36 is a similar graph for the lower energy beams. The percent energy spread varies from ±0.35 at 325 MeV to ±16.4 at 40 MeV. The difference in energy spread at 595 MeV and 325 MeV is related to the fact that two different extraction systems are used at these energies. This difference indicates that the lower energy beams, obtained by degrading through copper, were less monoenergetic than the primary-extracted beams (595 MeV and 380 MeV).

Total Beam Intensity Measurements

The proton beam intensity was determined by using two methods. The higher energy beams at 595, 480, 380, and 325 MeV were monitored with the $C^{12}(p,pn)C^{11}$ reaction; and the other beams at 225, 155, 95, 75, 50, and 40 MeV, because of their large size, were monitored with a calibrated secondary emission chamber.

The total activity from an irradiated polystyrene disk was calculated from the relation

$$A_T = N_O \sigma \Phi(t)\left(1 - e^{-\lambda t}\right)$$

where

N_O number of C^{12} atoms/cm^2

σ cross section for $C^{12}(p,pn)C^{11}$ reaction

$\Phi(t)$ beam intensity, protons/sec

$\lambda = \frac{0.693}{T_{1/2}} = 0.0338$ min^{-1}

$T_{1/2}$ half-life, 20.5 min

t duration of irradiation, min

The total activity A_T was found by integrating the peak associated with the 0.511-MeV gamma rays. Then, $\Phi(t)$ could be determined from the following equation:

$$\Phi(t) = \frac{A_T}{N_O \sigma\left(1 - e^{-\lambda t}\right)}$$

Figure 37 shows the results of the intensity measurements for all beams. The intensity of the 595-MeV beam was 5.3×10^{10} protons/sec. A value of 3.0×10^{10} protons/sec for the 325-MeV beam was found in the present investigation by using the $C^{12}(p,pn)C^{11}$ reaction. The difference in the two values can be attributed to a change in the ion source which was accomplished between the independent measurements. A measurement from the secondary emission chamber indicated an intensity of 6.8×10^8 protons/sec for the 40-MeV beam.

The largest error involved in the $C^{12}(p,pn)C^{11}$ reaction technique for proton beam monitoring is in the uncertainty of the value of the cross section σ for the $C^{12}(p,pn)C^{11}$ reaction. This error is reported to be approximately ±5 percent over the energy range of the investigation. (See ref. 3.)

Several investigators (refs. 9 and 10) have reported a loss of activity in this technique due to the diffusion process of C^{11} atoms into a gaseous form. As much as a 15-percent loss has been reported for very thin samples. However, the loss in activity for the thick samples used in this experiment was found to be less than ±0.5 percent,

which was determined by sandwiching three polystyrene samples together, bombarding, and then making an individual count on each sample. Other errors are discussed in the appendix.

Relative Intensity Profile Measurements

Relative intensity profile measurements were made on each of the proton beams. The data, normalized to unity, are shown in figures 38 to 47. Profiles of the 595-, 480-, 380-, and 325-MeV proton beams were obtained by using the scanning solid-state ionization chamber (diode) shown in figure 14. Profiles of the remaining beams were obtained by irradiating a matrix of polystyrene disks and determining the incident flux per disk from the $C^{12}(p,pn)C^{11}$ reaction. The total activity A_T of each disk was determined by integrating the counts under the peak associated with the 0.511-MeV gamma rays.

Both horizontal and vertical relative intensity profile measurements were made for all beams. As indicated in figures 38 to 47, the profiles are not completely symmetrical. In most cases, the vertical profiles have a larger full width at half maximum (called FWHM in the figures) than the horizontal profiles. Each figure has the horizontal profile indicated from left to right and the vertical profile indicated from top to bottom. This convention assumes that the beam is into the paper.

At 10 feet (3.05 m) from the BM4 window, the data show that the 595-MeV beam has full widths at half maximum of 0.4 inch and 1.1 inches (1.02 cm and 2.79 cm) for the horizontal and vertical profiles, respectively; and the 40-MeV beam has full widths at half maximum of 13.8 inches and 14.6 inches (35.05 cm and 37.08 cm) for the horizontal and vertical profiles, respectively. Focusing the low-energy beams and keeping the intensity up was very difficult, since they were scattered through thick copper degraders. An error of ±5 percent is estimated for the profiles which were obtained with the diode and ±8 percent for those obtained by using the $C^{12}(p,pn)C^{11}$ reaction. A summary of the data is tabulated in table 11.

CONCLUDING REMARKS

The data presented herein show that at the NASA Space Radiation Effects Laboratory an experimenter has at his command an energy range of 40 MeV to 595 MeV and an intensity range from 6.8×10^8 to approximately 5×10^{10} protons/sec. The lower energy beams, obtained by degrading through copper, were less monoenergetic than the higher energy beams obtained with the primary-beam extraction system. Energy spreads of ±4.9 MeV and ±1.13 MeV were measured for the 595-MeV and 325-MeV beams, respectively. Beam size availability varies from 0.4-inch (1.02-cm) to 14.6-inch (37.08-cm)

full width at half maximum for the small-area beams. Magnetic defocusing allows the experimenter much flexibility in choosing the desired beam shape at the target position. Although not discussed in this report, large-area beams are available for irradiating such targets as space vehicles, monkeys, and rabbits. Table 12 is a summary of the large-area beams available in the combined target area at SREL. (See ref. 11.)

Langley Research Center,
National Aeronautics and Space Administration,
Langley Station, Hampton, Va., August 18, 1969.

APPENDIX

DISCUSSION OF ERRORS

The largest error involved in the $C^{12}(p,pn)C^{11}$ reaction technique for proton beam monitoring is in the uncertainty of the value of the cross section for the $C^{12}(p,pn)C^{11}$ reaction. This error is reported to be approximately ±5 percent over the energy range of the investigation. (See ref. 3.)

Several investigators (refs. 5 and 6) have reported a loss of activity in this technique due to the diffusion process of C^{11} atoms into a gaseous form. As much as a 15-percent loss has been reported for very thin samples. However, the loss of activity for the "thick" samples used in this experiment was observed to be less than ±0.5 percent. This loss of activity was experimentally determined by irradiating a stack of three identical polystyrene targets for a time period of 3 half-lives corresponding to the $C^{12}(p,pn)C^{11}$ reaction. Each target was then counted and relative activities were determined. All targets were found to have the same activity within ±0.5 percent.

All the standard gamma sources used were calibrated to an accuracy within ±2 percent by the International Atomic Energy Agency, Vienna, Austria.

In order to determine the total number of emitted gamma rays, it was necessary to integrate the peak associated with the 0.511-MeV gamma rays. This integration was accomplished by using a computer to subtract out background counts and to determine the limits of integration. The error in the total integration was then found, since the error was known for the number of counts in each channel. A ±3-percent error was found for evaluation of the peak area.

The proton beam intensity fluctuation during an irradiation was determined by continuous monitoring of the current from a secondary emission chamber. Current readings were recorded at 1-minute intervals and found to fluctuate ±2 percent during the entire irradiation.

Contributions of the $C^{12}(n,2n)C^{11}$ reaction and other reactions to the total sample activity were found to be negligible for the energies considered. This fact was verified by counting several targets for 10 half-lives and noting the linearity of the data.

The attenuation of gamma rays in the polystyrene target and aluminum capsule also contributed an error. This attenuation can be calculated quite easily if it is assumed that all gamma rays are created at the geometrical center of the polystyrene target. The intensity of gamma rays reaching the NaI(Tl) crystal is given by

$$I = I_o e^{-\left(\mu_p d_p + \mu_{Al} d_{Al} + \mu_a d_a\right)}$$

where

I_o total intensity of gamma rays produced at origin

μ_p attenuation coefficient of polystyrene, 0.218 $inch^{-1}$ (0.086 cm^{-1})

μ_{Al} attenuation coefficient of aluminum, 0.584 $inch^{-1}$ (0.23 cm^{-1})

μ_a attenuation coefficient of air, 0.282×10^{-3} $inch^{-1}$ (0.111×10^{-3} cm^{-1})

d_p thickness of polystyrene, 0.063 inch (0.159 cm)

d_{Al} thickness of aluminum, 0.039 inch (0.100 cm)

d_a thickness of air, 3.94 inches (10.000 cm)

By using the above information, it is easily seen that the gamma-ray intensity at the face of the NaI(Tl) crystal is

$$I = 0.963I_o$$

A total of 3.7 percent of the gamma rays were attenuated.

Other errors, such as inaccuracy in the calculated number of C^{12} atoms/cm^2 and time measurements, were estimated to be ±2 percent. Therefore, the overall root-mean-square error was calculated and found to be ±7.8 percent.

REFERENCES

1. Koehler, A. M.: Dosimetry of Proton Beams Using Small Silicon Diodes. Radiation Research Supplement 7, Philip E. Schambra, George E. Stapleton, and Nathaniel F. Barr, eds., Academic Press, 1967, pp. 53-63.

2. Raju, M. R.: The Use of the Miniature Silicon Diode as a Radiation Dosemeter. Phys. Med. Biol., vol. 11, no. 3, 1966, pp. 371-376.

3. Cumming, J. B.: Monitor Reactions for High Energy Proton Beams. Annual Review of Nuclear Science, Vol. 13, Emilio Segrè, Gerhart Friedlander, and H. Pierre Noyes, eds., Annu. Rev., Inc., 1963, pp. 261-286.

4. Mather, R.; and Segrè, E.: Range Energy Relation for 340-Mev Protons. Phys. Rev., Second ser., vol. 84, no. 2, Oct. 15, 1951, pp. 191-193.

5. Bakker, C. J.; and Segrè, E.: Stopping Power and Energy Loss for Ion Pair Production for 340-MeV Protons. Phys. Rev., Second ser., vol. 81, no. 4, Feb. 15, 1951, pp. 489-492.

6. Anon.: Studies in Penetration of Charged Particles in Matter. Publ. 1133, Nat. Acad. Sci.-Nat. Res. Counc., 1964.

7. Janni, Joseph F.: Calculations of Energy Loss, Range, Pathlength, Straggling, Multiple Scattering, and the Probability of Inelastic Nuclear Collisions for 0.1- to 1000-MeV Protons. AFWL-TR-65-150, U.S. Air Force, Sept. 1966. (Available from DDC as AD643837.)

8. Blake, K. R.; Boles, L. A.; Nelson, J. B.; and Parker, C. V., Jr.: Large Area Proton Beams for Radiobiological Research From the NASA-SREL Synchrocyclotron. Vol. I – Investigation of the Nominal 300 MeV Primary Beam. USAF Sch. Aerosp. Med., Aerosp. Med. Div. (Brooks AFB, Texas), Jan. 30, 1968.

9. Fuchs, H.; and Lindenberger, K. H.: Loss of Activity From Betatron Irradiated Samples by Diffusion. Nucl. Instrum. Methods, vol. 7, Apr.-June 1960, pp. 219-220.

10. Measday, David F.: The $^{12}C(p,pn)^{11}C$ Reaction From 50 to 160 MeV. Nucl. Phys., vol. 78, no. 2, Apr. 1966, pp. 476-480.

11. Hill, Gerald F.; and Honaker, William C.: Large-Area Proton Beams Established at the NASA Space Radiation Effects Laboratory in the Energy Range From 31 to 225 MeV. NASA TN D-5479, 1970.

TABLE 1.- MAGNET POWER SUPPLY SETTINGS FOR A SMALL 595-MeV PROTON BEAM IN THE COMBINED TARGET AREA AT SREL

Extraction platter used	600 MeV
Copper degrader thickness (BD1)	0 in. (0 cm), (0 g/cm^2)
Degraded energy	595 MeV
Distance of energy measurement from BM4 exit window	10 ft (3.05 m)
Beam dimension (full width at half maximum) for –	
Horizontal profile	0.4 in. (1.02 cm)
Vertical profile	1.1 in. (2.79 cm)
Main magnet reading	74.00 mV
Diverted current	+15.0 A

Power supply and shunt numbers	Magnet	Digital voltmeter reading, mV
PS 1	M2 and M3	43.42
PS 2	M4	50.24
PS 3	M5	47.50
PS 4	Q1A and Q2A	18.85
PS 5	Q5	16.66
PS 6	Q8	41.35
PS 7	Q2 and Q3	19.47
PS 8	Q6 and Q10	30.75
PS 9	----------	-----
PS 10	Q1	26.43
PS 11	Q7	68.22
PS 12	Q9	58.83
PS 13	----------	-----
PS 14	----------	-----
PS 15	Q4	13.87
PS 16	Q11	60.50
PS 17	Q12	51.43
PS 18	Q13	54.15
PS 19	Q14	30.34
PS 20	M1	5.21
Shunt 1	M2 and M3	-----
Shunt 2	Q1A and Q2A	-----
Shunt 3	Q2 and Q3	+11.99
Shunt 4	Q6 and Q10	-5.60
Shunt 5	----------	-----

TABLE 2.- MAGNET POWER SUPPLY SETTINGS FOR A SMALL 480-MeV PROTON BEAM IN THE COMBINED TARGET AREA AT SREL

Extraction platter used . . . . . 600 MeV
Copper degrader thickness (BD1) . . . . . 2.50 in. (6.35 cm), (56.64 g/cm^2)
Degraded energy . . . . . 480 MeV
Distance of energy measurement from BM4 exit window . . . . . 10 ft (3.05 m)
Beam dimension (full width at half maximum) for –
  Horizontal profile . . . . . 0.7 in. (1.78 cm)
  Vertical profile . . . . . 0.6 in. (1.52 cm)
Main magnet reading . . . . . 74.00 mV
Diverted current . . . . . +9.66 A

Power supply and shunt numbers	Magnet	Digital voltmeter reading, mV
PS 1	M2 and M3	43.68
PS 2	M4	43.57
PS 3	M5	43.24
PS 4	Q1A and Q2A	28.46
PS 5	Q5	45.30
PS 6	Q8	50.76
PS 7	Q2 and Q3	21.85
PS 8	Q6 and Q10	56.13
PS 9	----------	-----
PS 10	Q1	31.55
PS 11	Q7	50.79
PS 12	Q9	32.09
PS 13	----------	-----
PS 14	----------	-----
PS 15	Q4	41.04
PS 16	Q11	33.91
PS 17	Q12	62.37
PS 18	Q13	47.32
PS 19	Q14	18.27
PS 20	M1	4.13
Shunt 1	M2 and M3	-----
Shunt 2	Q1A and Q2A	-----
Shunt 3	Q2 and Q3	+13
Shunt 4	Q6 and Q10	-7.5
Shunt 5	----------	-----

TABLE 3.- MAGNET POWER SUPPLY SETTINGS FOR A SMALL 380-MeV PROTON BEAM IN THE COMBINED TARGET AREA AT SREL

Extraction platter used . . . . . 600 MeV
Copper degrader thickness (BD1) . . . . . 4.75 in. (12.07 cm), (107.62 g/cm^2)
Degraded energy . . . . . 380 MeV
Distance of energy measurement from BM4 exit window . . . . . 10 ft (3.05 m)
Beam dimension (full width at half maximum) for –
  Horizontal profile . . . . . 1.0 in. (2.54 cm)
  Vertical profile . . . . . 0.7 in. (1.78 cm)
Main magnet reading . . . . . 74.02 mV
Diverted current . . . . . +14.0 A

Power supply and shunt numbers	Magnet	Digital voltmeter reading, mV
PS 1	M2 and M3	43.63
PS 2	M4	38.33
PS 3	M5	38.26
PS 4	Q1A and Q2A	28.50
PS 5	Q5	39.33
PS 6	Q8	51.92
PS 7	Q2 and Q3	22.66
PS 8	Q6 and Q10	54.90
PS 9	----------	-----
PS 10	Q1	31.57
PS 11	Q7	61.62
PS 12	Q9	30.06
PS 13	----------	-----
PS 14	----------	-----
PS 15	Q4	38.86
PS 16	Q11	18.89
PS 17	Q12	29.82
PS 18	Q13	44.25
PS 19	Q14	36.09
PS 20	M1	4.66
Shunt 1	M2 and M3	-----
Shunt 2	Q1A and Q2A	-----
Shunt 3	Q2 and Q3	+14.35
Shunt 4	Q6 and Q10	-----
Shunt 5	----------	-----

TABLE 4.- MAGNET POWER SUPPLY SETTINGS FOR A SMALL 325-MeV PROTON BEAM IN THE COMBINED TARGET AREA AT SREL

Extraction platter used			300 MeV
Copper degrader thickness (BD1)	0 in.	(0 cm),	(0 g/cm^2)
Degraded energy			325 MeV
Distance of energy measurement from BM4 exit window		10 ft	(3.05 m)
Beam dimension (full width at half maximum) for –			
Horizontal profile		2.1 in.	(5.33 cm)
Vertical profile		2.1 in.	(5.33 cm)
Main magnet reading			67.30 mV
Diverted current			+85.0 A

Power supply and shunt numbers	Magnet	Digital voltmeter reading, mV
PS 1	M2 and M3	32.50
PS 2	M4	33.72
PS 3	M5	34.31
PS 4	Q1A and Q2A	19.07
PS 5	Q5	15.24
PS 6	Q8	30.45
PS 7	Q2 and Q3	16.01
PS 8	Q6 and Q10	25.45
PS 9	----------	----
PS 10	Q1	22.80
PS 11	Q7	41.75
PS 12	Q9	10.21
PS 13	----------	----
PS 14	----------	----
PS 15	Q4	22.48
PS 16	Q11	31.67
PS 17	Q12	38.20
PS 18	Q13	50.04
PS 19	Q14	68.02
PS 20	M1	8.94
Shunt 1	M2 and M3	----
Shunt 2	Q1A and Q2A	----
Shunt 3	Q2 and Q3	+9.56
Shunt 4	Q6 and Q10	-4.45
Shunt 5	----------	----

TABLE 5.- MAGNET POWER SUPPLY SETTINGS FOR A SMALL 225-MeV PROTON BEAM IN THE COMBINED TARGET AREA AT SREL

Extraction platter used . . . . . 300 MeV
Copper degrader thickness (BD1) . . . . . 1.75 in. (4.45 cm), (39.65 g/cm^2)
Degraded energy . . . . . 225 MeV
Distance of energy measurement from BM4 exit window . . . . . 10 ft (3.05 m)
Beam dimension (full width at half maximum) for –
  Horizontal profile . . . . . 1.7 in. (4.32 cm)
  Vertical profile . . . . . 3.7 in. (9.40 cm)
Main magnet reading . . . . . 67.92 mV
Diverted current . . . . . +27 A

Power supply and shunt numbers	Magnet	Digital voltmeter reading, mV
PS 1	M2 and M3	31.71
PS 2	M4	27.39
PS 3	M5	27.50
PS 4	Q1A and Q2A	16.12
PS 5	Q5	30.20
PS 6	Q8	21.00
PS 7	Q2 and Q3	19.60
PS 8	Q6 and Q10	31.70
PS 9	----------	----
PS 10	Q1	22.81
PS 11	Q7	27.10
PS 12	Q9	22.80
PS 13	----------	----
PS 14	----------	----
PS 15	Q4	22.00
PS 16	Q11	42.06
PS 17	Q12	30.05
PS 18	Q13	41.12
PS 19	Q14	27.01
PS 20	M1	7.98
Shunt 1	M2 and M3	----
Shunt 2	Q1A and Q2A	----
Shunt 3	Q2 and Q3	11.82
Shunt 4	Q6 and Q10	5.30
Shunt 5	----------	----

TABLE 6.- MAGNET POWER SUPPLY SETTINGS FOR A SMALL 155-MeV PROTON BEAM IN THE COMBINED TARGET AREA AT SREL

Extraction platter used . . . . . 300 MeV
Copper degrader thickness (BD1) . . . . . 2.25 in. (5.72 cm), (50.98 g/cm^2)
Degraded energy . . . . . 155 MeV
Distance of energy measurement from BM4 exit window . . . . . 10 ft (3.05 m)
Beam dimension (full width at half maximum) for –
  Horizontal profile . . . . . 2.4 in. (6.10 cm)
  Vertical profile . . . . . 5.5 in. (13.97 cm)
Main magnet reading . . . . . 67.39 mV
Diverted current . . . . . +80.0 A

Power supply and shunt numbers	Magnet	Digital voltmeter reading, mV
PS 1	M2 and M3	31.71
PS 2	M4	24.89
PS 3	M5	24.89
PS 4	Q1A and Q2A	16.04
PS 5	Q5	30.49
PS 6	Q8	18.80
PS 7	Q2 and Q3	19.60
PS 8	Q6 and Q10	30.90
PS 9	----------	-----
PS 10	Q1	22.81
PS 11	Q7	25.43
PS 12	Q9	22.51
PS 13	----------	-----
PS 14	----------	-----
PS 15	Q4	22.05
PS 16	Q11	37.70
PS 17	Q12	25.13
PS 18	Q13	32.00
PS 19	Q14	20.00
PS 20	M1	8.00
Shunt 1	M2 and M3	-----
Shunt 2	Q1A and Q2A	-----
Shunt 3	Q2 and Q3	+11.8
Shunt 4	Q6 and Q10	-5.14
Shunt 5	----------	-----

TABLE 7.- MAGNET POWER SUPPLY SETTINGS FOR A SMALL 95-MeV PROTON BEAM IN THE COMBINED TARGET AREA AT SREL

Extraction platter used . . . . . 300 MeV
Copper degrader thickness (BD1) . . . . . 2.75 in. (6.99 cm), (62.31 g/cm^2)
Degraded energy . . . . . 95 MeV
Distance of energy measurement from BM4 exit window . . . . . 10 ft (3.05 m)
Beam dimension (full width at half maximum) for –
  Horizontal profile . . . . . 3.7 in. (9.40 cm)
  Vertical profile . . . . . 6.9 in. (17.53 cm)
Main magnet reading . . . . . 67.82 mV
Diverted current . . . . . +27 A

Power supply and shunt numbers	Magnet	Digital voltmeter reading, mV
PS 1	M2 and M3	31.74
PS 2	M4	21.99
PS 3	M5	22.72
PS 4	Q1A and Q2A	16.13
PS 5	Q5	27.20
PS 6	Q8	30.00
PS 7	Q2 and Q3	20.21
PS 8	Q6 and Q10	32.75
PS 9	----------	-----
PS 10	Q1	22.84
PS 11	Q7	29.76
PS 12	Q9	17.78
PS 13	----------	-----
PS 14	----------	-----
PS 15	Q4	23.06
PS 16	Q11	27.09
PS 17	Q12	31.03
PS 18	Q13	35.00
PS 19	Q14	20.00
PS 20	M1	8.00
Shunt 1	M2 and M3	-----
Shunt 2	Q1A and Q2A	-----
Shunt 3	Q2 and Q3	+12.34
Shunt 4	Q6 and Q10	-5.60
Shunt 5	----------	-----

TABLE 8.- MAGNET POWER SUPPLY SETTINGS FOR A SMALL 75-MeV PROTON BEAM IN THE COMBINED TARGET AREA AT SREL

Extraction platter used . . . . . 300 MeV
Copper degrader thickness (BD1) . . . . . 3.375 in. (8.57 cm), (76.47 g/cm^2)
Degraded energy . . . . . 75 MeV
Distance of energy measurement from BM4 exit window . . . . . 10 ft (3.05 m)
Beam dimension (full width at half maximum) for –
  Horizontal profile . . . . . 3.6 in. (9.14 cm)
  Vertical profile . . . . . 4.0 in. (10.16 cm)
Main magnet reading . . . . . 67.43 mV
Diverted current . . . . . +80.0 A

Power supply and shunt numbers	Magnet	Digital voltmeter reading, mV
PS 1	M2 and M3	31.87
PS 2	M4	17.02
PS 3	M5	17.02
PS 4	Q1A and Q2A	15.59
PS 5	Q5	18.06
PS 6	Q8	20.56
PS 7	Q2 and Q3	20.76
PS 8	Q6 and Q10	24.05
PS 9	----------	-----
PS 10	Q1	24.21
PS 11	Q7	22.65
PS 12	Q9	13.33
PS 13	----------	-----
PS 14	----------	-----
PS 15	Q4	30.02
PS 16	Q11	18.32
PS 17	Q12	16.42
PS 18	Q13	16.52
PS 19	Q14	18.49
PS 20	M1	8.39
Shunt 1	M2 and M3	-----
Shunt 2	Q1A and Q2A	-----
Shunt 3	Q2 and Q3	+12.48
Shunt 4	Q6 and Q10	-14.50
Shunt 5	----------	-----

TABLE 9.- MAGNET POWER SUPPLY SETTINGS FOR A SMALL 50-MeV PROTON BEAM IN THE COMBINED TARGET AREA AT SREL

Extraction platter used . . . . . 300 MeV
Copper degrader thickness (BD1) . . . . . 3.50 in. (8.89 cm), (79.30 g/cm^2)
Degraded energy . . . . . 50 MeV
Distance of energy measurement from BM4 exit window . . . . . 10 ft (3.05 m)
Beam dimension (full width at half maximum) for –
  Horizontal profile . . . . . 6.3 in. (16.00 cm)
  Vertical profile . . . . . 6.4 in. (16.26 cm)
Main magnet reading . . . . . 67.55 mV
Diverted current . . . . . +80.0 A

Power supply and shunt numbers	Magnet	Digital voltmeter reading, mV
PS 1	M2 and M3	31.88
PS 2	M4	15.58
PS 3	M5	15.54
PS 4	Q1A and Q2A	15.56
PS 5	Q5	19.23
PS 6	Q8	19.21
PS 7	Q2 and Q3	20.75
PS 8	Q6 and Q10	21.44
PS 9	----------	-----
PS 10	Q1	24.21
PS 11	Q7	18.63
PS 12	Q9	15.64
PS 13	----------	-----
PS 14	----------	-----
PS 15	Q4	30.00
PS 16	Q11	15.00
PS 17	Q12	15.00
PS 18	Q13	20.00
PS 19	Q14	15.00
PS 20	M1	8.38
Shunt 1	M2 and M3	-----
Shunt 2	Q1A and Q2A	-----
Shunt 3	Q2 and Q3	+12.45
Shunt 4	Q6 and Q10	-4.00
Shunt 5	----------	-----

TABLE 10.- MAGNET POWER SUPPLY SETTINGS FOR A SMALL 40-MeV PROTON BEAM IN THE COMBINED TARGET AREA AT SREL

Extraction platter used . . . . . 300 MeV
Copper degrader thickness (BD1) . . . . . 3.75 in. (9.53 cm), (84.96 g/cm^2)
Degraded energy . . . . . 40 MeV
Distance of energy measurement from BM4 exit window . . . . . 10 ft (3.05 m)
Beam dimension (full width at half maximum) for.–
  Horizontal profile . . . . . 13.8 in. (35.05 cm)
  Vertical profile . . . . . 14.6 in. (37.08 cm)
Main magnet reading . . . . . 67.40 mV
Diverted current . . . . . +80.0 A

Power supply and shunt numbers	Magnet	Digital voltmeter reading, mV
PS 1	M2 and M3	32.50
PS 2	M4	13.40
PS 3	M5	13.74
PS 4	Q1A and Q2A	14.00
PS 5	Q5	18.02
PS 6	Q8	17.82
PS 7	Q2 and Q3	20.20
PS 8	Q6 and Q10	20.99
PS 9	----------	-----
PS 10	Q1	24.23
PS 11	Q7	17.90
PS 12	Q9	9.76
PS 13	----------	-----
PS 14	----------	-----
PS 15	Q4	29.75
PS 16	Q11	14.48
PS 17	Q12	14.74
PS 18	Q13	10.98
PS 19	Q14	3.07
PS 20	M1	8.39
Shunt 1	M2 and M3	-----
Shunt 2	Q1A and Q2A	-----
Shunt 3	Q2 and Q3	+12.17
Shunt 4	Q6 and Q10	-13.60
Shunt 5	----------	-----

TABLE 11.- SUMMARY OF PROTON BEAM MEASUREMENTS

Proton energy, MeV	Energy spread, MeV	Full width at half maximum of beam profile				Beam intensity, protons/sec
		Horizontal		Vertical		
		in.	cm	in.	cm	
595	±4.9	0.4	1.02	1.1	2.79	5.3×10^{10}
480	±4.7	.7	1.78	.6	1.52	2.0×10^{10}
380	±5.7	1.0	2.54	.7	1.78	4.9×10^{9}
325	±1.13	2.1	5.33	2.1	5.33	3.0×10^{10}
225	±2.7	1.7	4.32	3.7	9.40	6.2×10^{9}
155	±4.1	2.4	6.10	5.5	13.97	3.5×10^{9}
95	±4.1	3.7	9.40	6.9	17.53	1.5×10^{9}
75	±4.8	3.6	9.14	4.0	10.16	1.3×10^{9}
50	±4.8	6.3	16.00	6.4	16.26	7.8×10^{8}
40	±6.1	13.8	35.05	14.6	37.08	6.8×10^{8}

TABLE 12.- LARGE-AREA BEAMS AVAILABLE IN COMBINED TARGET AREA AT SREL

Proton energy, MeV	Full width at half maximum, cm, for –				Maximum flux, $\frac{\text{protons/cm}^2}{\text{min}}$, for –			
	Horizontal profile at –		Vertical profile at –		Horizontal profile at –		Vertical profile at –	
	3.05 m	7.62 m	3.05 m	7.62 m	3.05 m	7.62 m	3.05 m	7.62 m
225	11.3	18.2	9.7	18.2	9.15×10^9	2.55×10^9	8.25×10^9	2.55×10^9
155	17.2	32.8	26.6	47.2	1.8×10^9	4.45×10^8	1.35×10^9	3×10^8
95	19.0	53.0	22.6	45.0	4.8×10^8	8.66×10^7	4.4×10^8	8.1×10^7
75	14.0	36.0	19.2	36.0	8.3×10^8	1.9×10^8	8.3×10^8	1.8×10^8
50	45.0	---	35.0	---	3.5×10^7	---------	3.5×10^7	---------
*194	24.0	---	24.0	---	2.0×10^9	---------	2.0×10^9	---------
*146	54.0	---	51.0	---	1.76×10^9	---------	1.80×10^9	---------
*142	40	---	41	---	3×10^9	---------	2.9×10^9	---------
*90	56.0	---	58.0	---	3.57×10^8	---------	3.37×10^8	---------
*31	78.0	---	78.5	---	2.7×10^8	---------	2.65×10^8	---------

*Coulomb scattered.

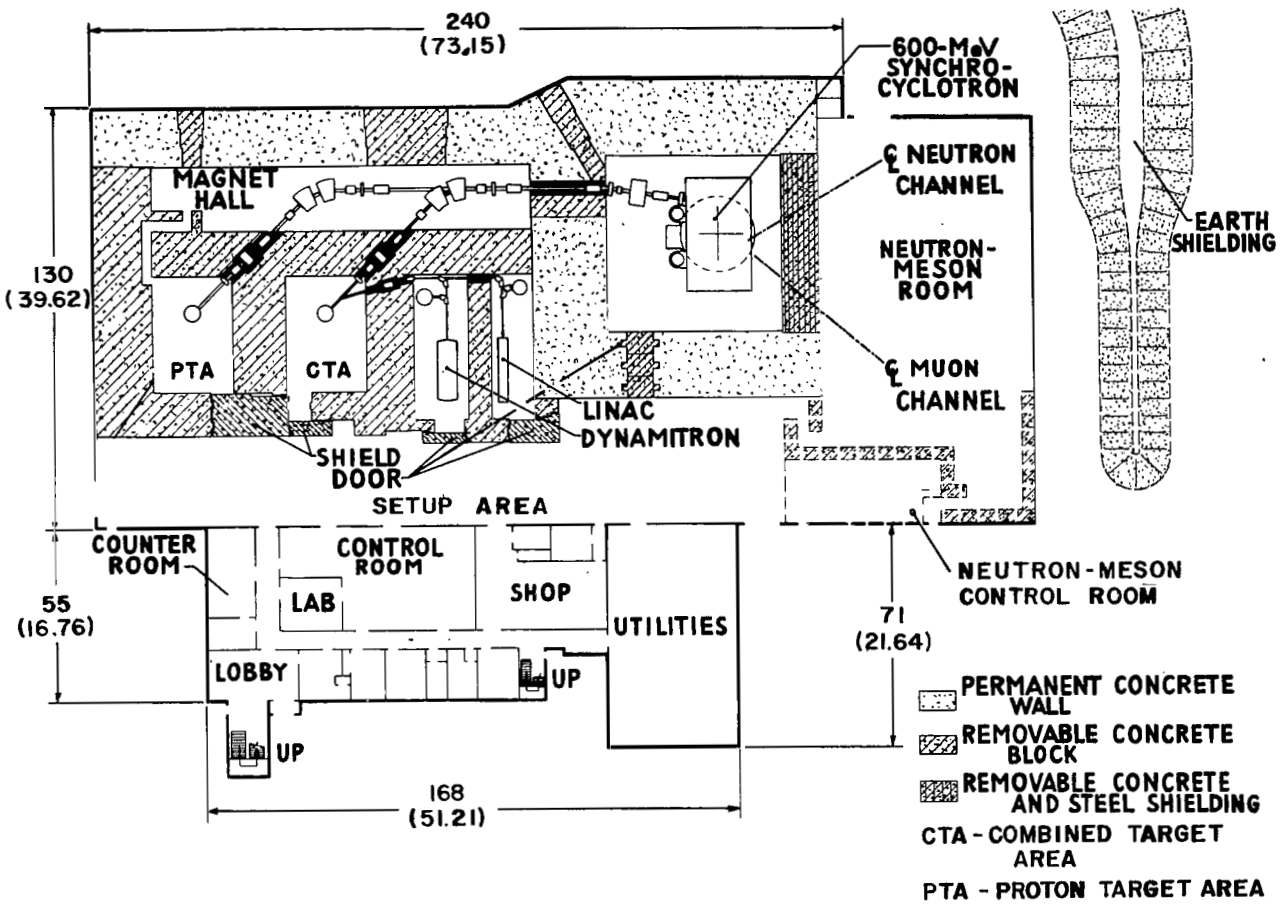

Figure 1.- Plan view of NASA Space Radiation Effects Laboratory (SREL). All dimensions are given in feet (meters).

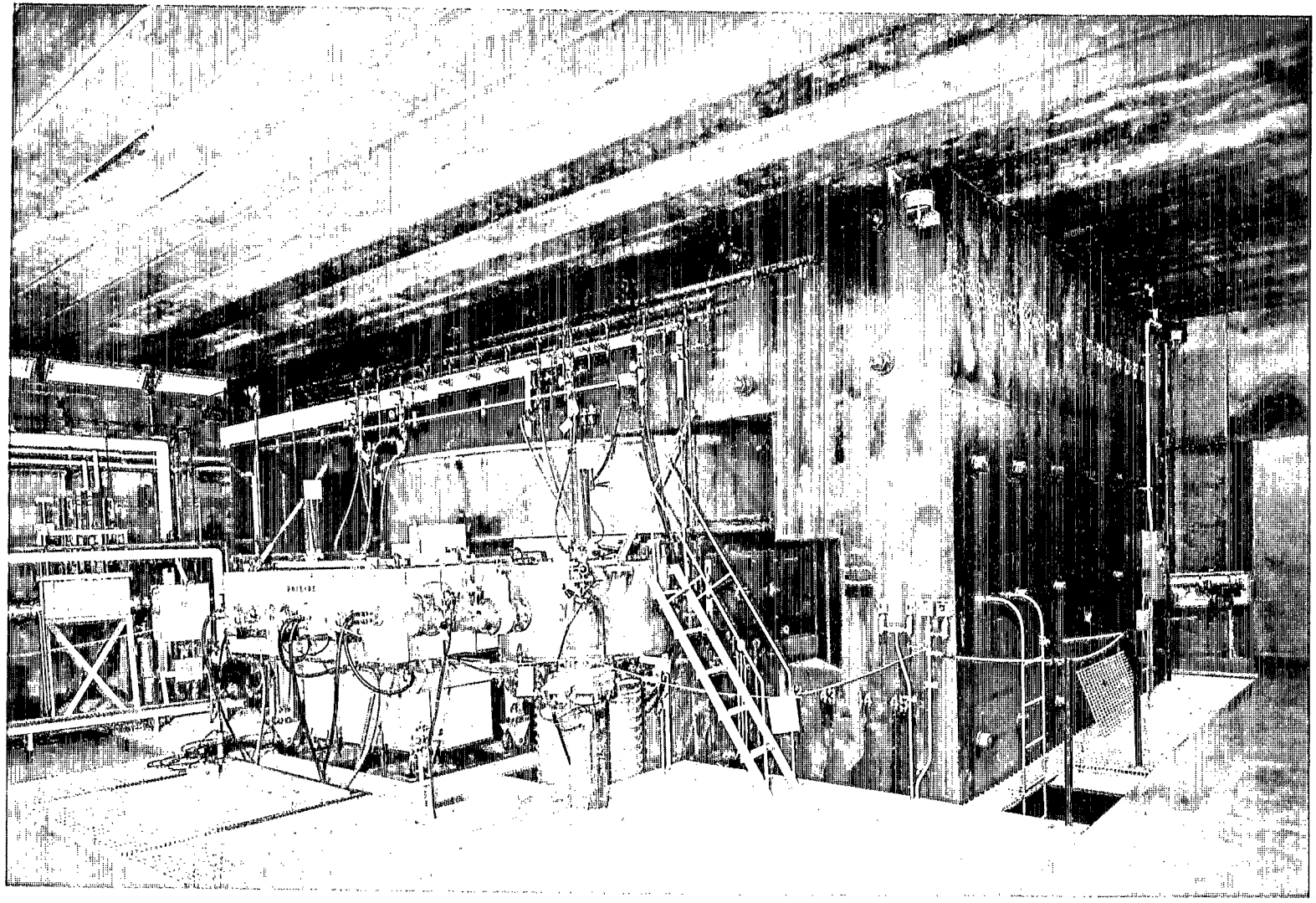

Figure 2.- SREL 600-MeV proton synchrocyclotron. L-65-8622

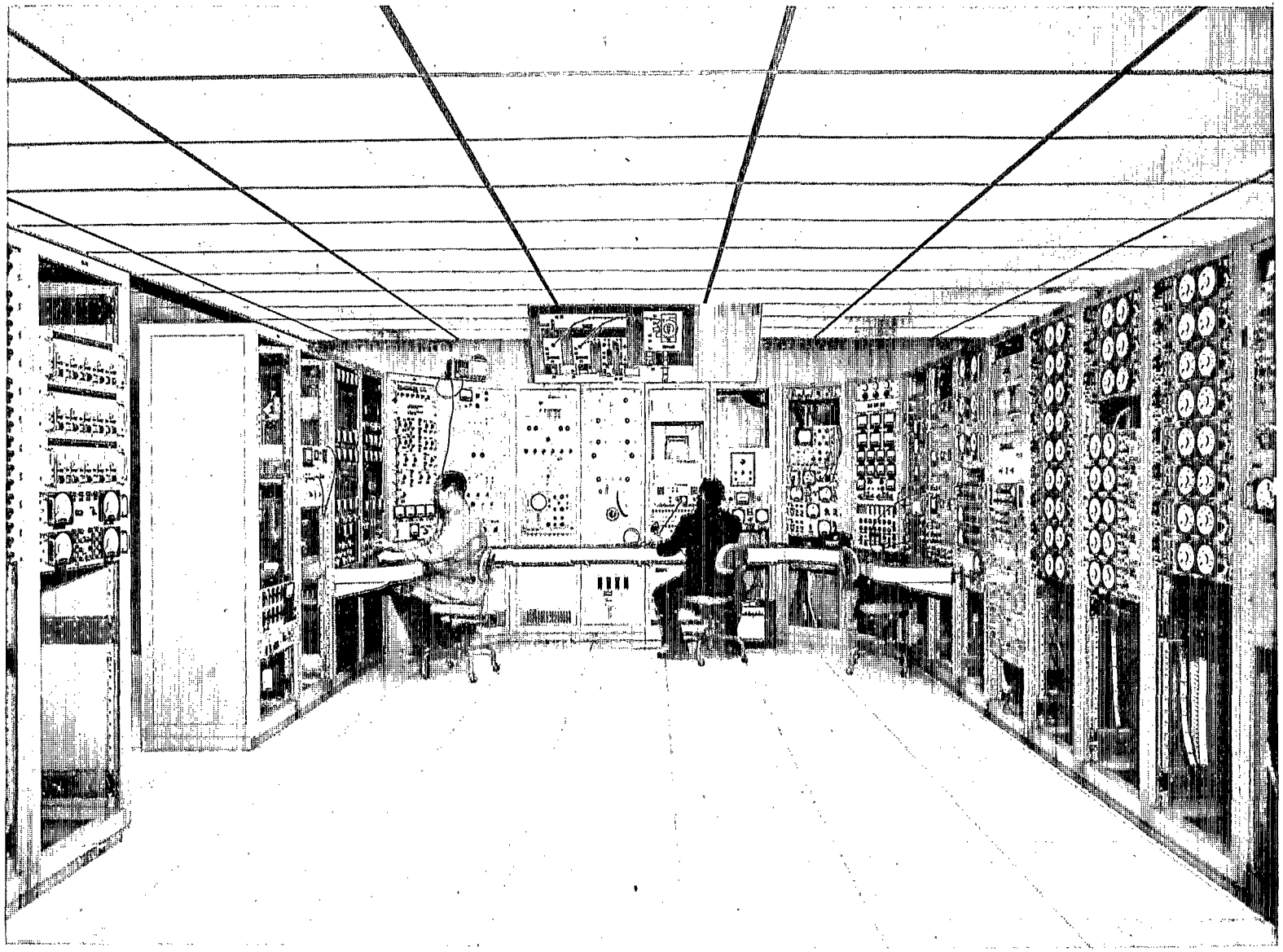

Figure 3.- Control panels for 600-MeV proton synchrocyclotron. L-65-8616

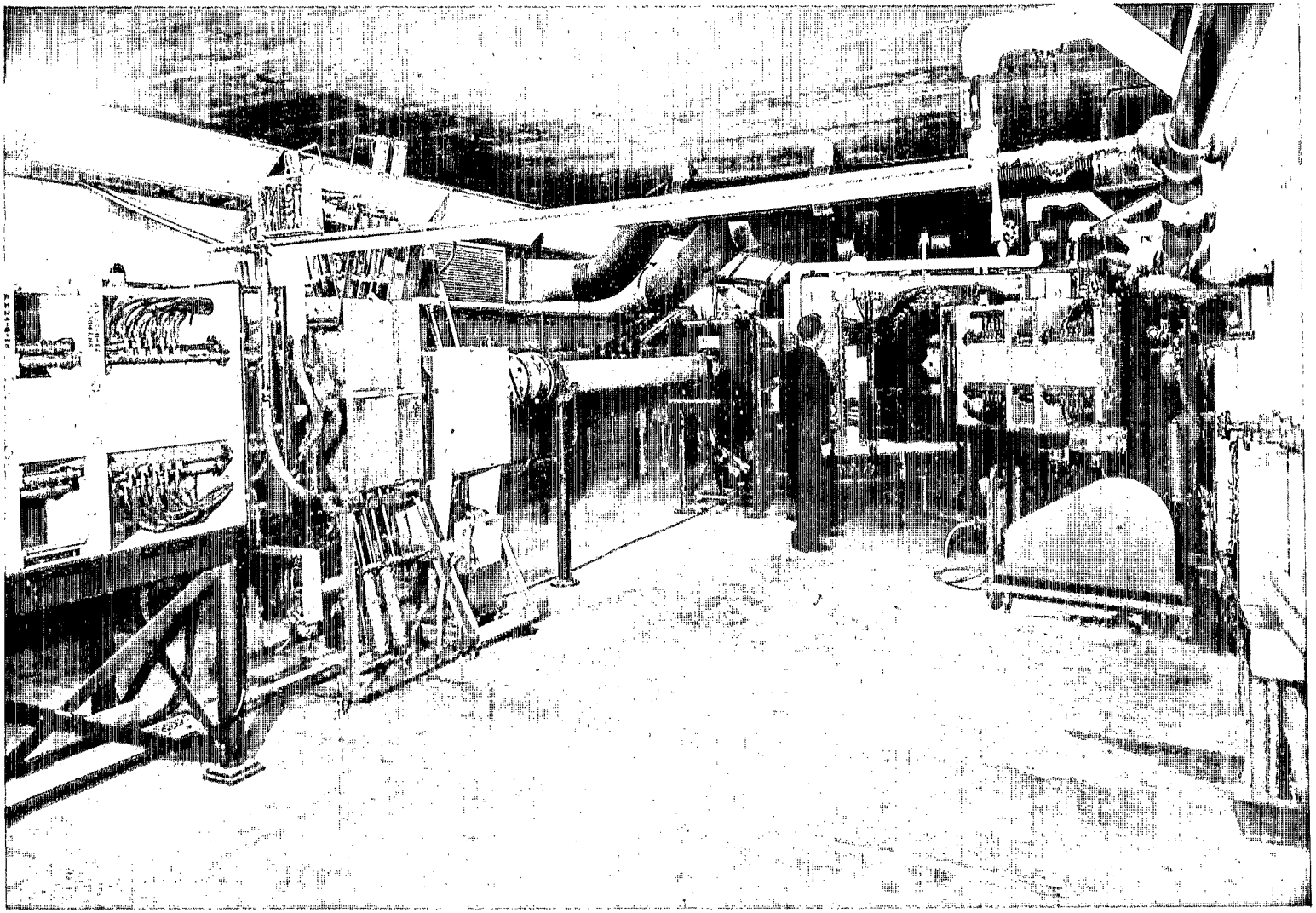

Figure 4.- Proton beam transport system showing section that transports beam into combined target area (CTA). L-65-8617

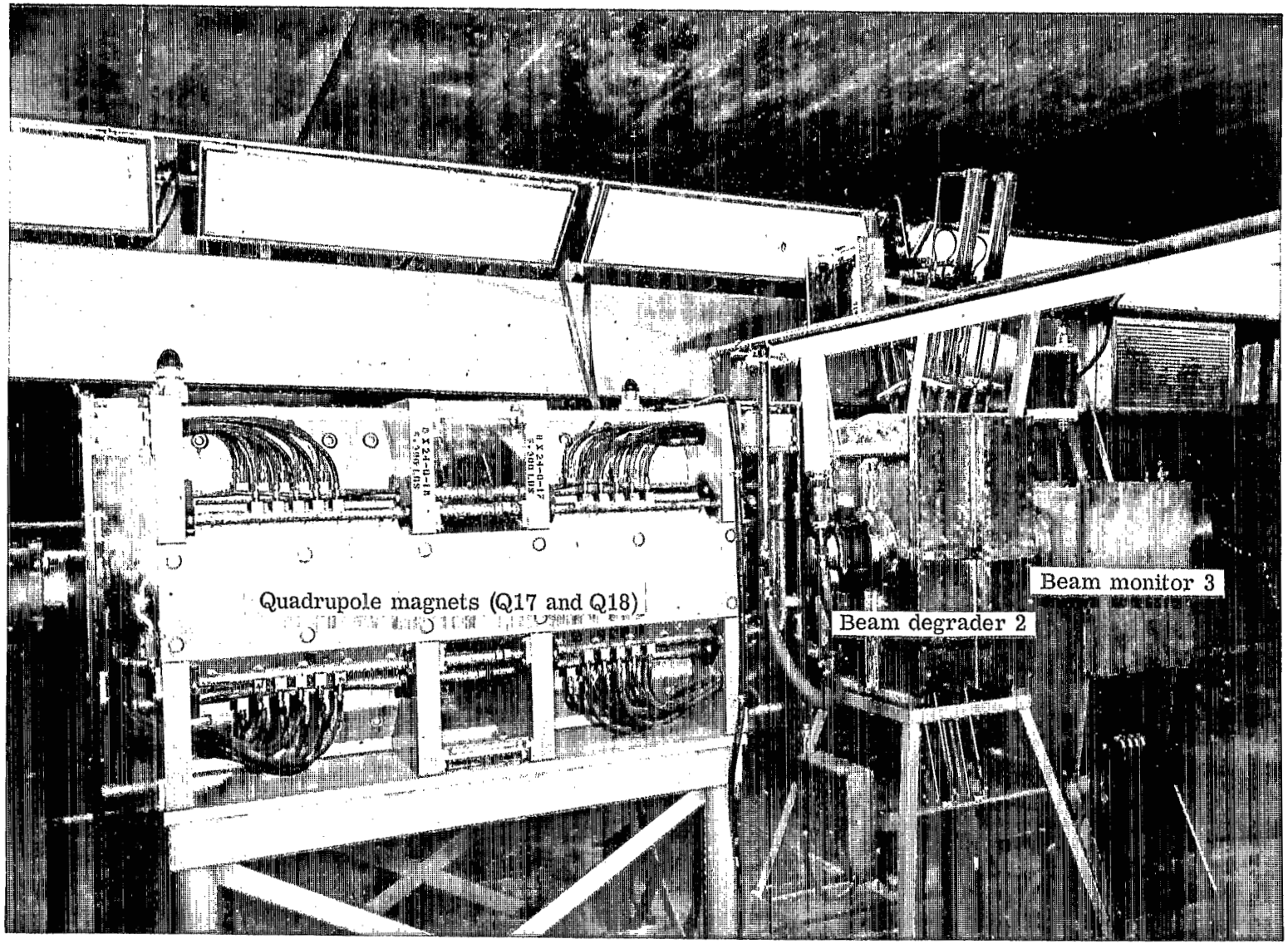

Figure 5.- Section of proton beam transport system showing a quadrupole pair, beam degrader, and beam monitor. L-65-8547.1

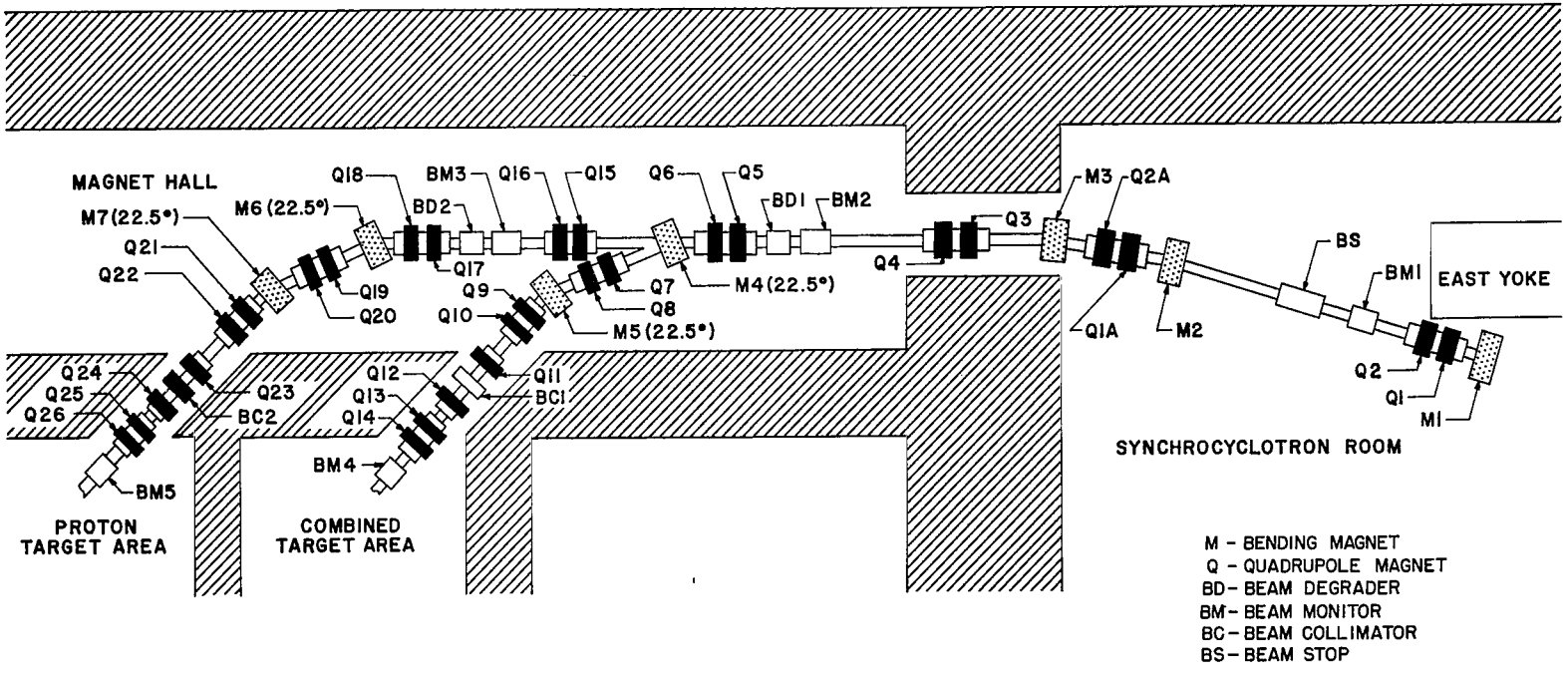

Figure 6.- Schematic diagram of proton beam transport system at SREL.

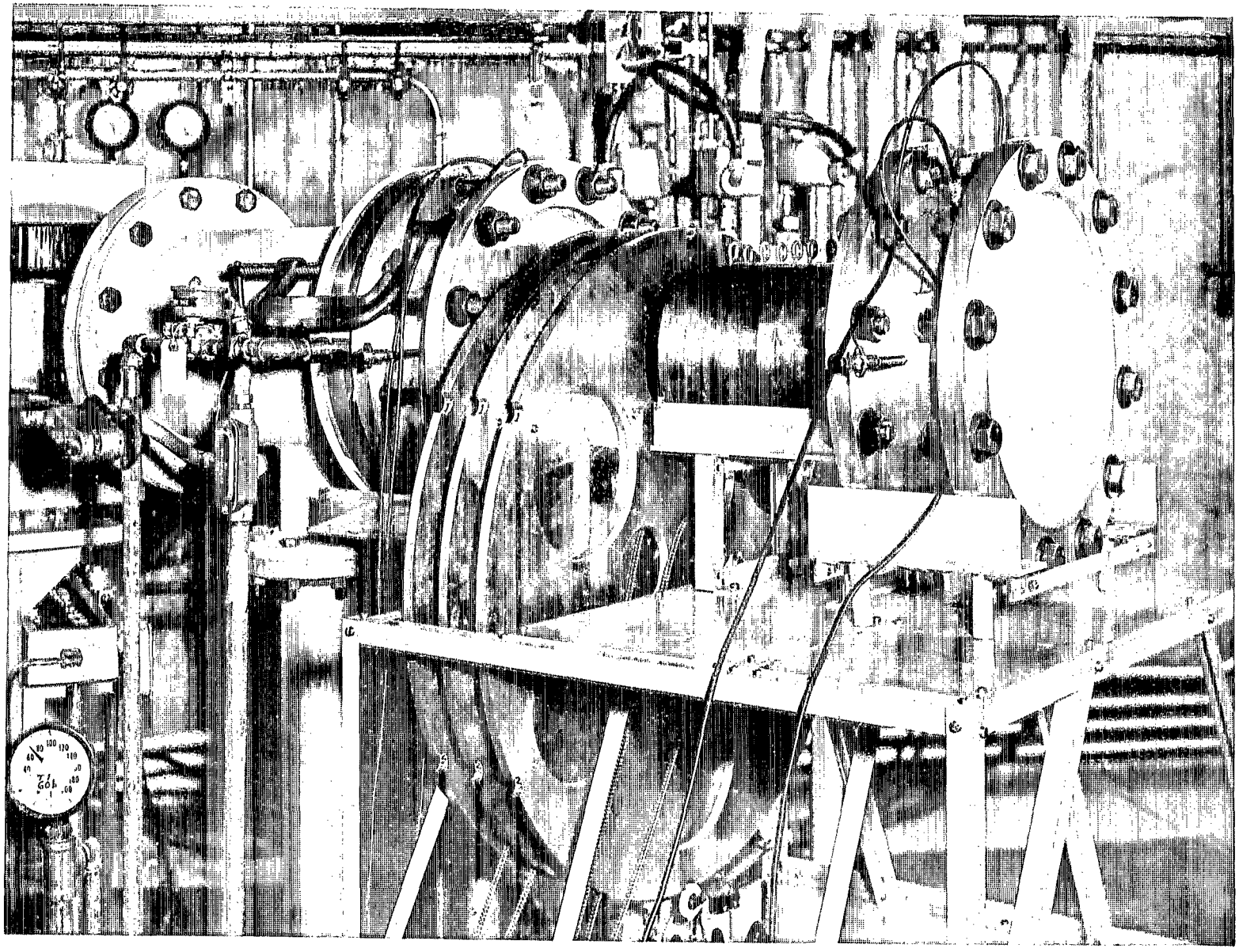

Figure 7.- Range-energy spectrometer as it is used in an experiment.

L-66-4811

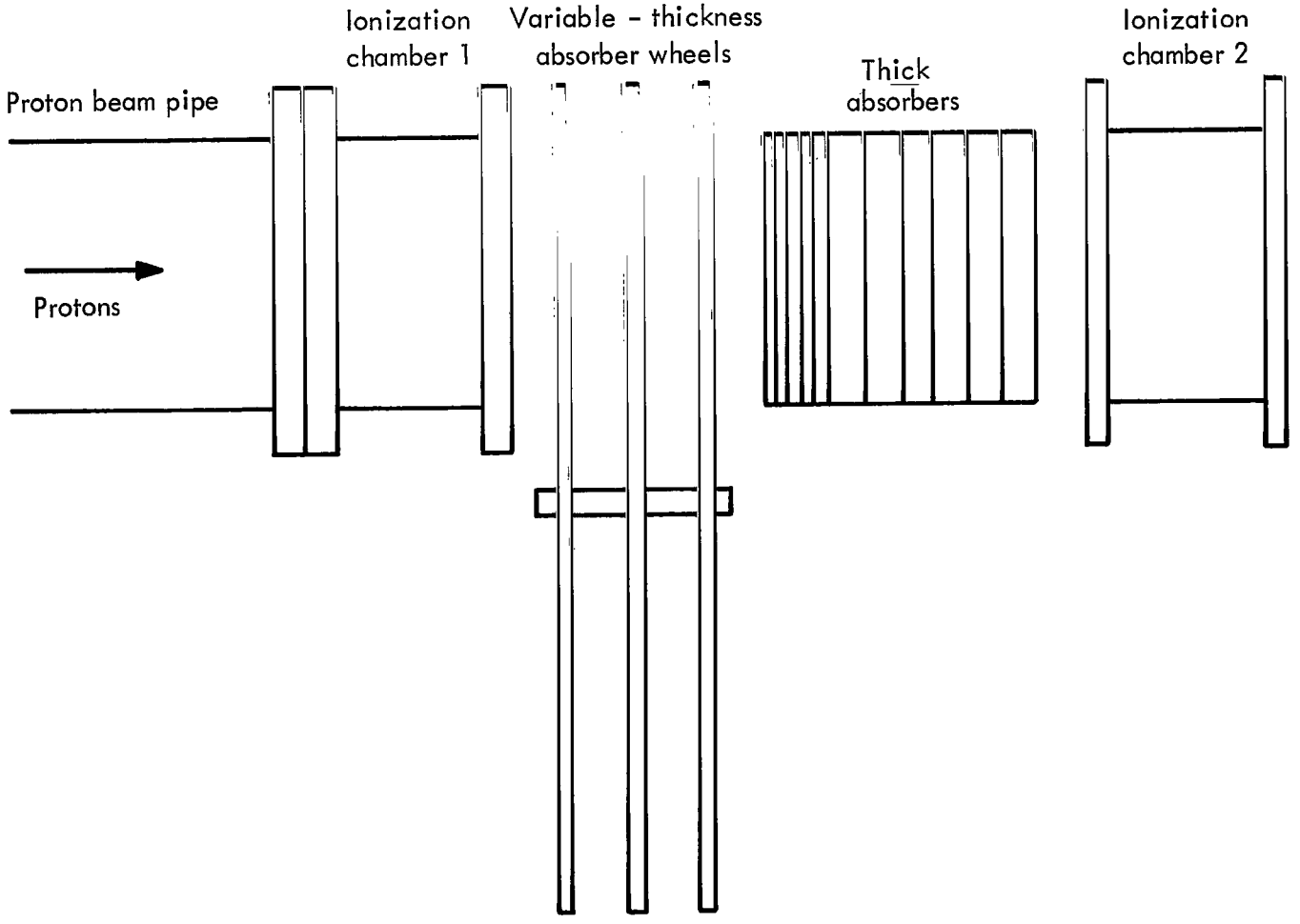

Figure 8.- Diagram of range-energy proton spectrometer.

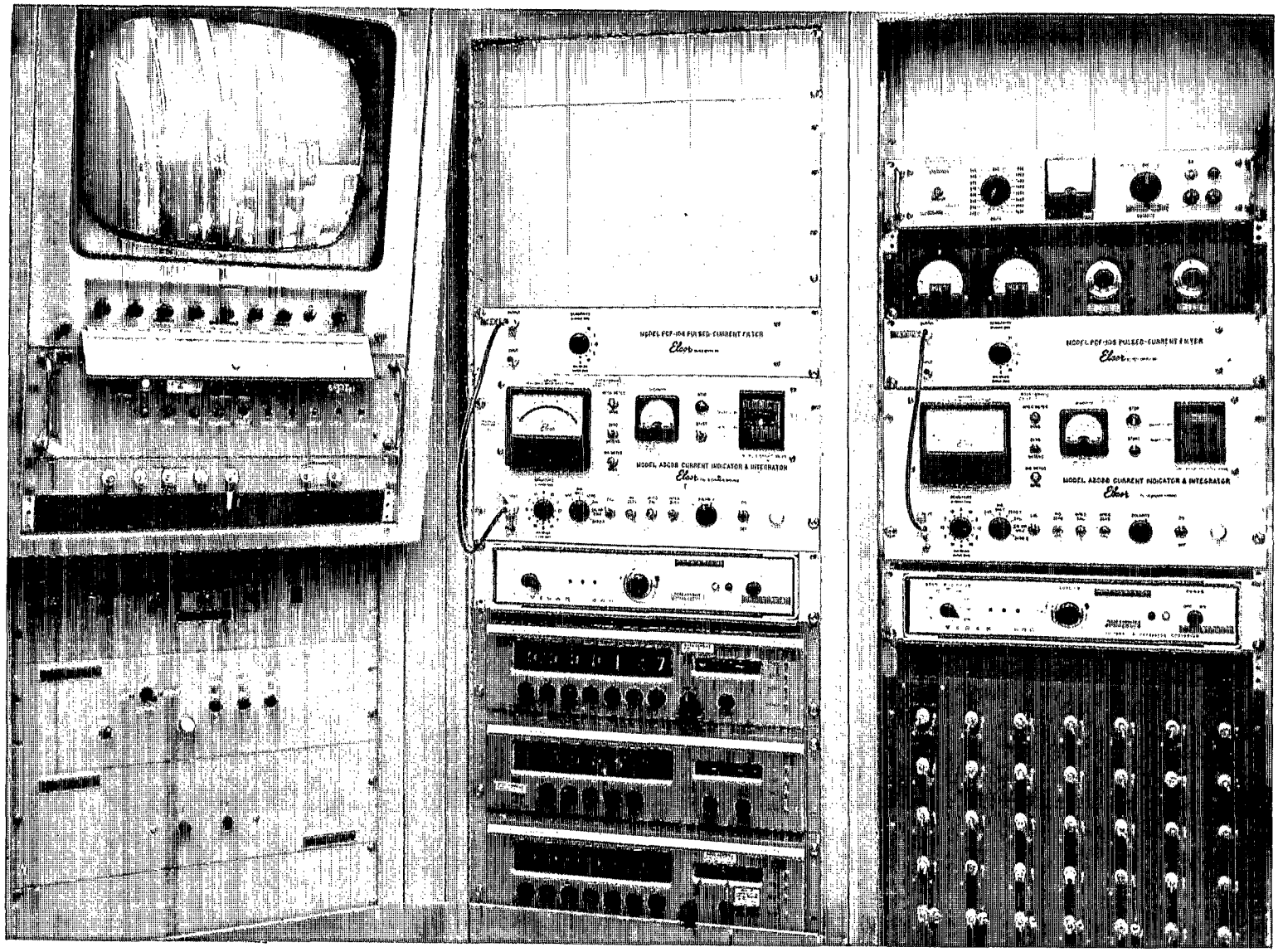

Figure 9.- Readout electronics and TV monitor for range-energy spectrometer. L-67-2109

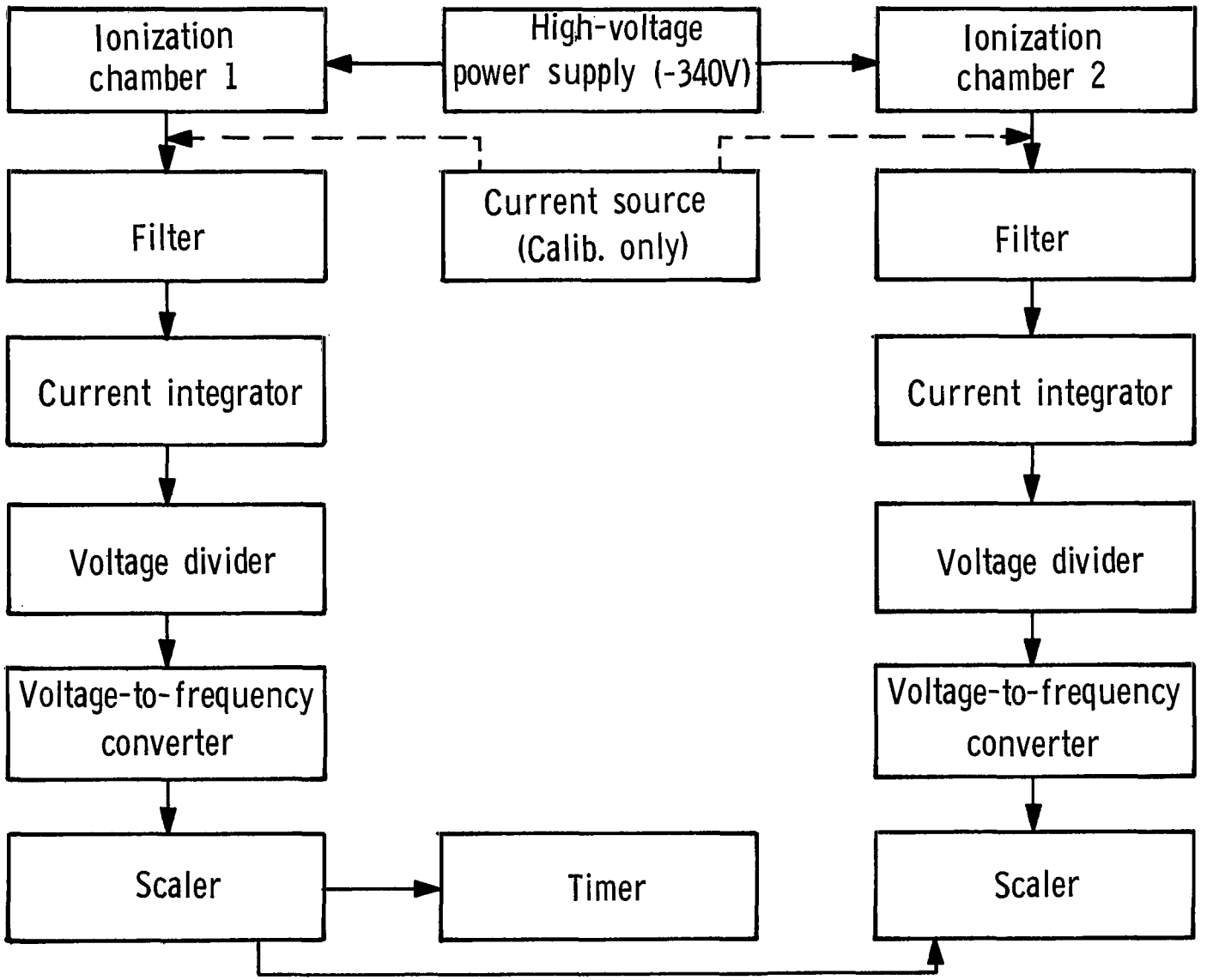

Figure 10.- Block diagram of electronics associated with range-energy spectrometer.

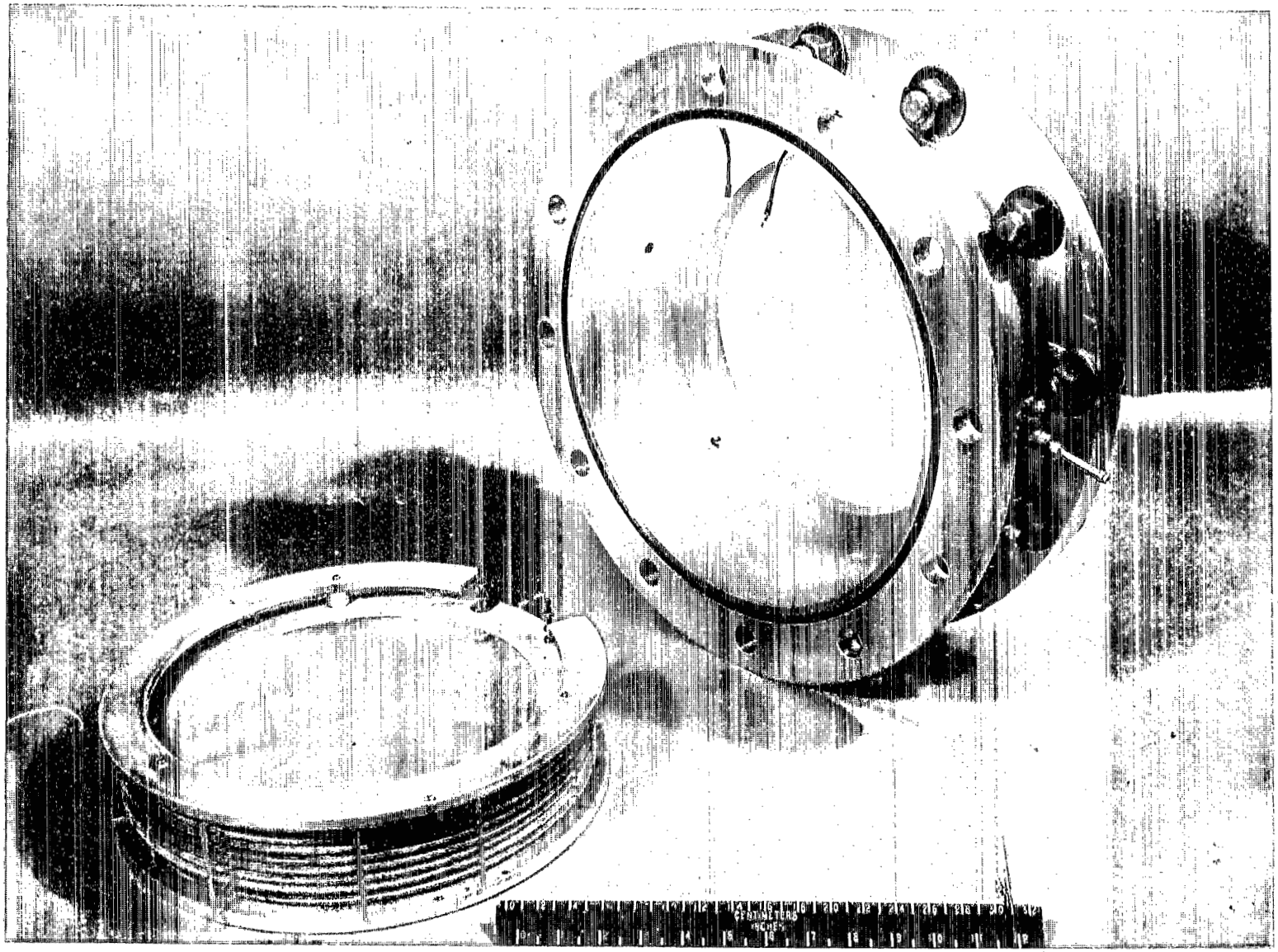

Figure 11.- Large-area, parallel-plate, ionization chamber showing removable, cartridge-type, plate assembly. L-67-4462

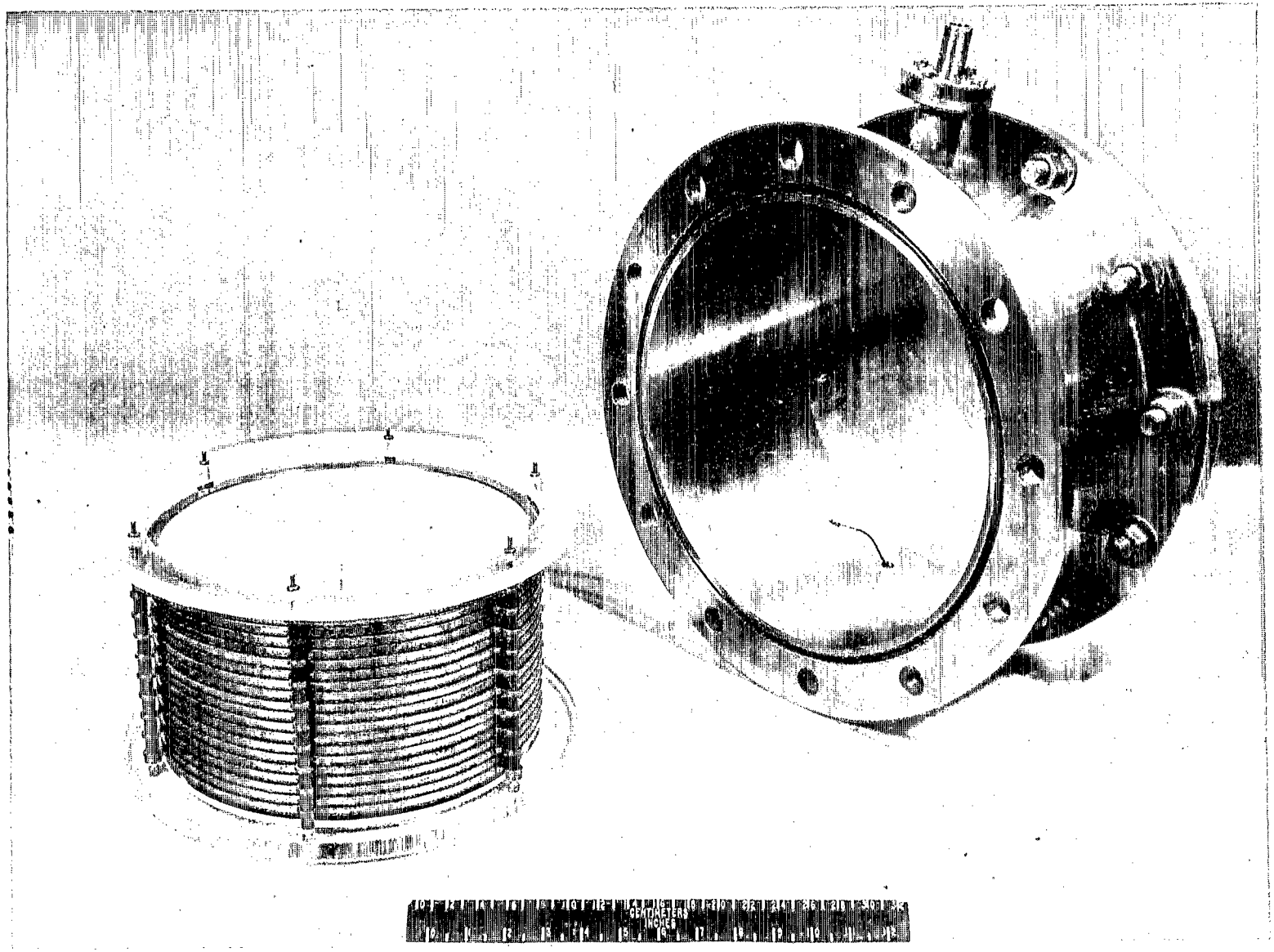

Figure 12.- Large-area, parallel-plate, secondary emission chamber showing removable, cartridge-type, plate assembly. L-67-4464

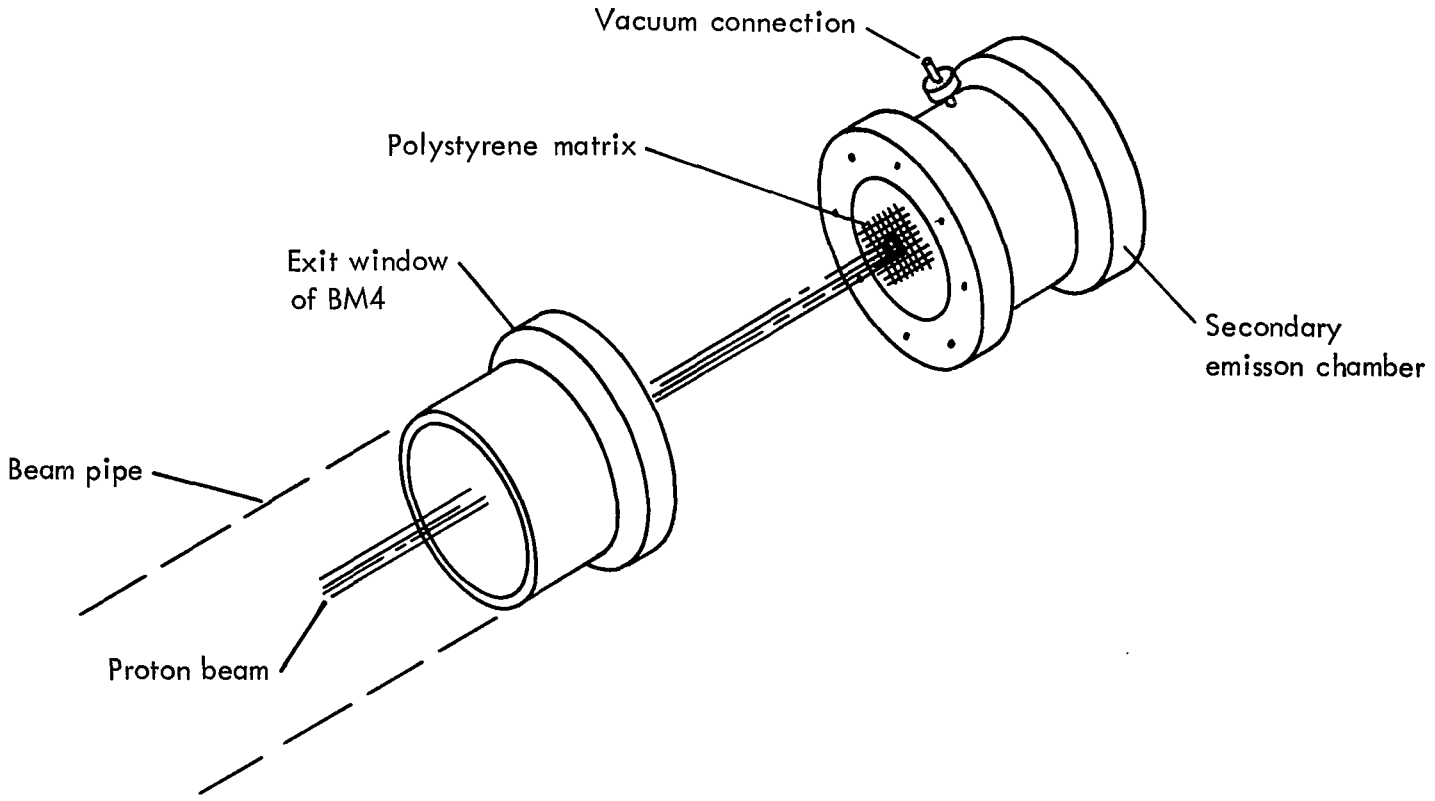

Figure 13.- Schematic diagram illustrating method used to monitor small-area beams while polystyrene disk is being irradiated.

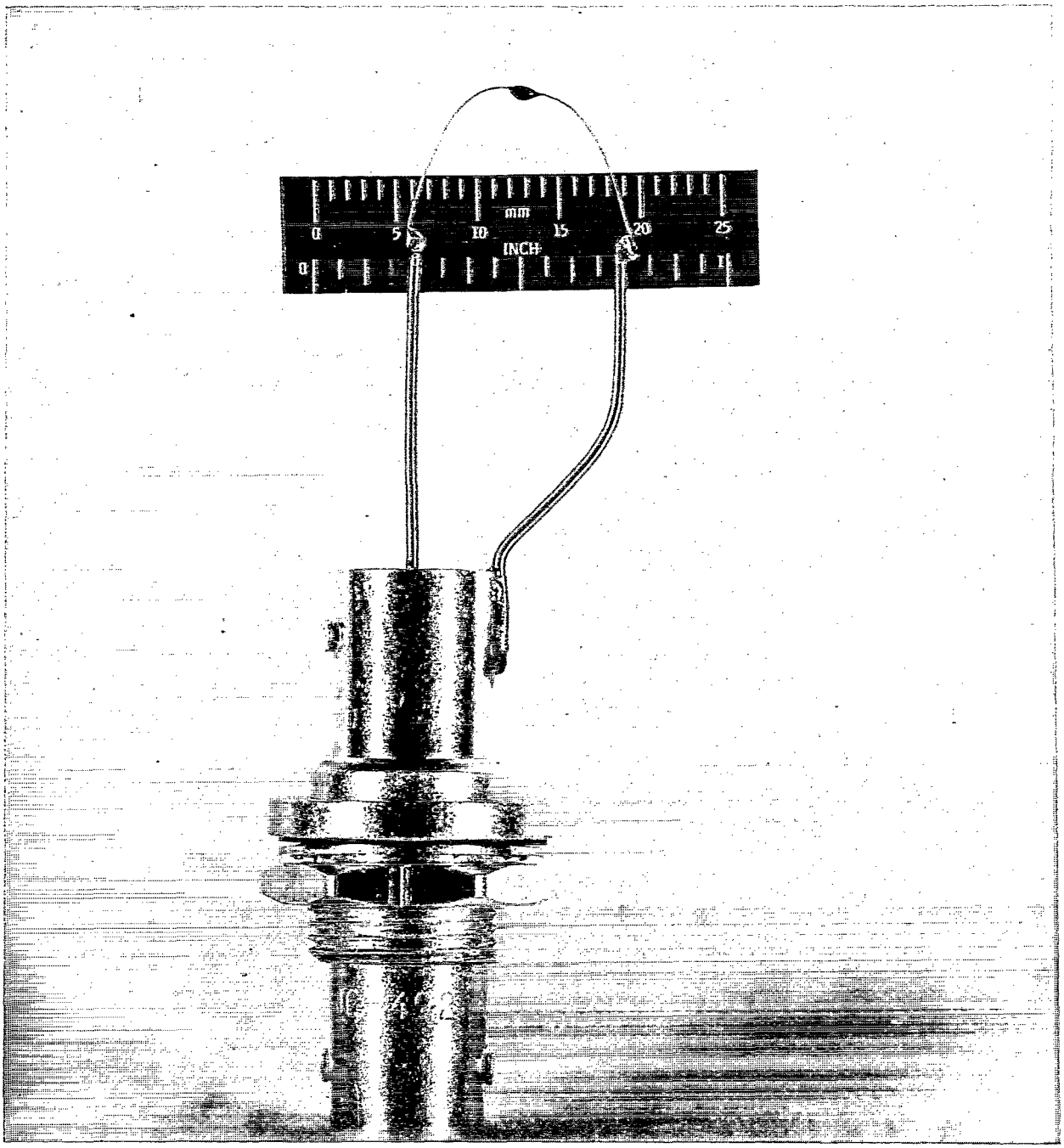

L-67-1781

Figure 14.- Solid-state ionization chamber (diode) mounted on a BNC connector used in determining relative spatial intensity profile of several small-area, high-intensity beams.

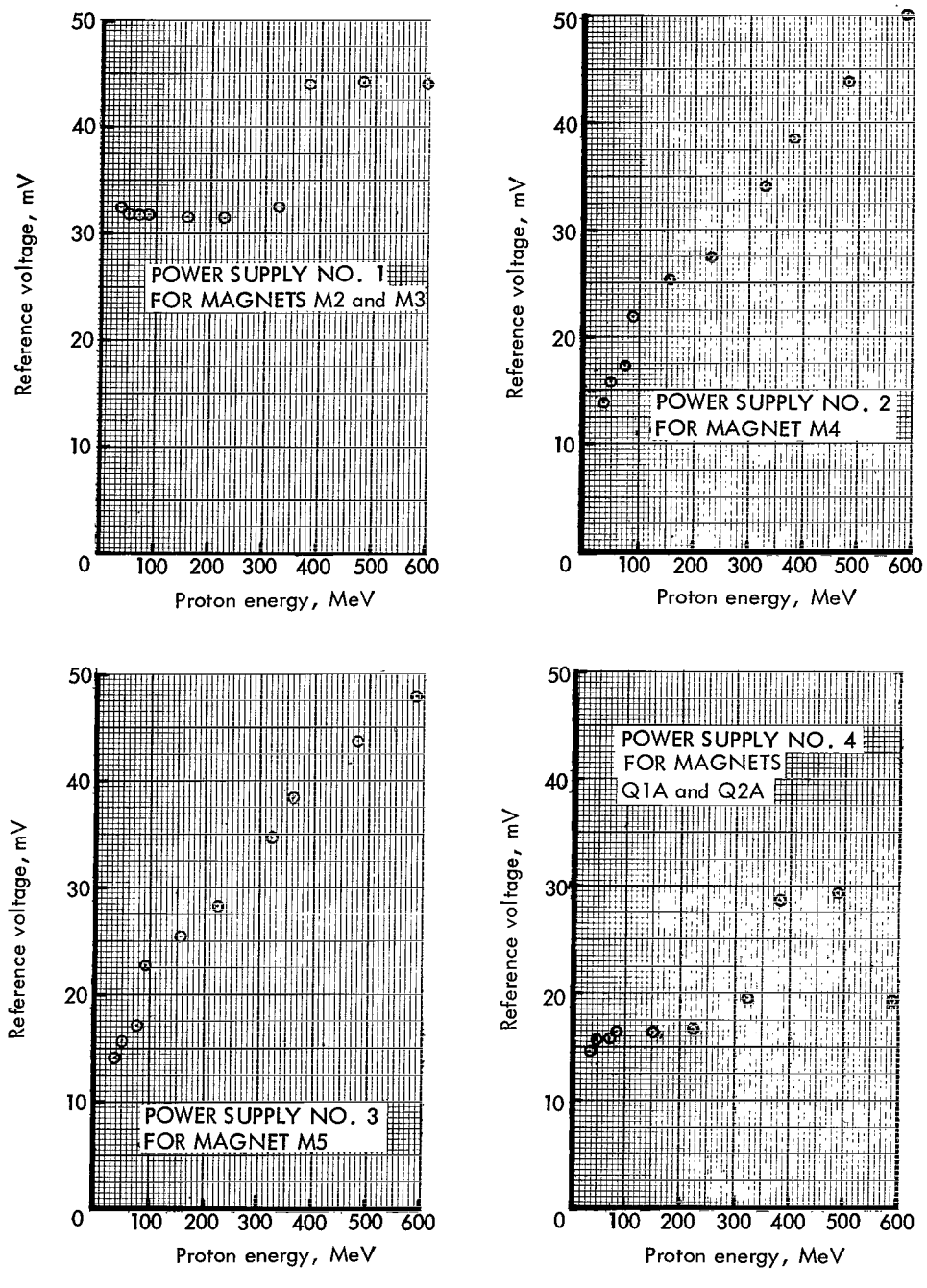

Figure 15.- Magnet settings as a function of proton energy.

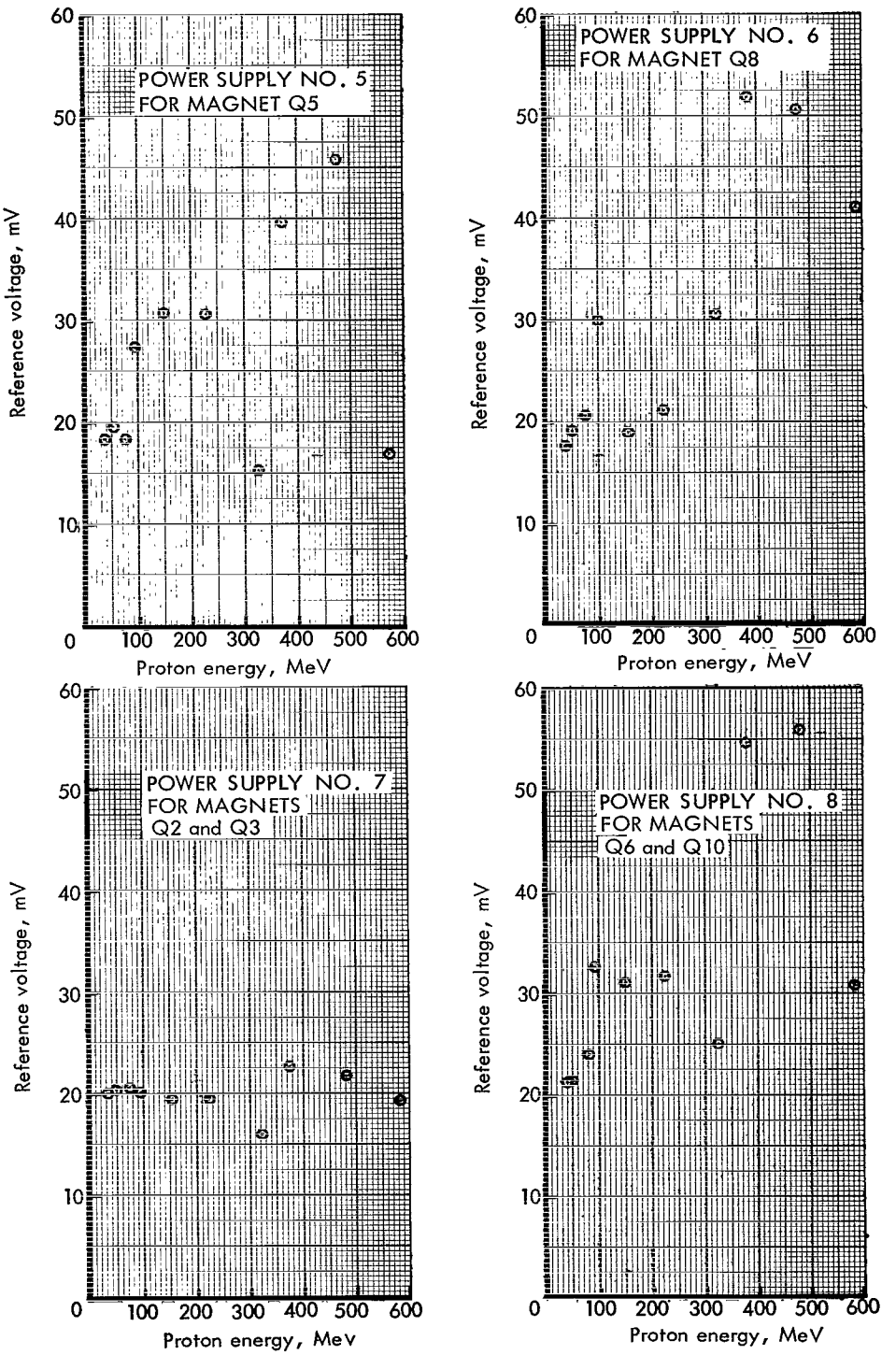

Figure 15.- Continued.

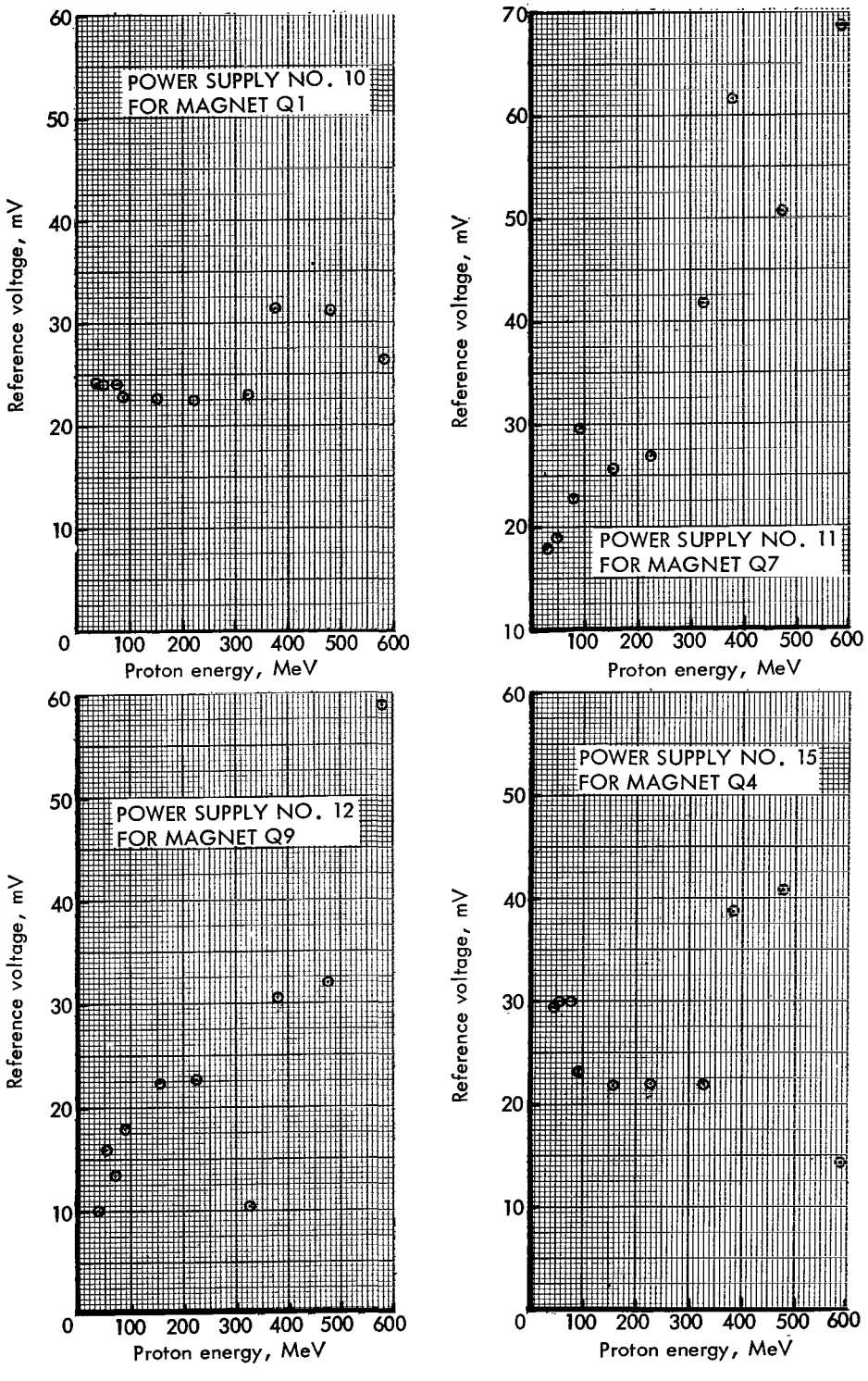

Figure 15.- Continued.

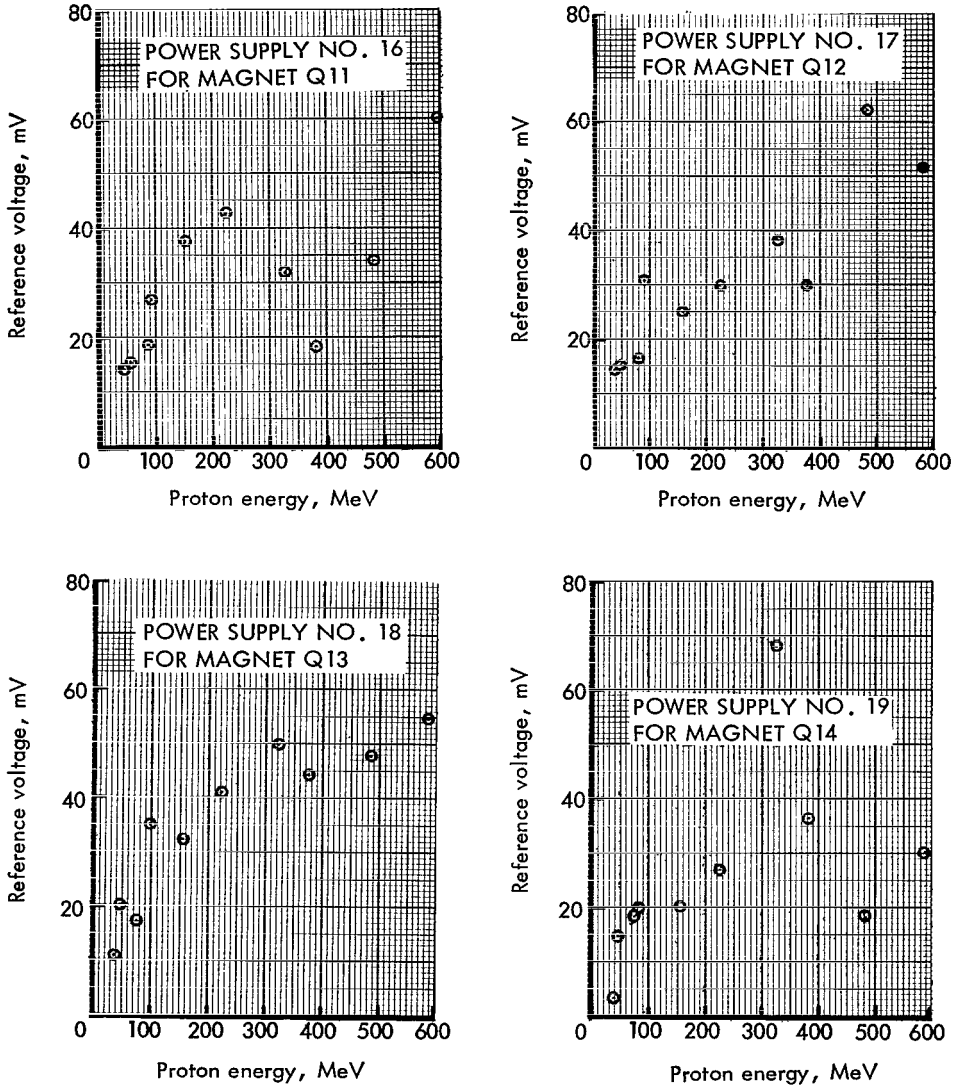

Figure 15.- Continued.

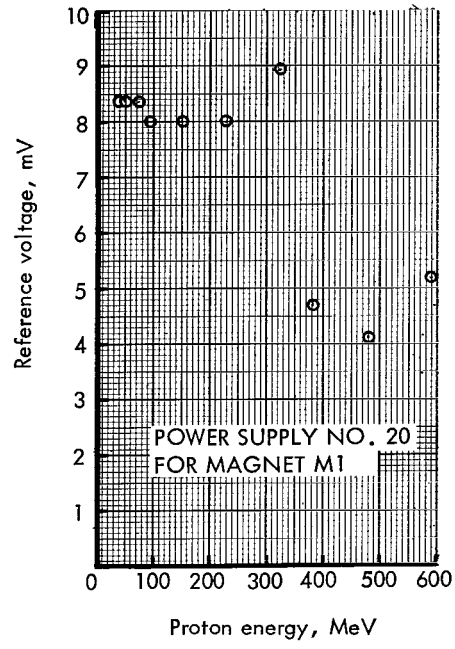

Figure 15.- Concluded.

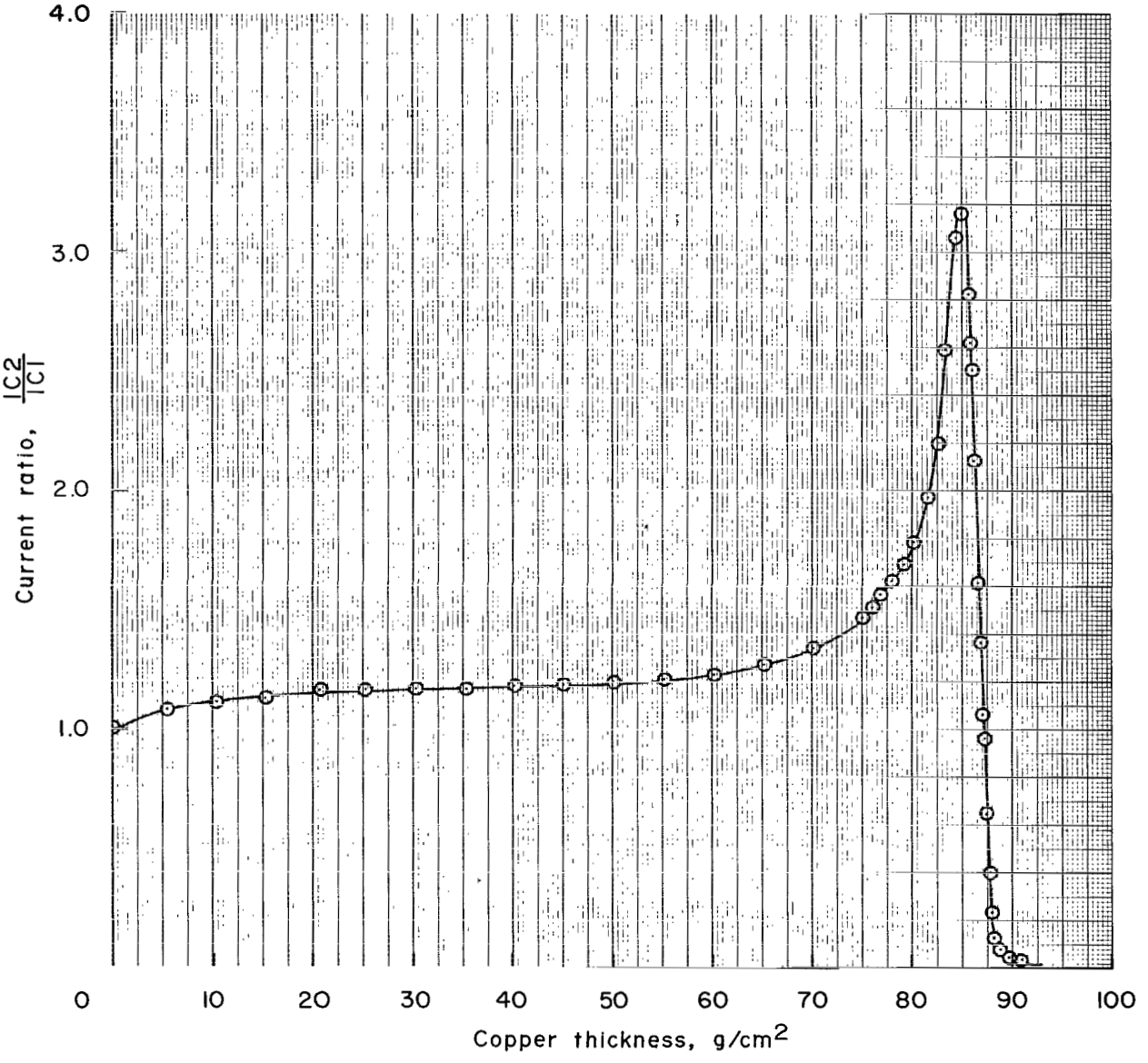

Figure 16.- Range-energy curve for 325-MeV proton beam in copper taken at Ω_1 = 2.59 steradians.

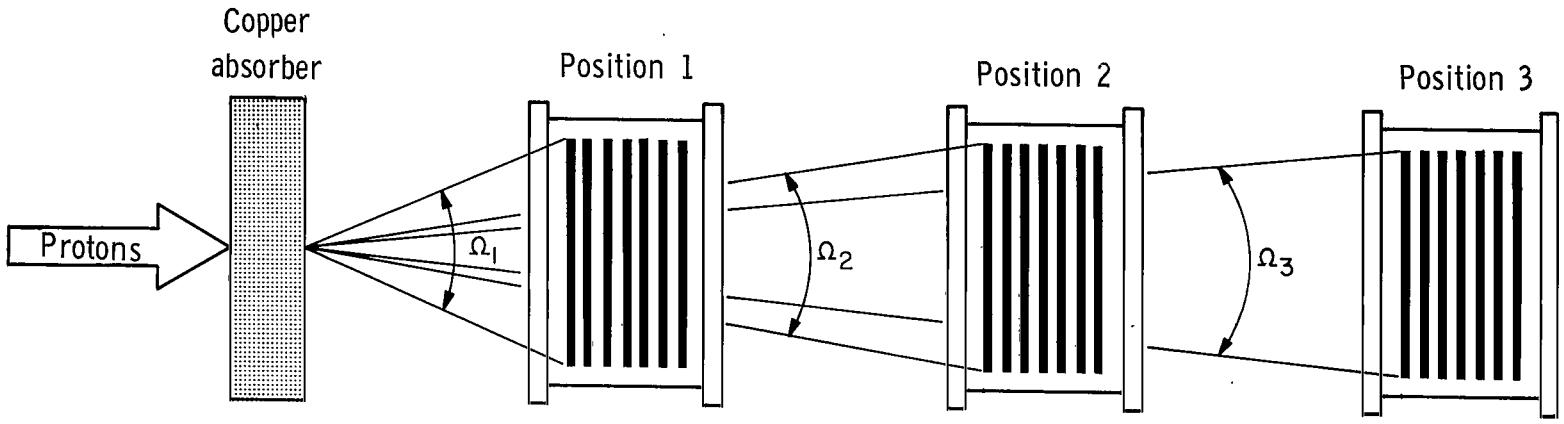

Figure 17.- Diagram showing positions of ionization chamber 2 for Coulomb scattering correction experiment.

0.00021	0.00033	0.00060	0.00116	0.00202	0.00120	0.00030
0.00028	0.00188	0.01563	0.02982	0.04901	0.01287	0.00098
0.00042	0.00852	0.08810	0.28687	0.33755	0.06375	0.00232
0.00031	0.00233	0.01788	0.02934	0.03213	0.00873	0.00070
0.00023	0.00033	0.00066	0.00100	0.00135	0.00079	0.00027

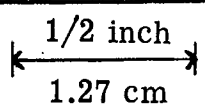

Figure 18.- Diagram showing polystyrene target matrix array used for intensity measurements.

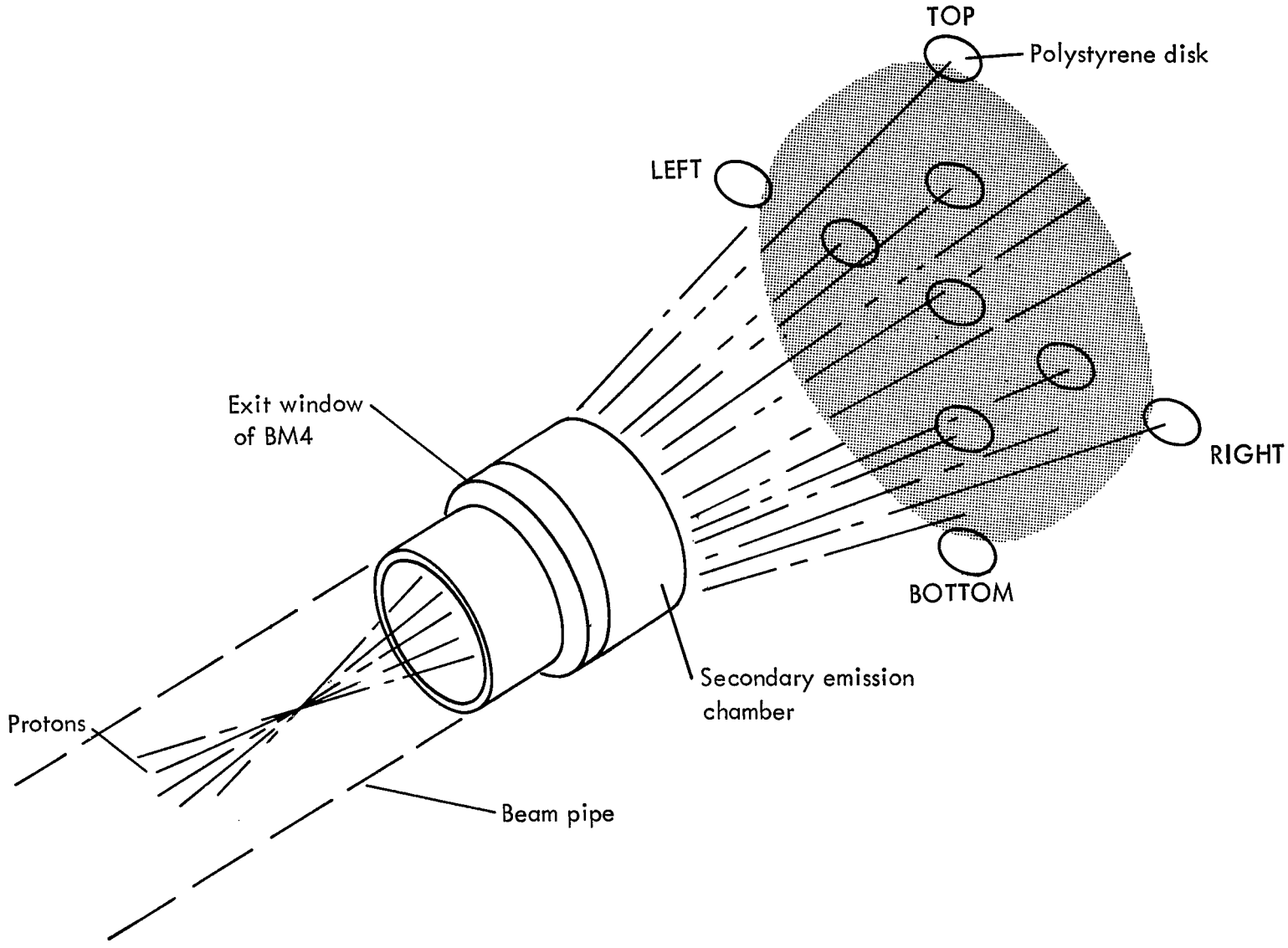

Figure 19.- Diagram showing experimental setup for determining relative intensity profiles for large-area proton beams.

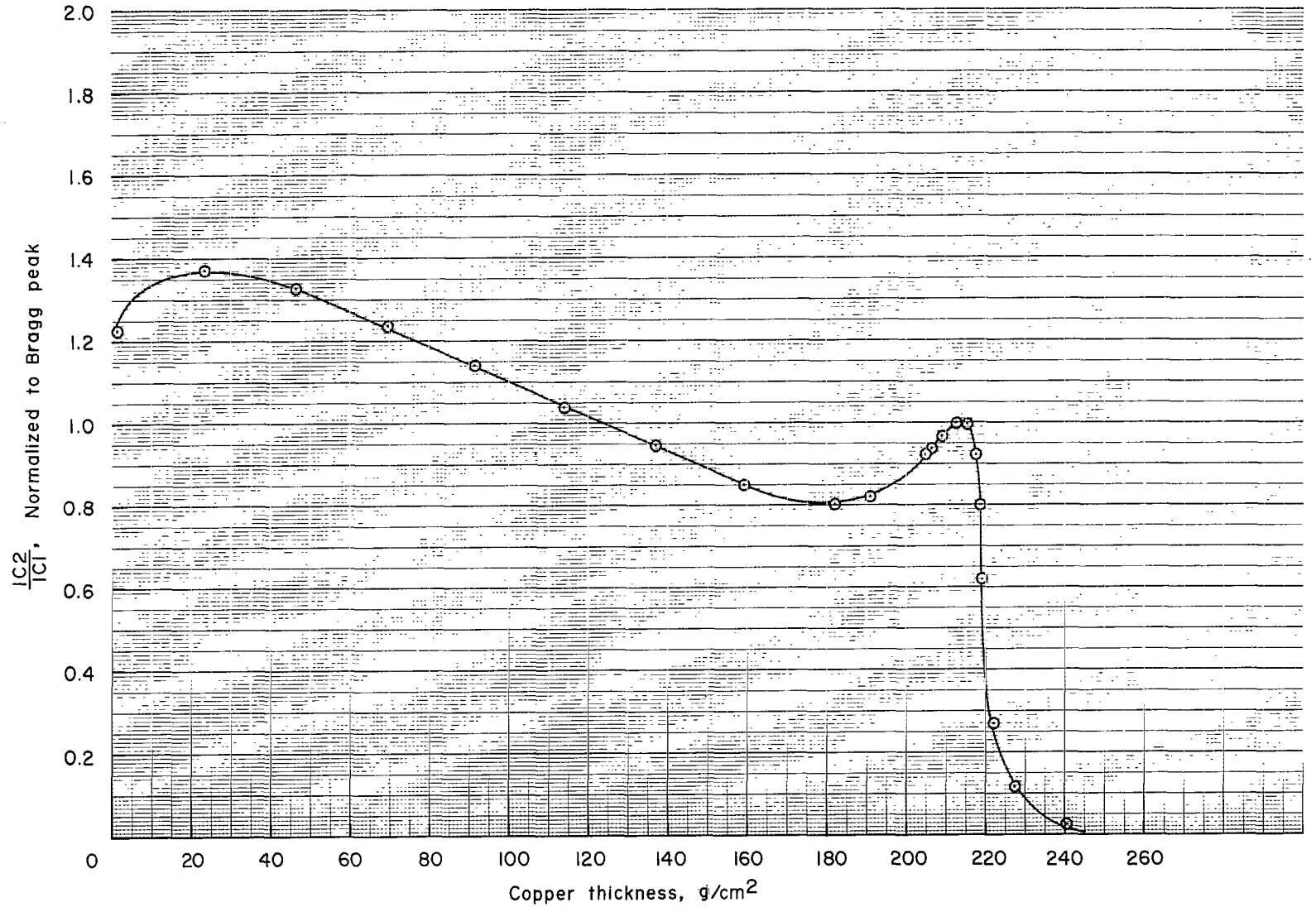

Figure 20.- Range-energy curve normalized to unity at Bragg peak for 595-MeV beam taken at Ω_1 = 2.59 steradians.

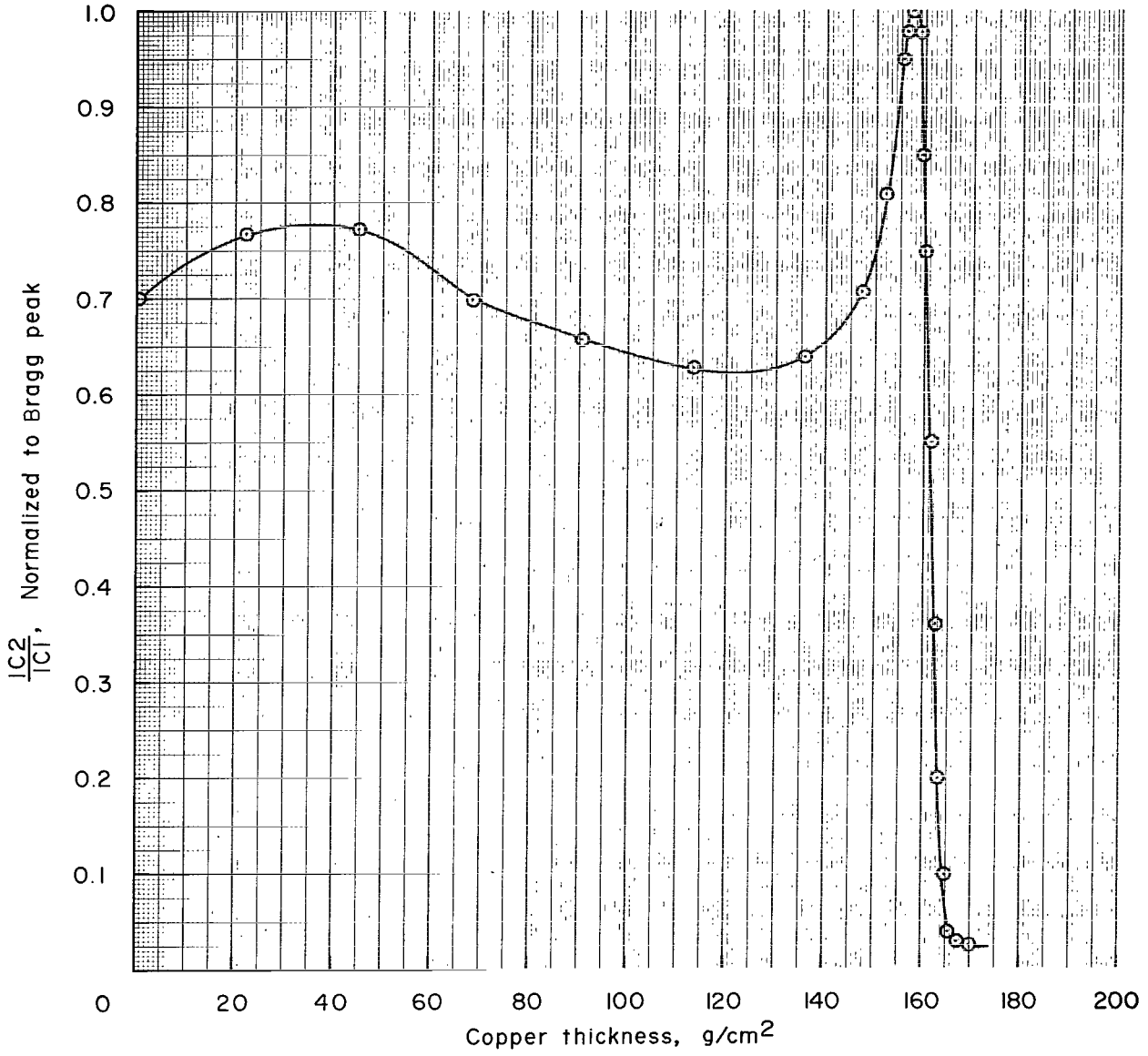

Figure 21.- Range-energy curve normalized to unity at Bragg peak for 480-MeV beam taken at $\Omega_1 = 2.59$ steradians.

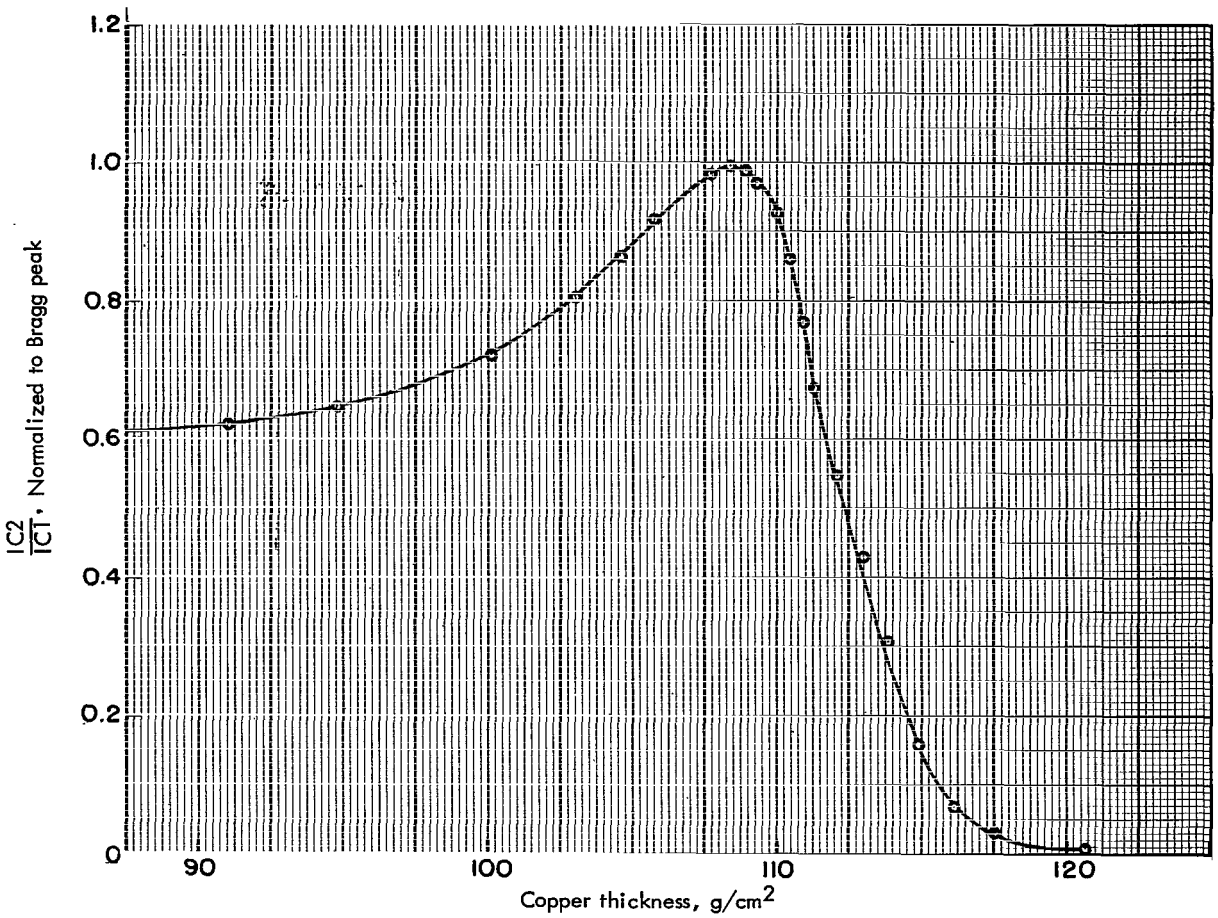

Figure 22.- Range-energy curve normalized to unity at Bragg peak for 380-MeV beam taken at Ω_1 = 2.59 steradians.

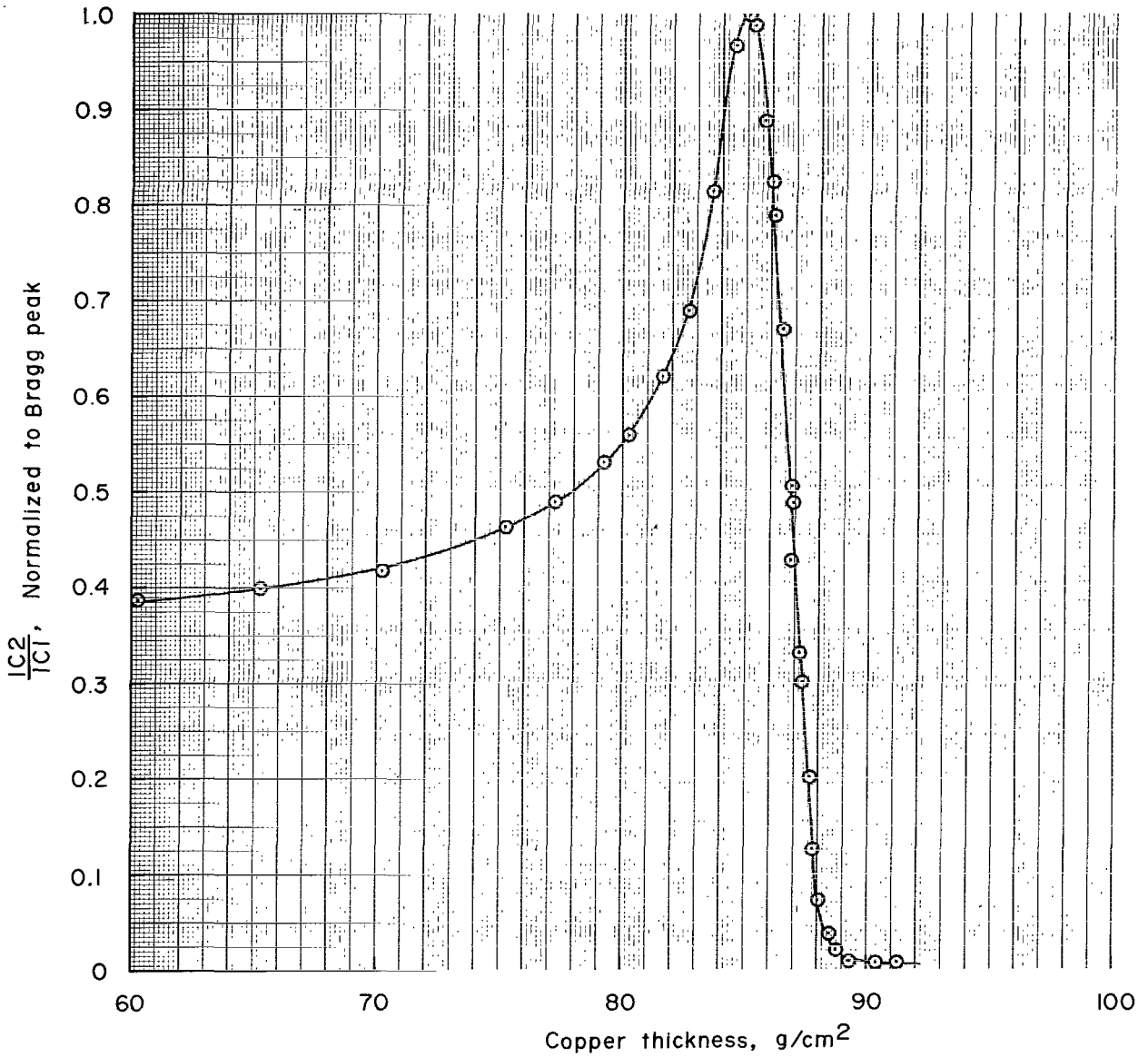

Figure 23.- Range-energy curve normalized to unity at Bragg peak for 325-MeV beam taken at Ω_1 = 2.59 steradians.

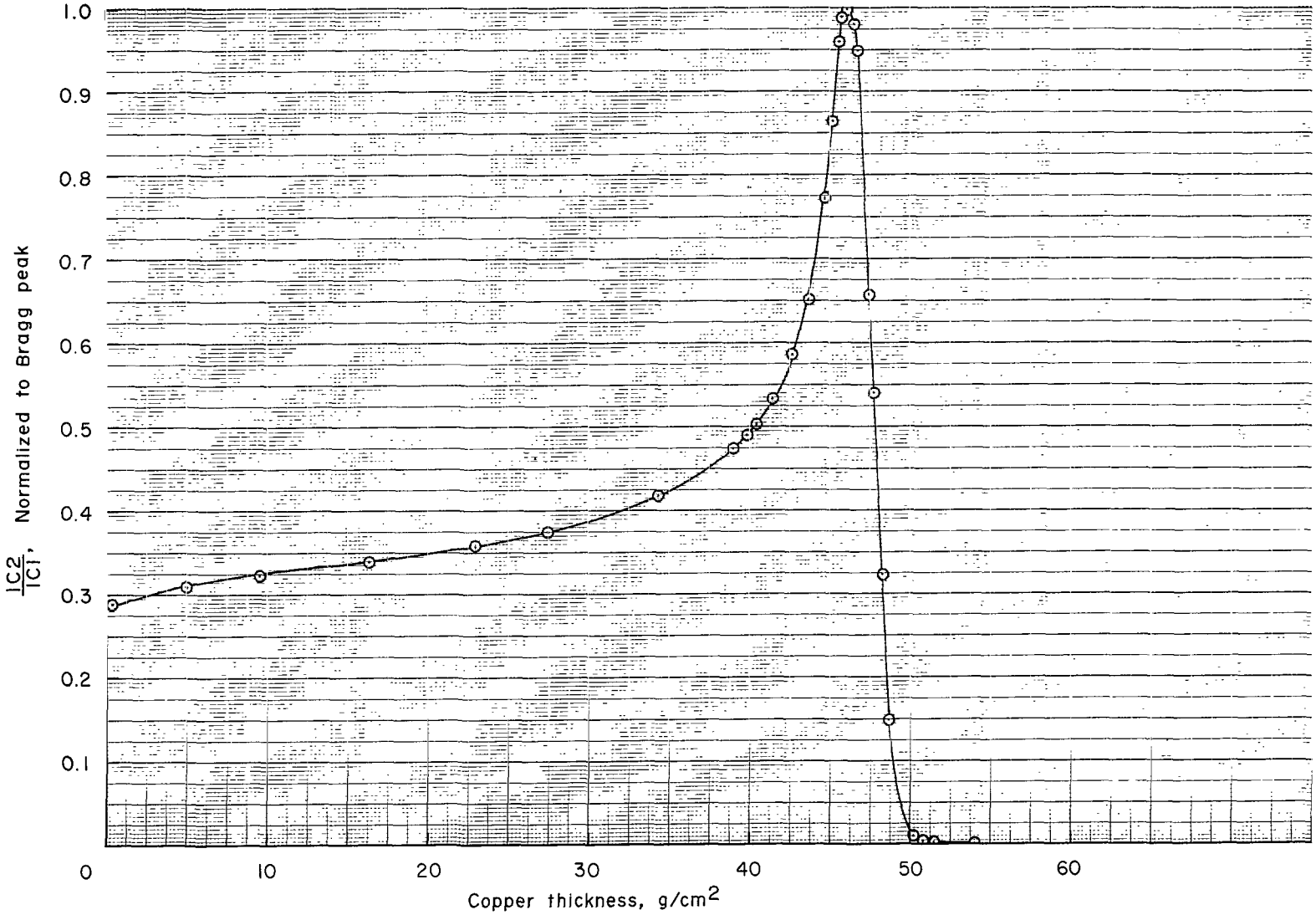

Figure 24.- Range-energy curve normalized to unity at Bragg peak for 225-MeV beam taken at Ω_1 = 2.59 steradians.

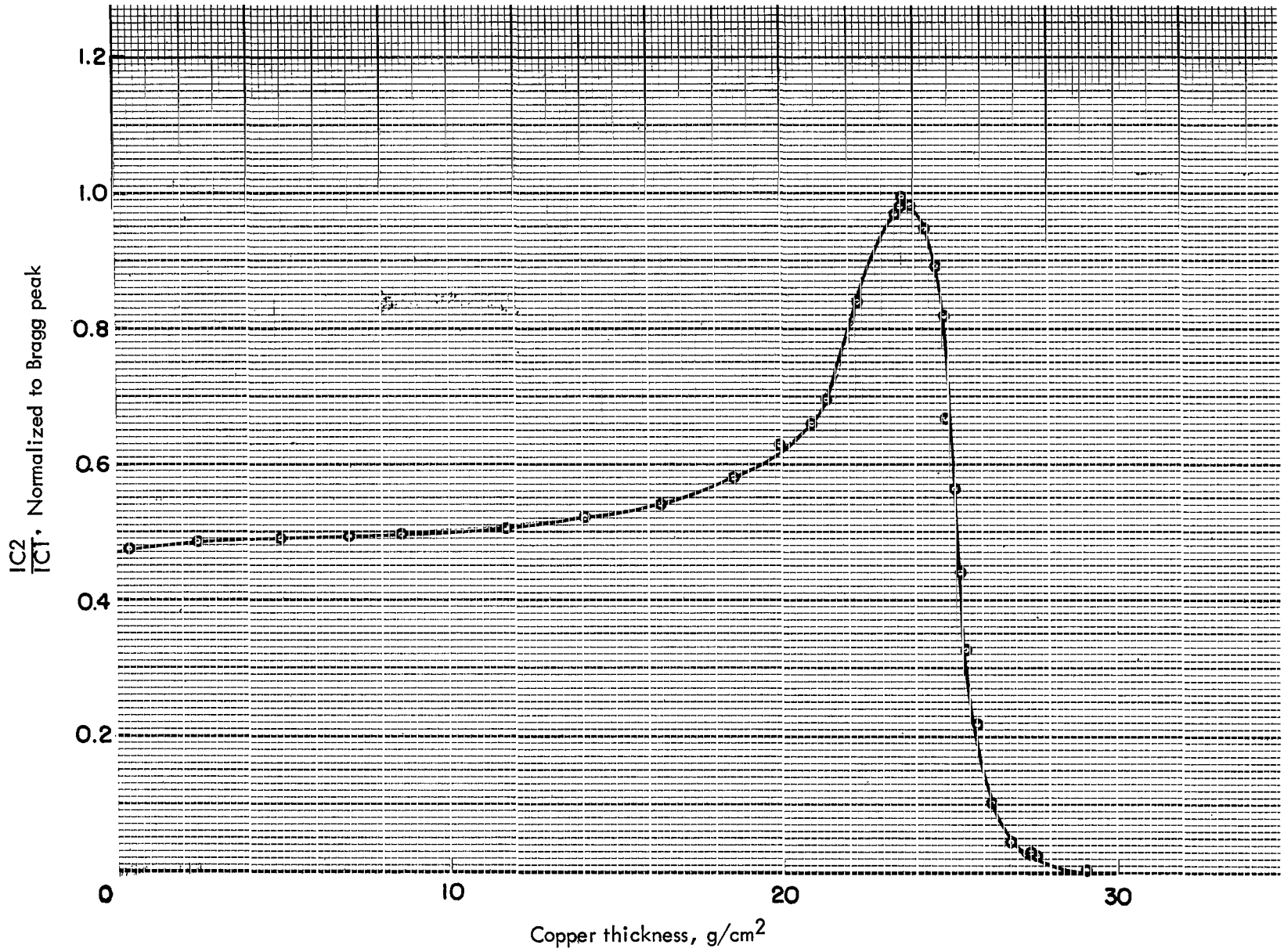

Figure 25.- Range-energy curve normalized to unity at Bragg peak for 155-MeV beam taken at Ω_1 = 2.59 steradians.

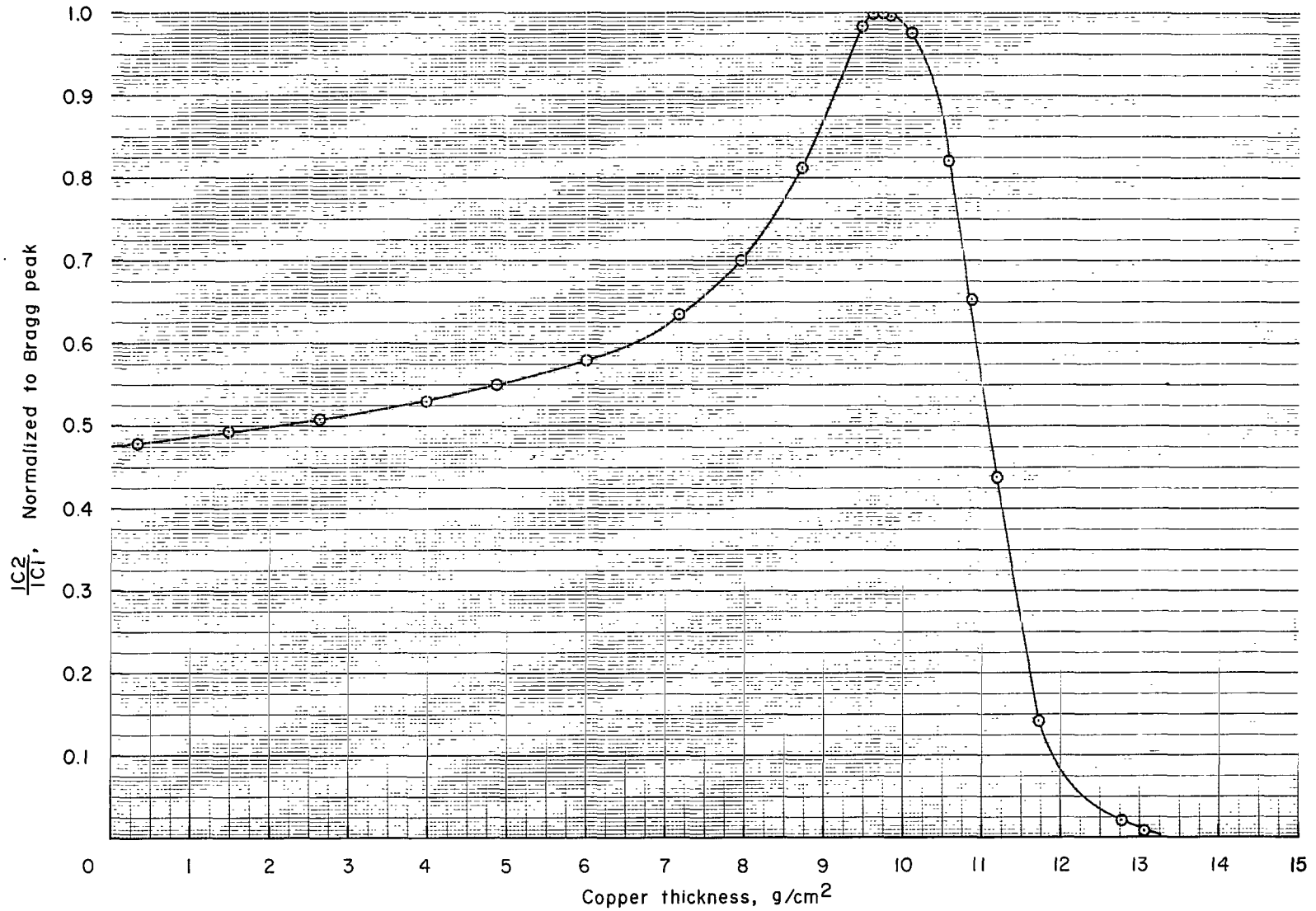

Figure 26.- Range-energy curve normalized to unity at Bragg peak for 95-MeV beam taken at Ω_1 = 2.59 steradians.

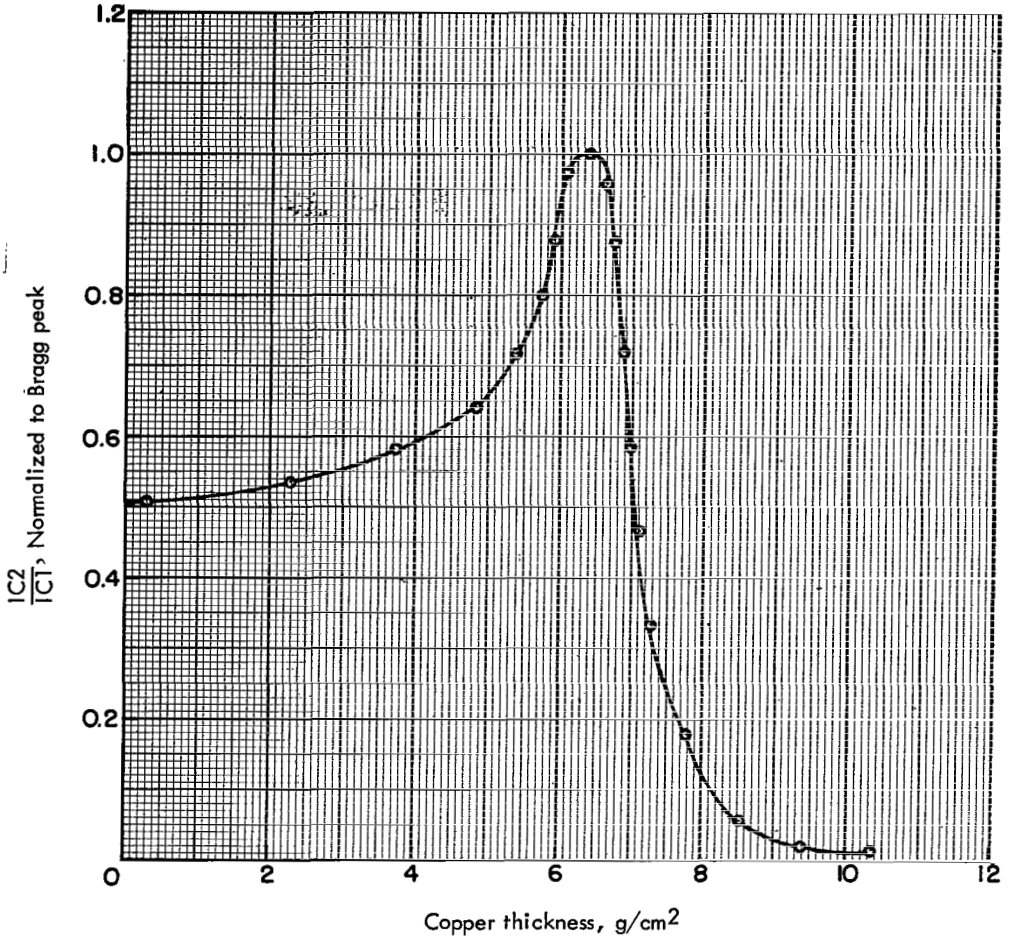

Figure 27.- Range-energy curve normalized to unity at Bragg peak for 75-MeV beam taken at Ω_1 = 2.59 steradians.

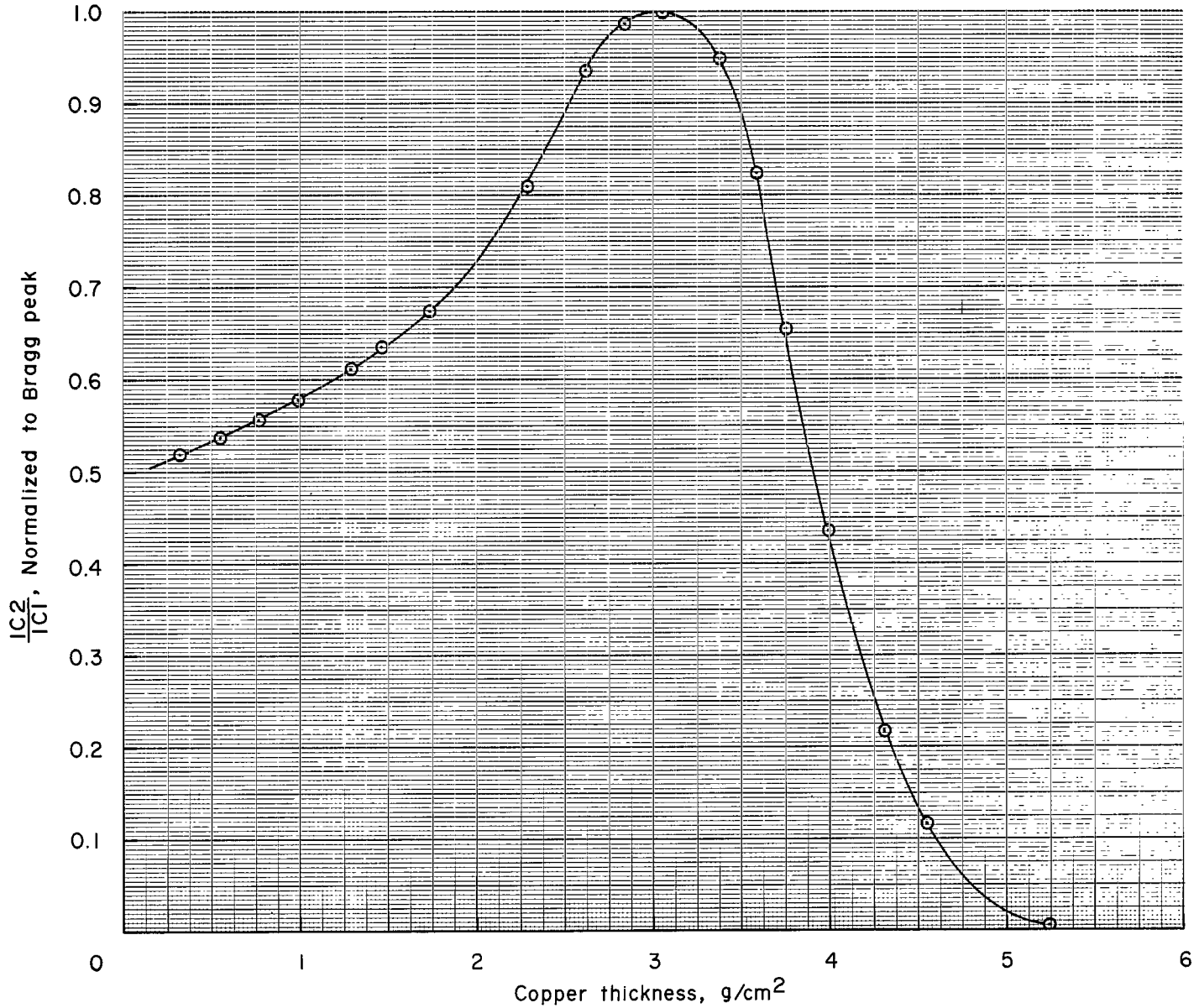

Figure 28.- Range-energy curve normalized to unity at Bragg peak for 50-MeV beam taken at Ω_1 = 2.59 steradians.

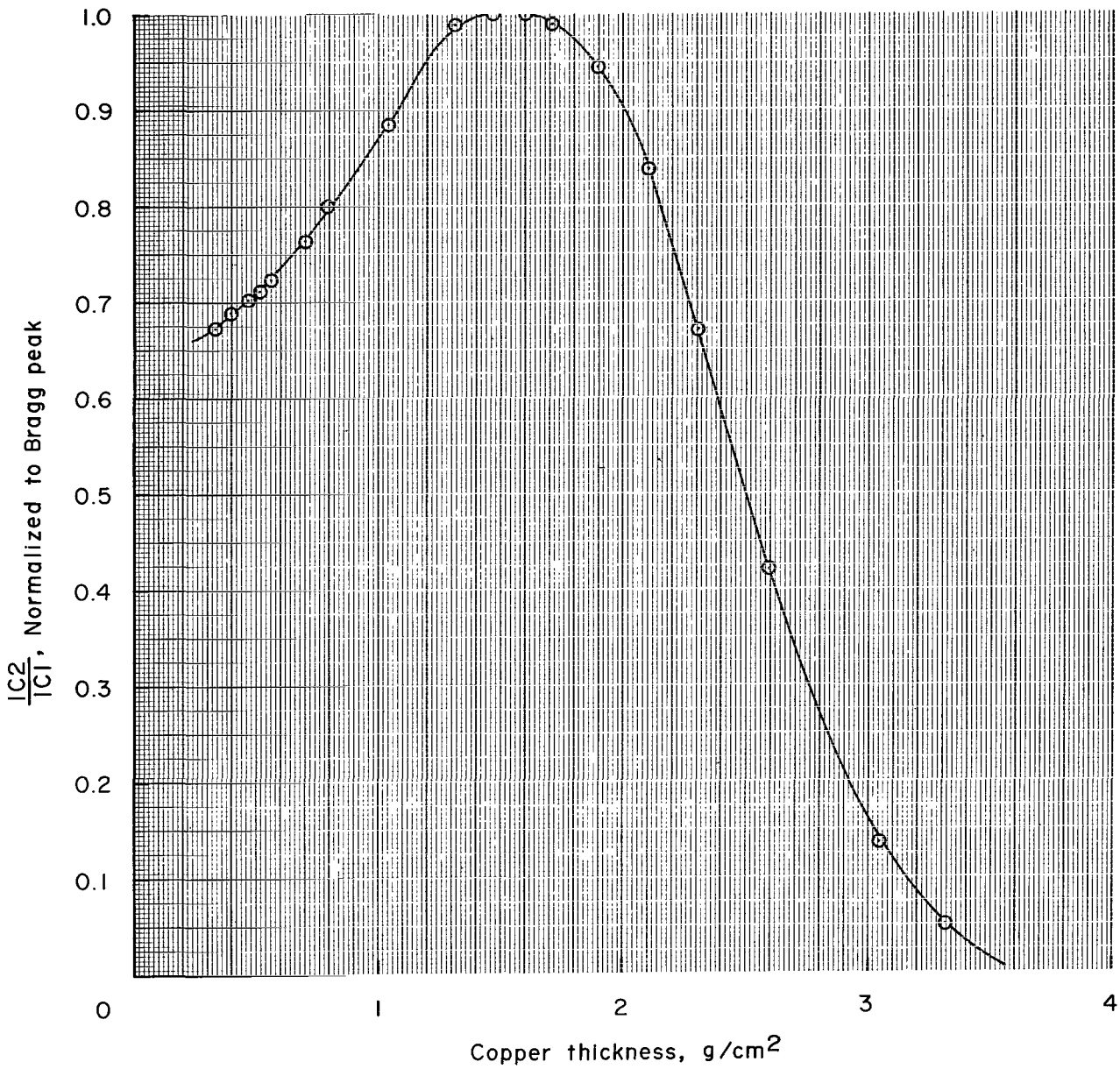

Figure 29.- Range-energy curve normalized to unity at Bragg peak for 40-MeV beam taken at Ω_1 = 2.59 steradians.

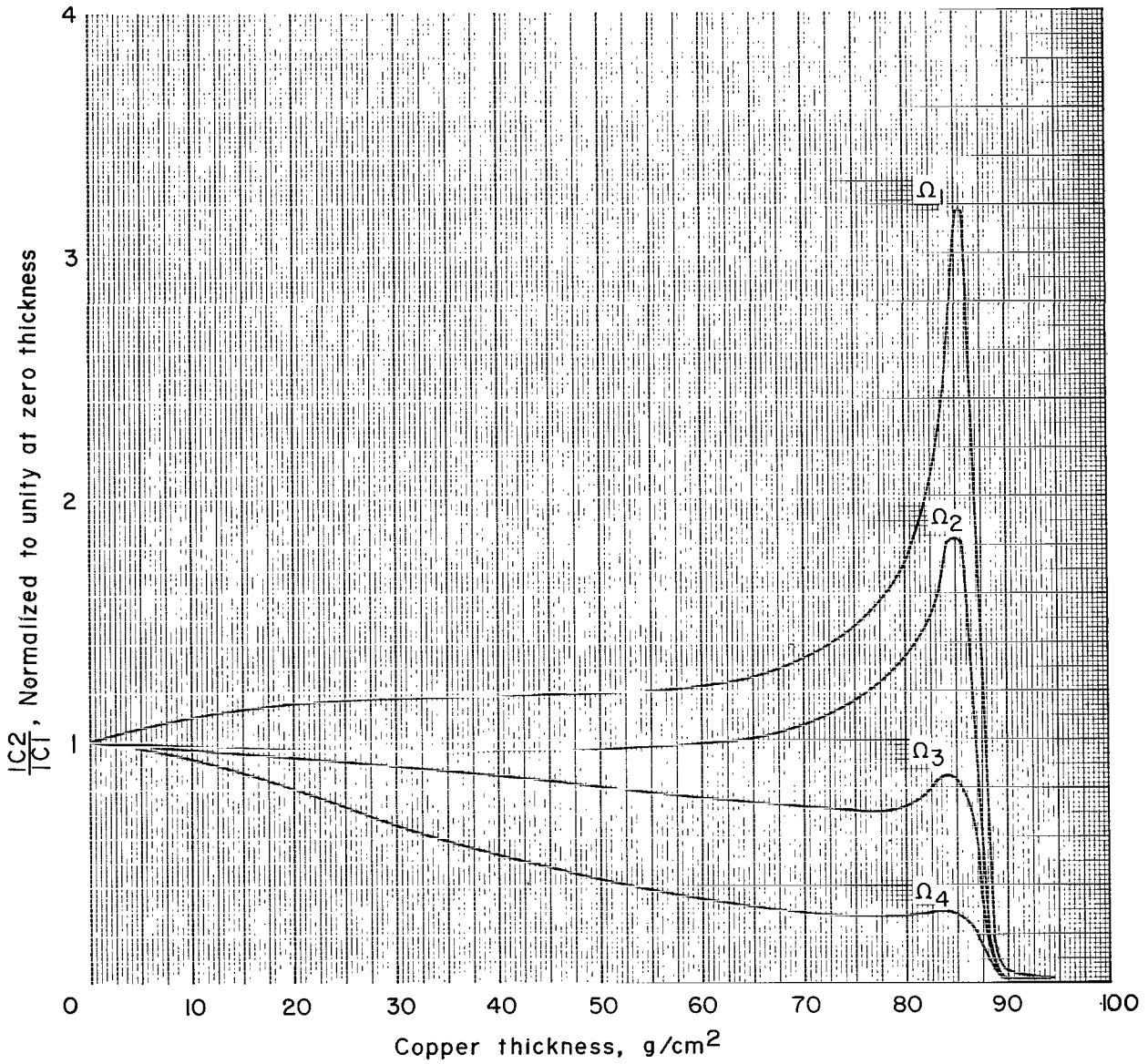

Figure 30.- Range-energy curves taken with ionization chamber 2 at four positions for 325-MeV proton beam.

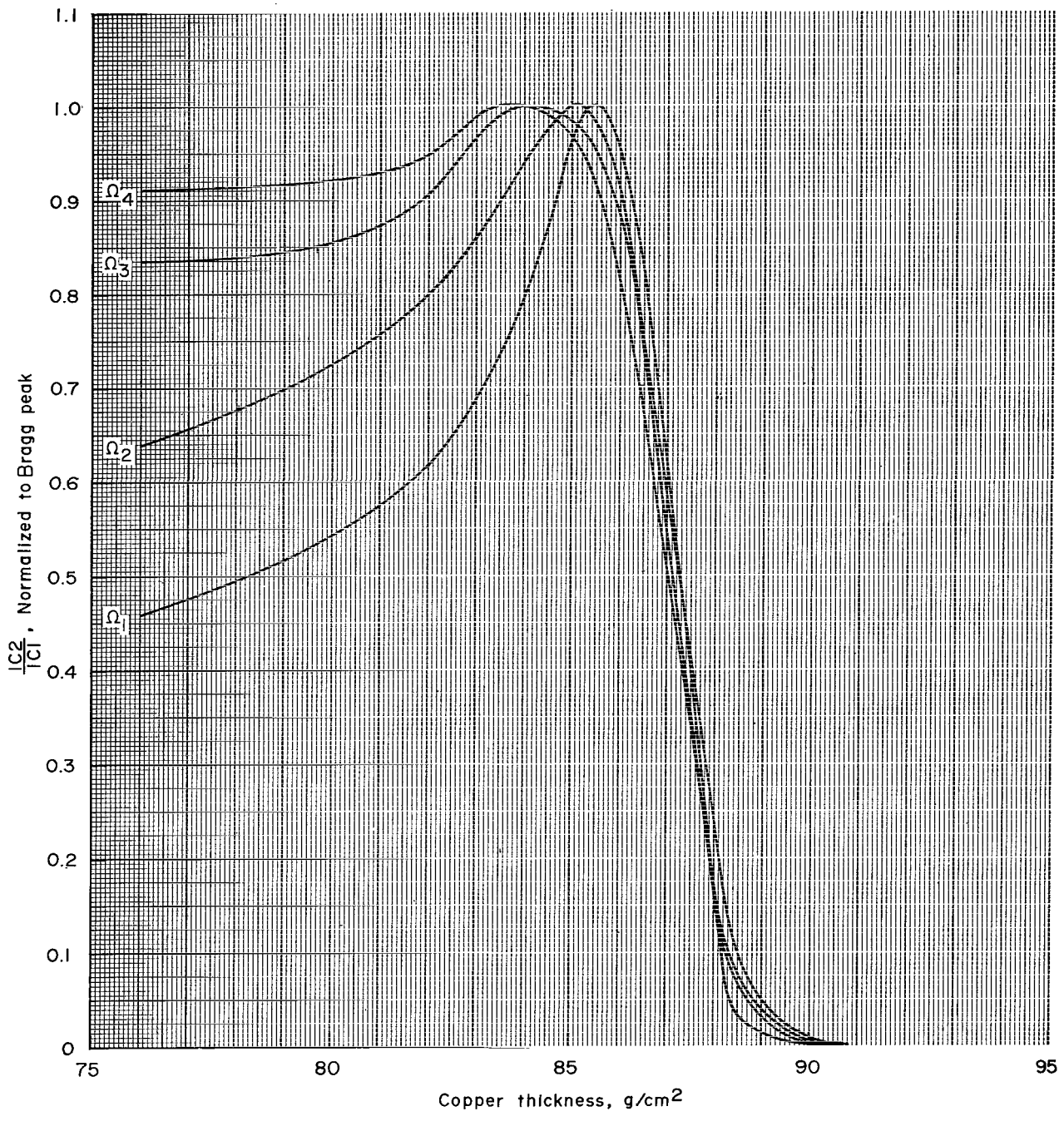

Figure 31.- Range-energy curves taken with ionization chamber 2 at four positions and normalized to unity for 325-MeV proton beam.

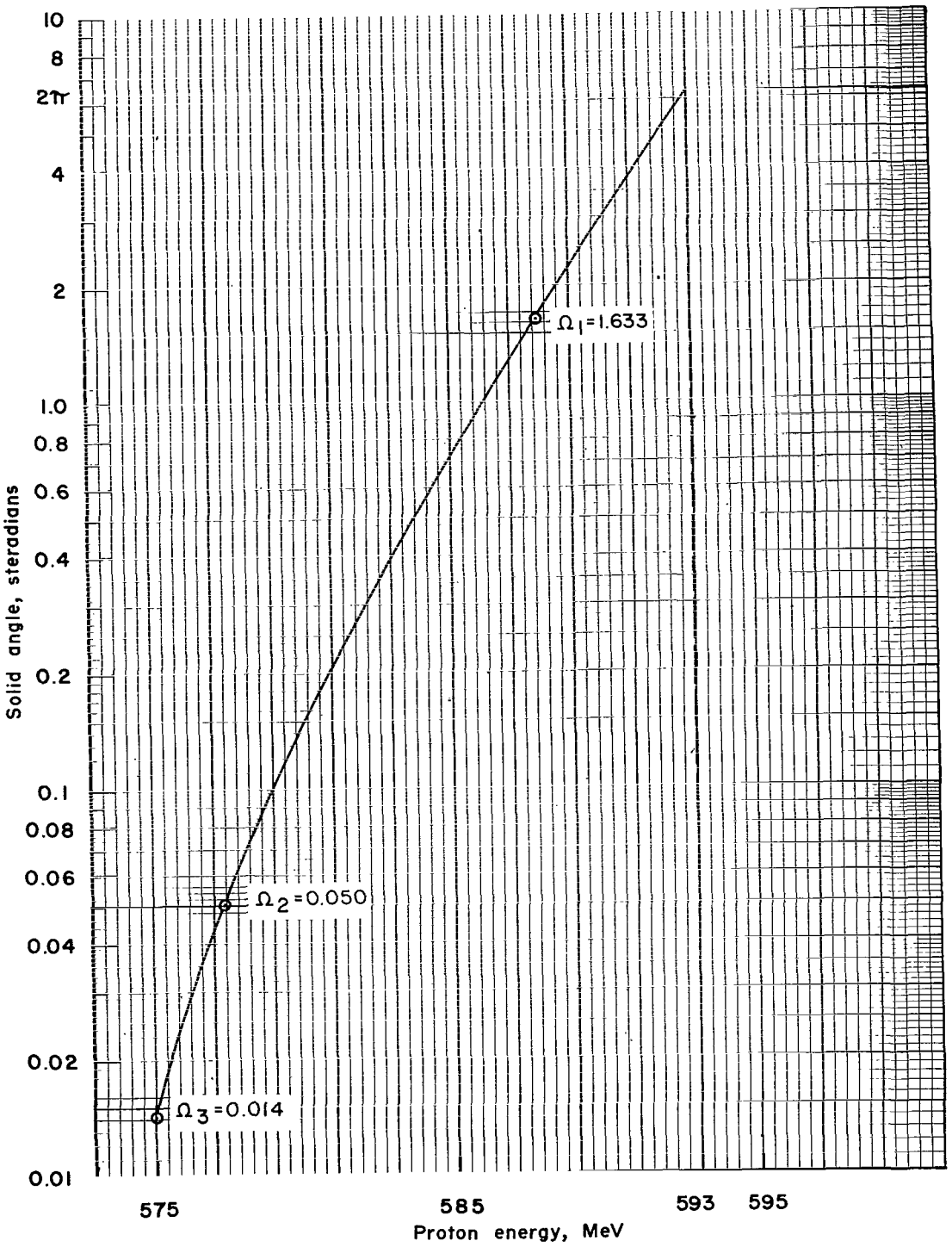

Figure 32.- Coulomb scattering corrections for 595-MeV beam.

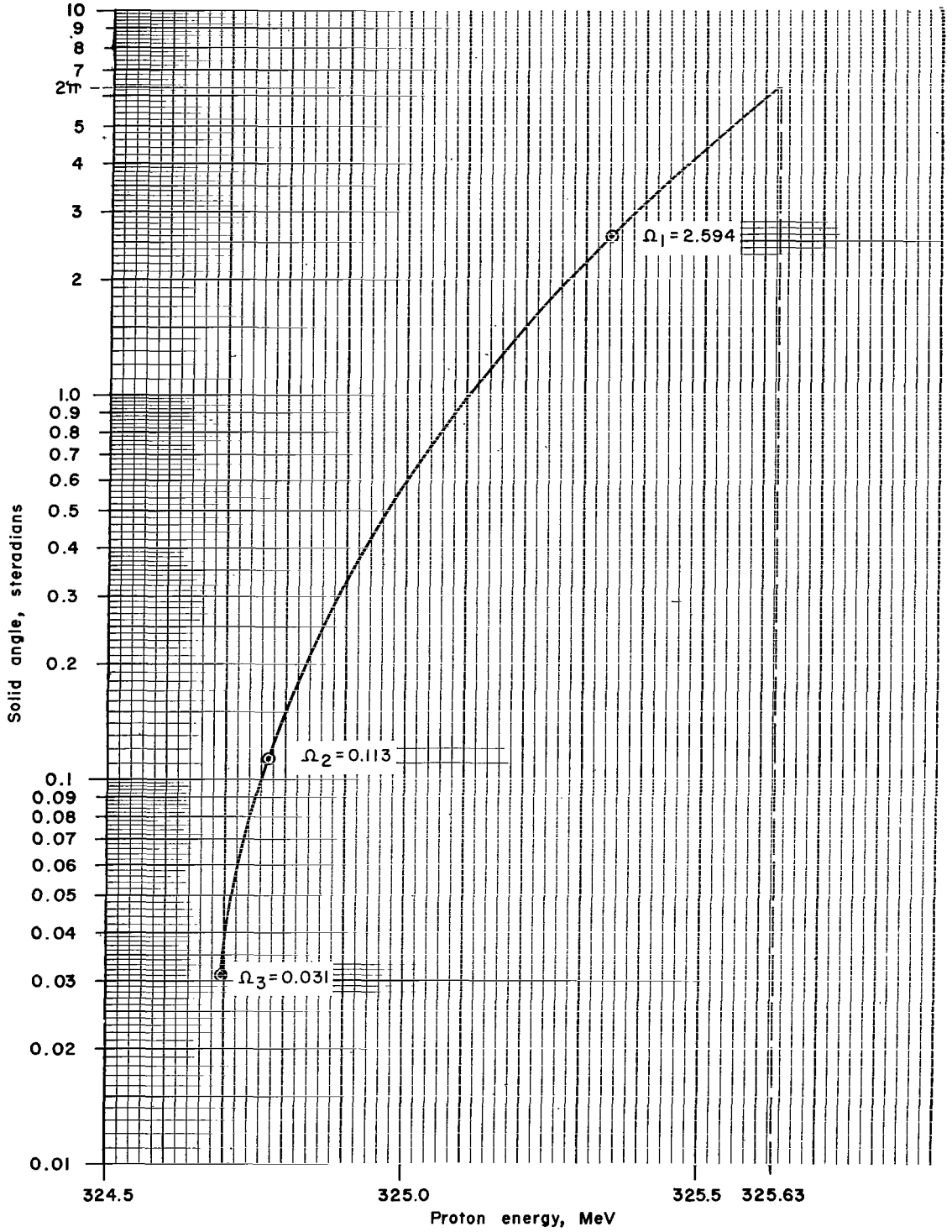

Figure 33.- Coulomb scattering corrections for 325-MeV beam.

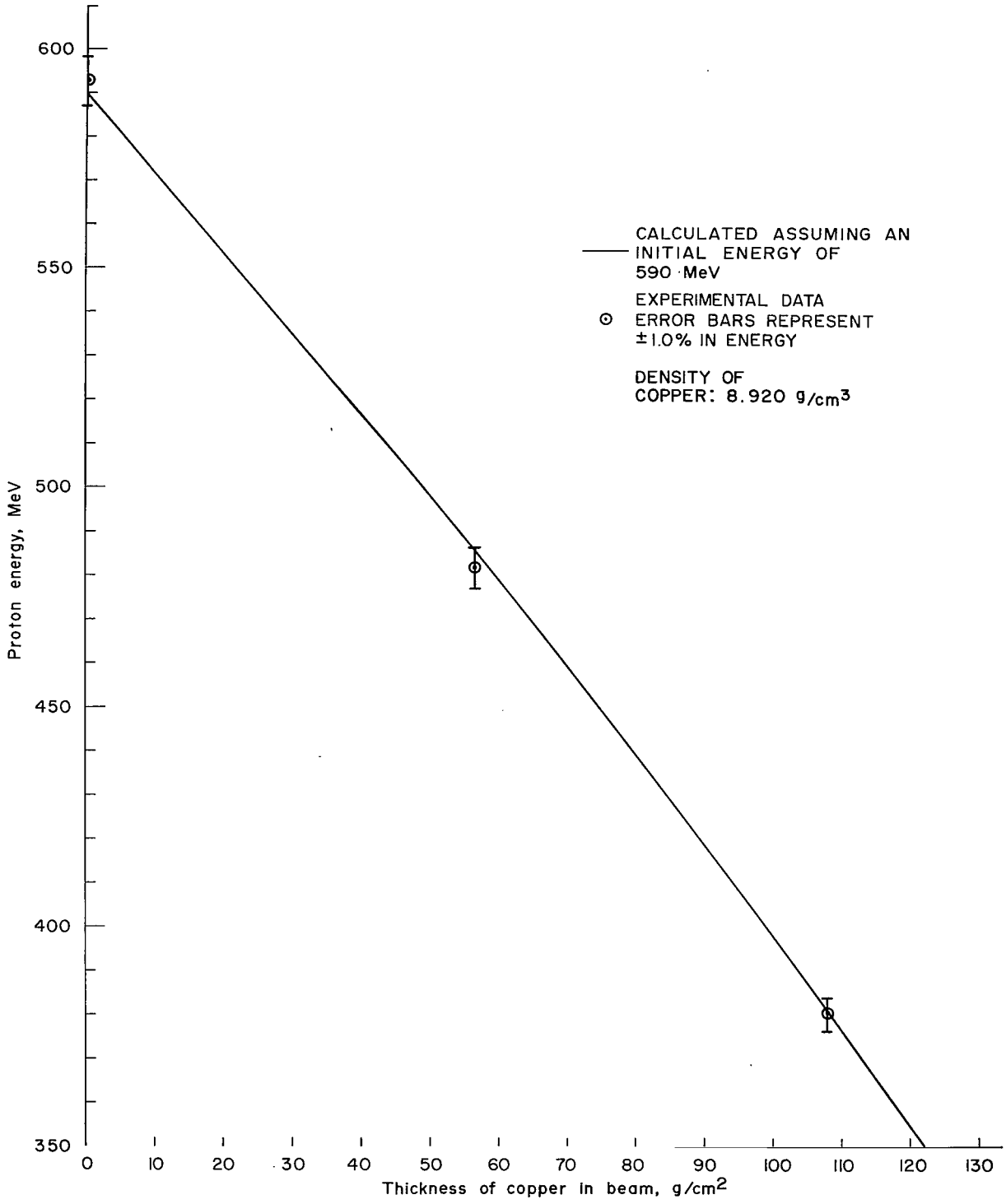

Figure 34.- Comparison of experimental data with calculated values in which an initial beam energy of 590 MeV is assumed.

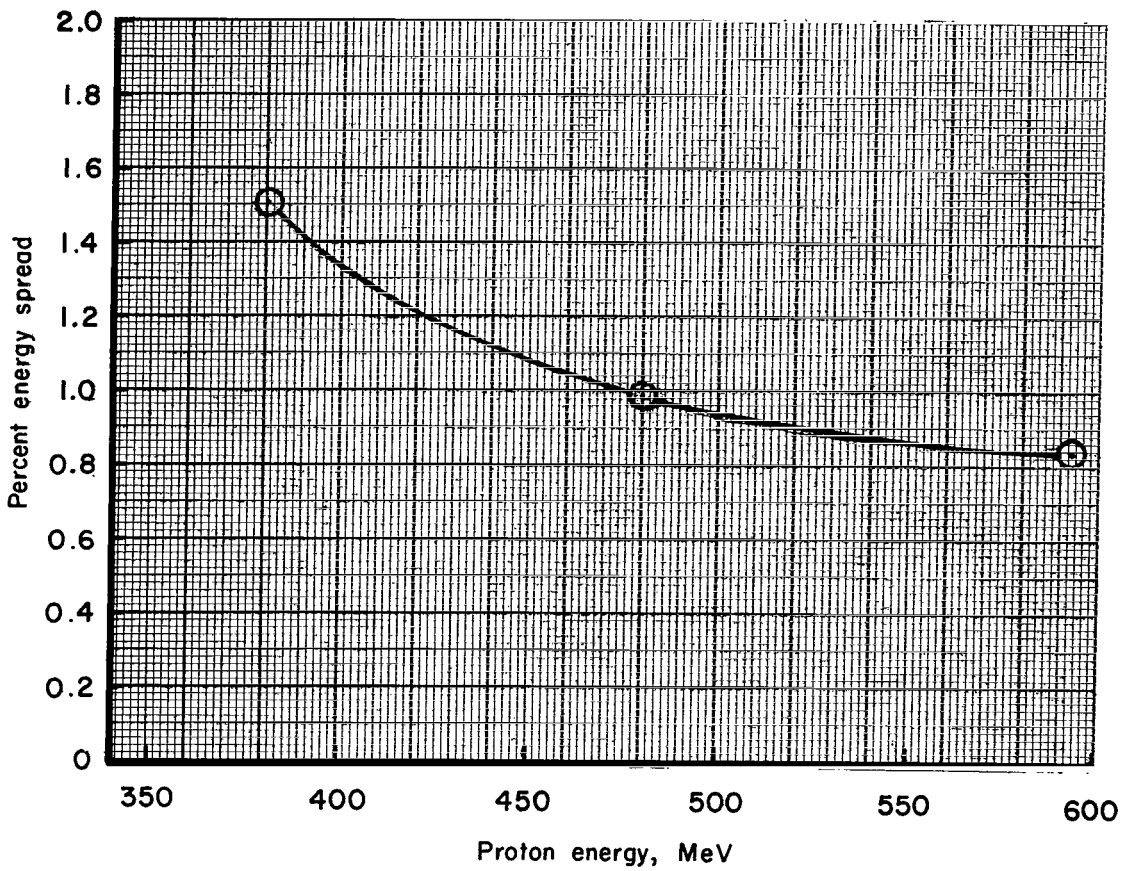

Figure 35.- Percent energy spread as a function of energy for higher energy beams.

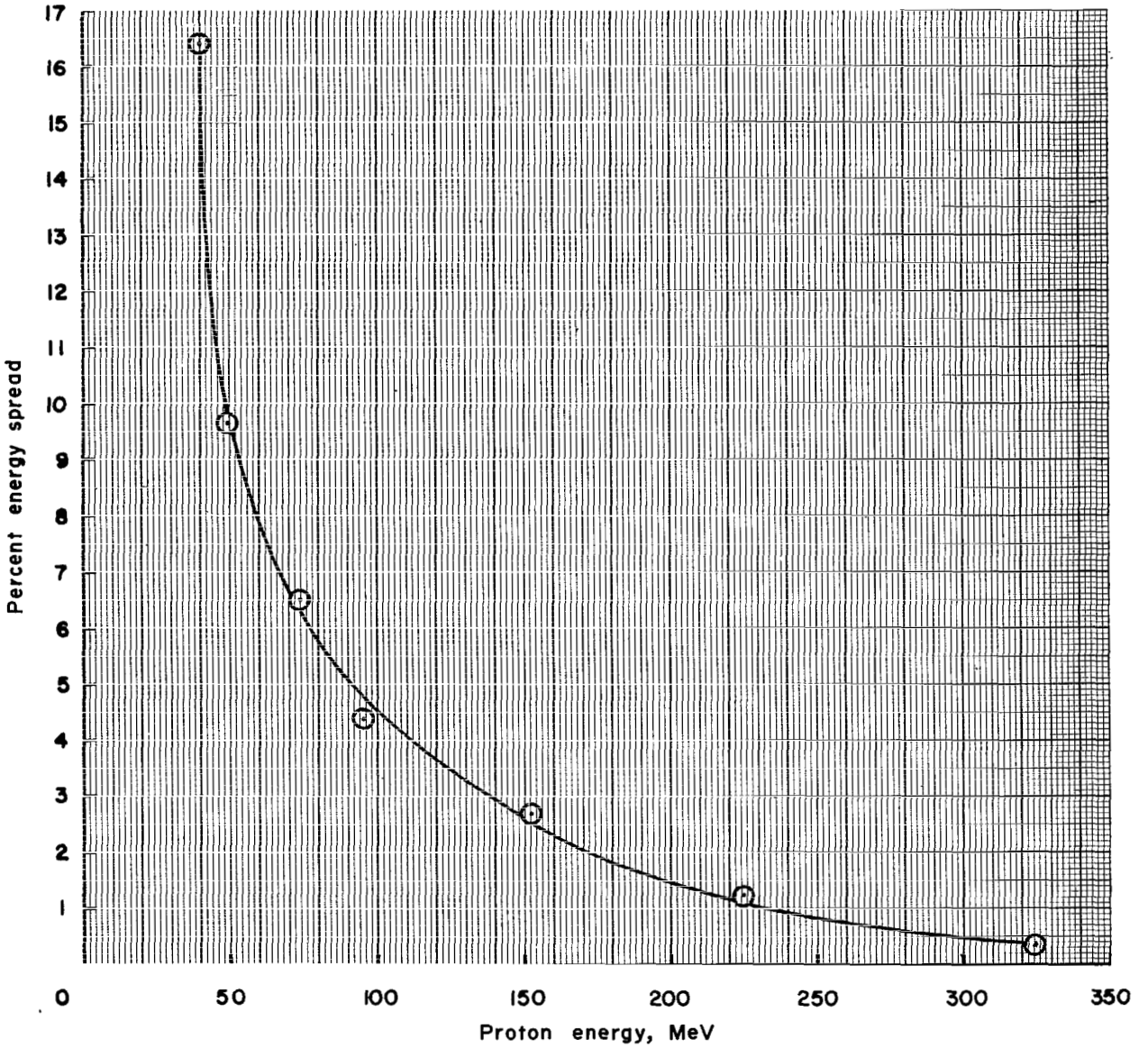

Figure 36.- Percent energy spread as a function of energy for lower energy beams.

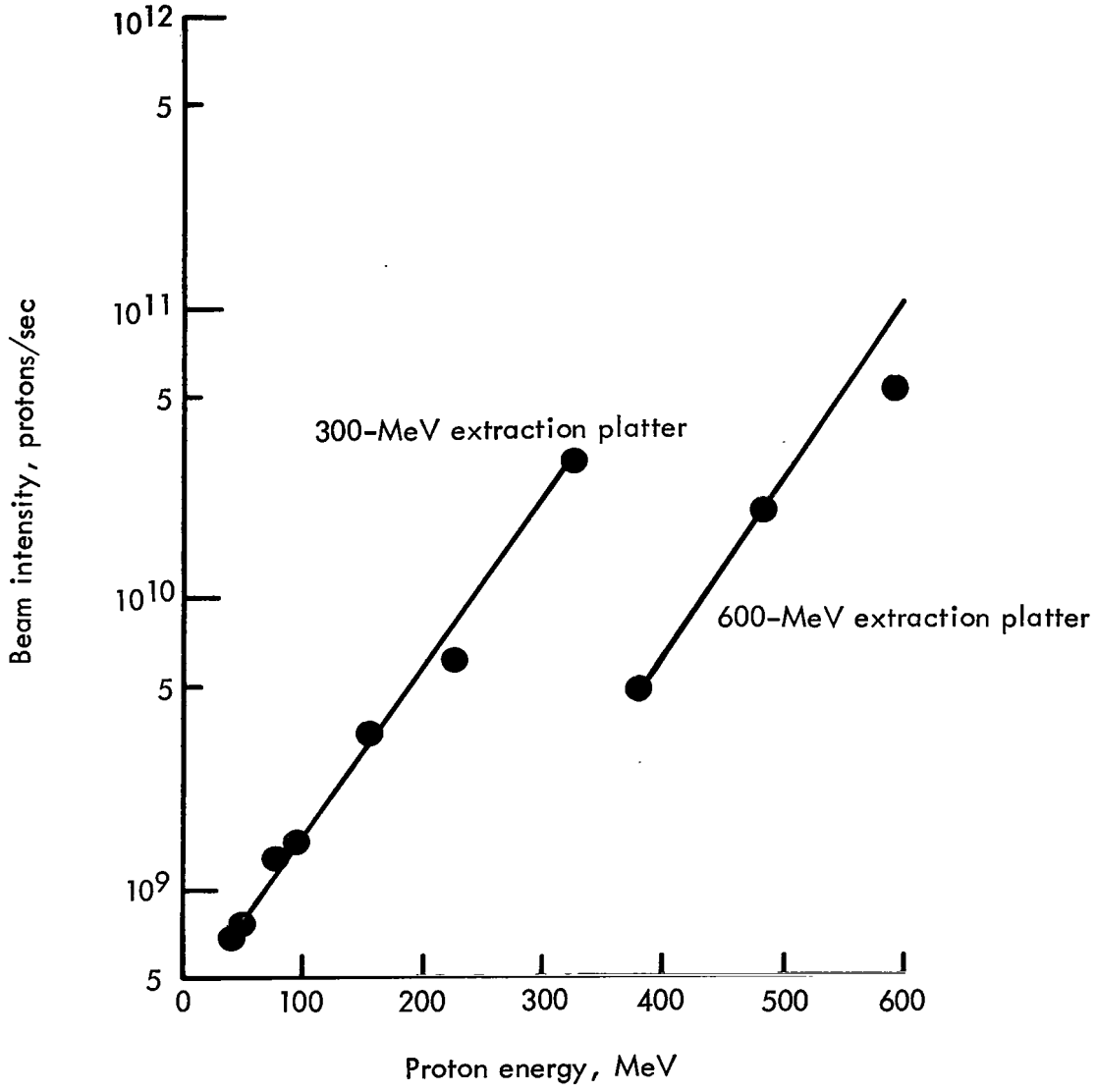

Figure 37.- Proton beam intensity as a function of proton energy.

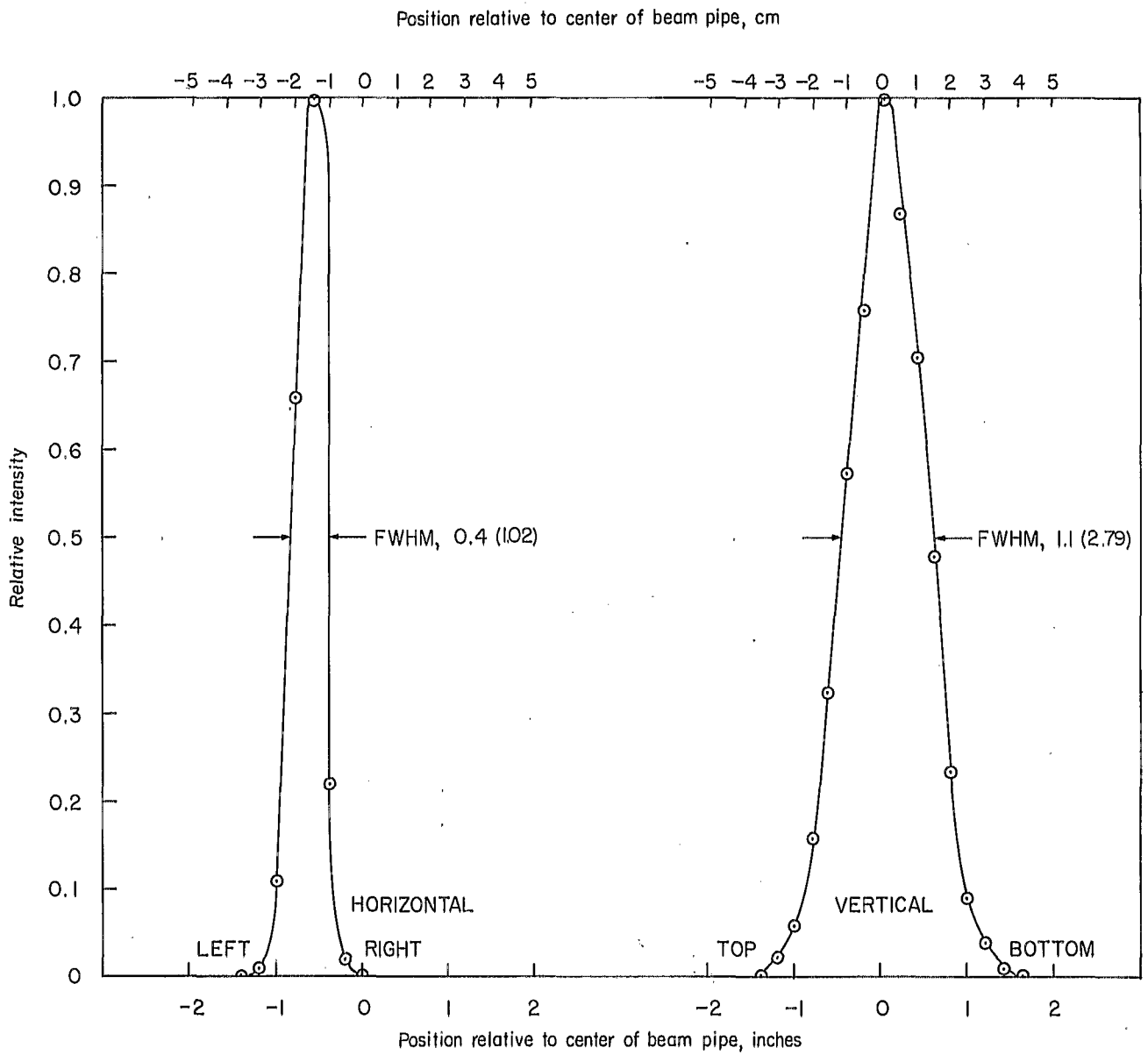

Figure 38.- Horizontal and vertical relative profiles of 595-MeV beam. Full width at half maximum is given in inches (centimeters).

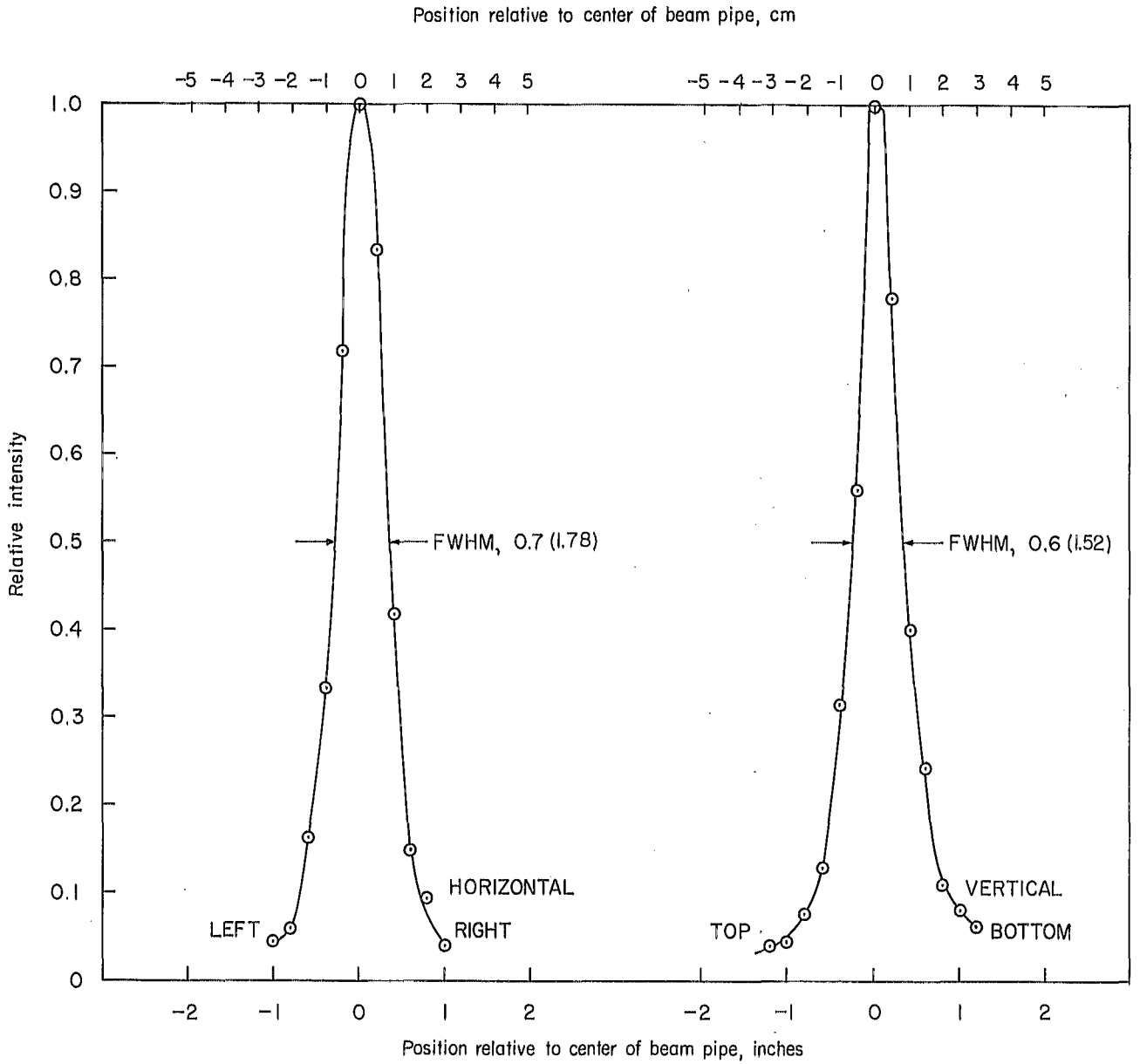

Figure 39.- Horizontal and vertical relative profiles of 480-MeV beam. Full width at half maximum is given in inches (centimeters).

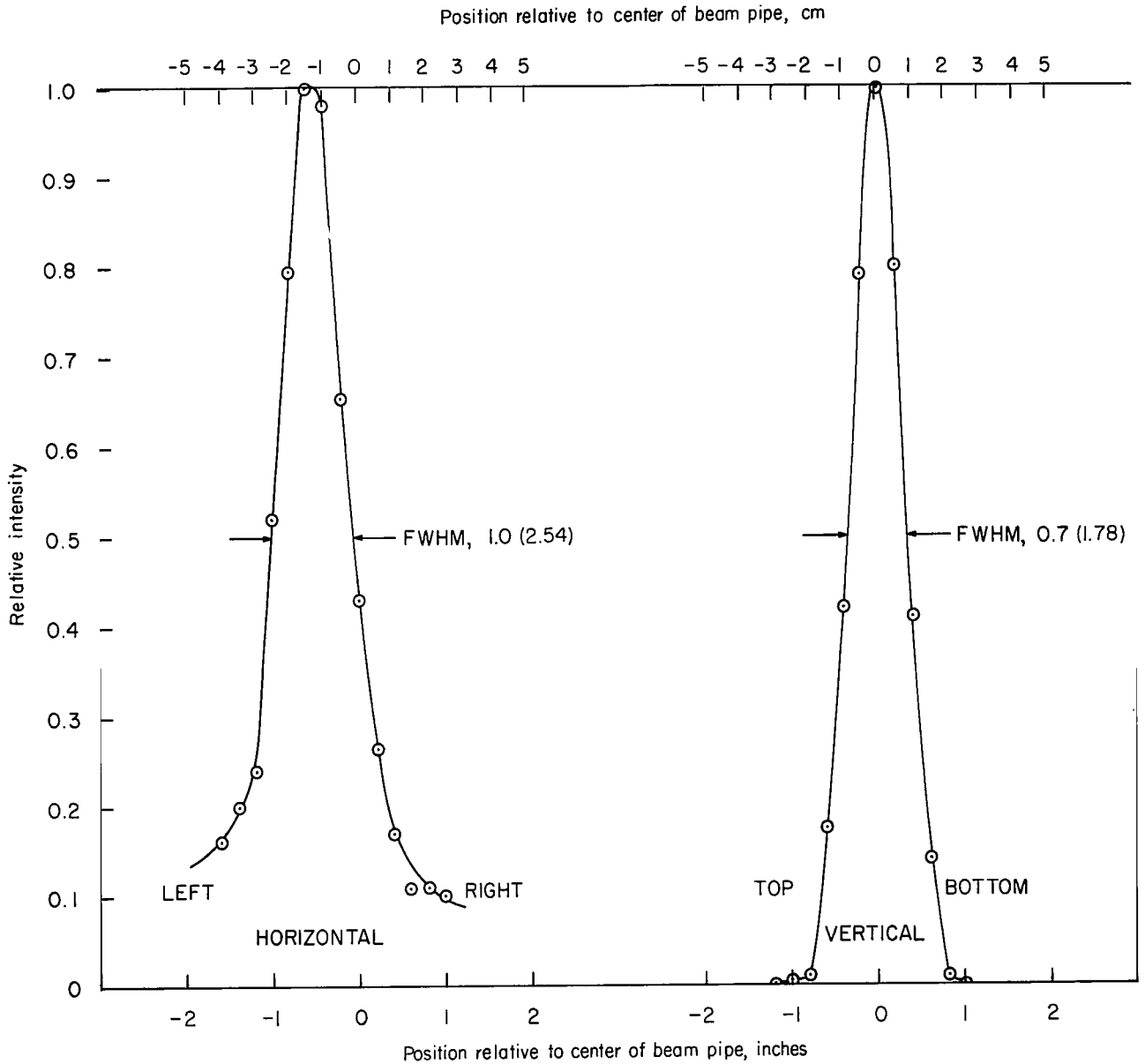

Figure 40.- Horizontal and vertical relative profiles of 380-MeV beam. Full width at half maximum is given in inches (centimeters).

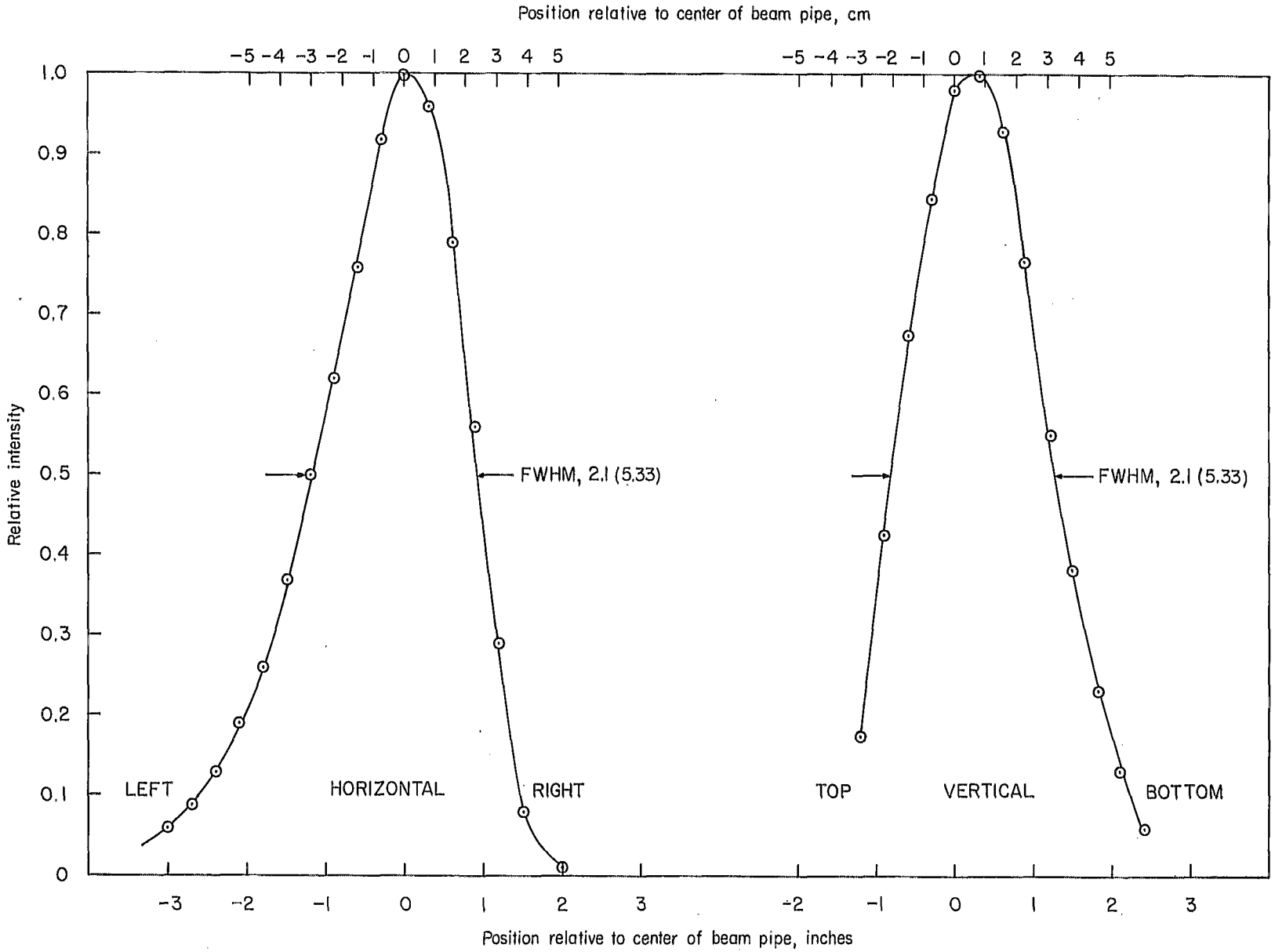

Figure 41.- Horizontal and vertical relative profiles of 325-MeV beam. Full width at half maximum is given in inches (centimeters).

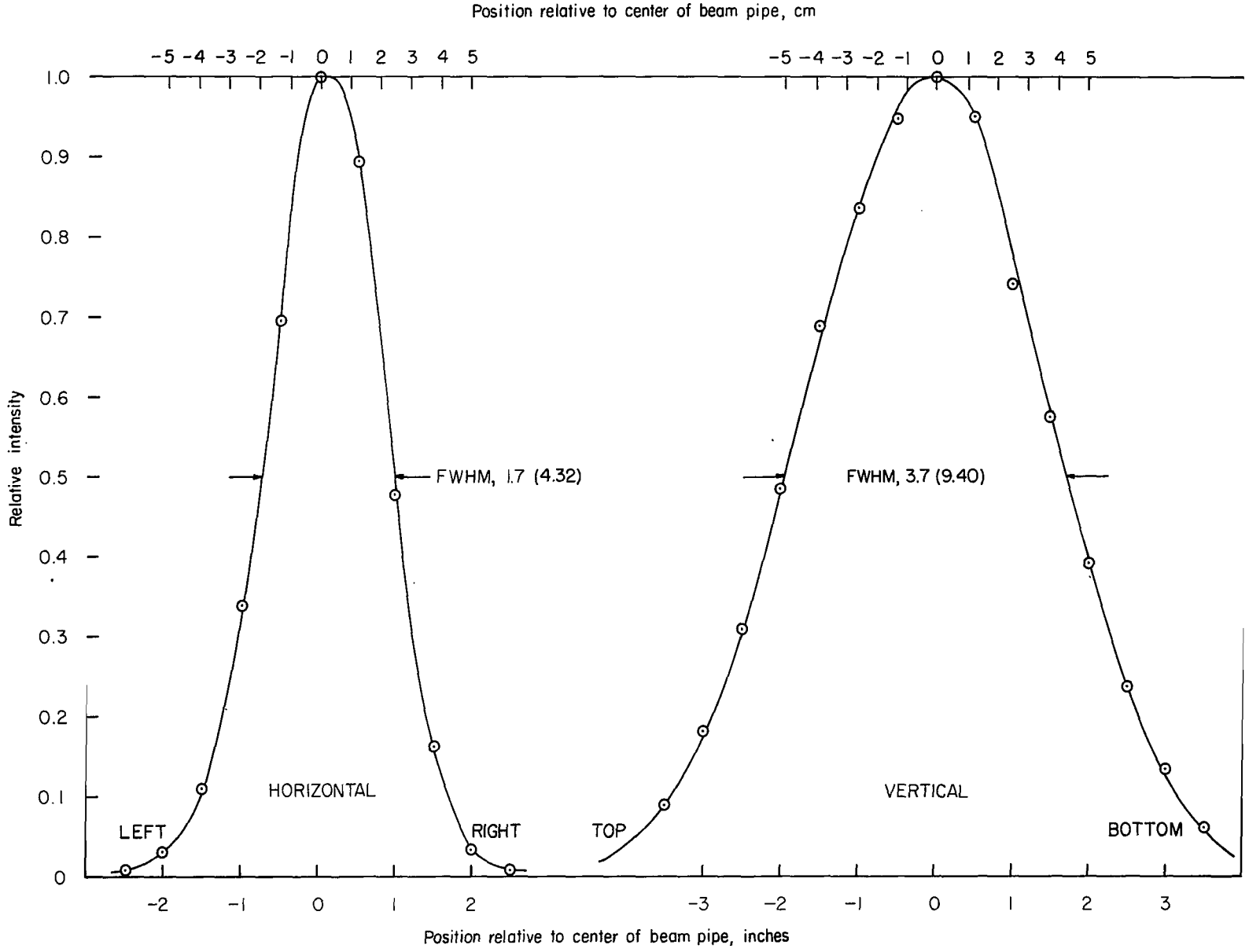

Figure 42.- Horizontal and vertical relative profiles of 225-MeV beam. Full width at half maximum is given in inches (centimeters).

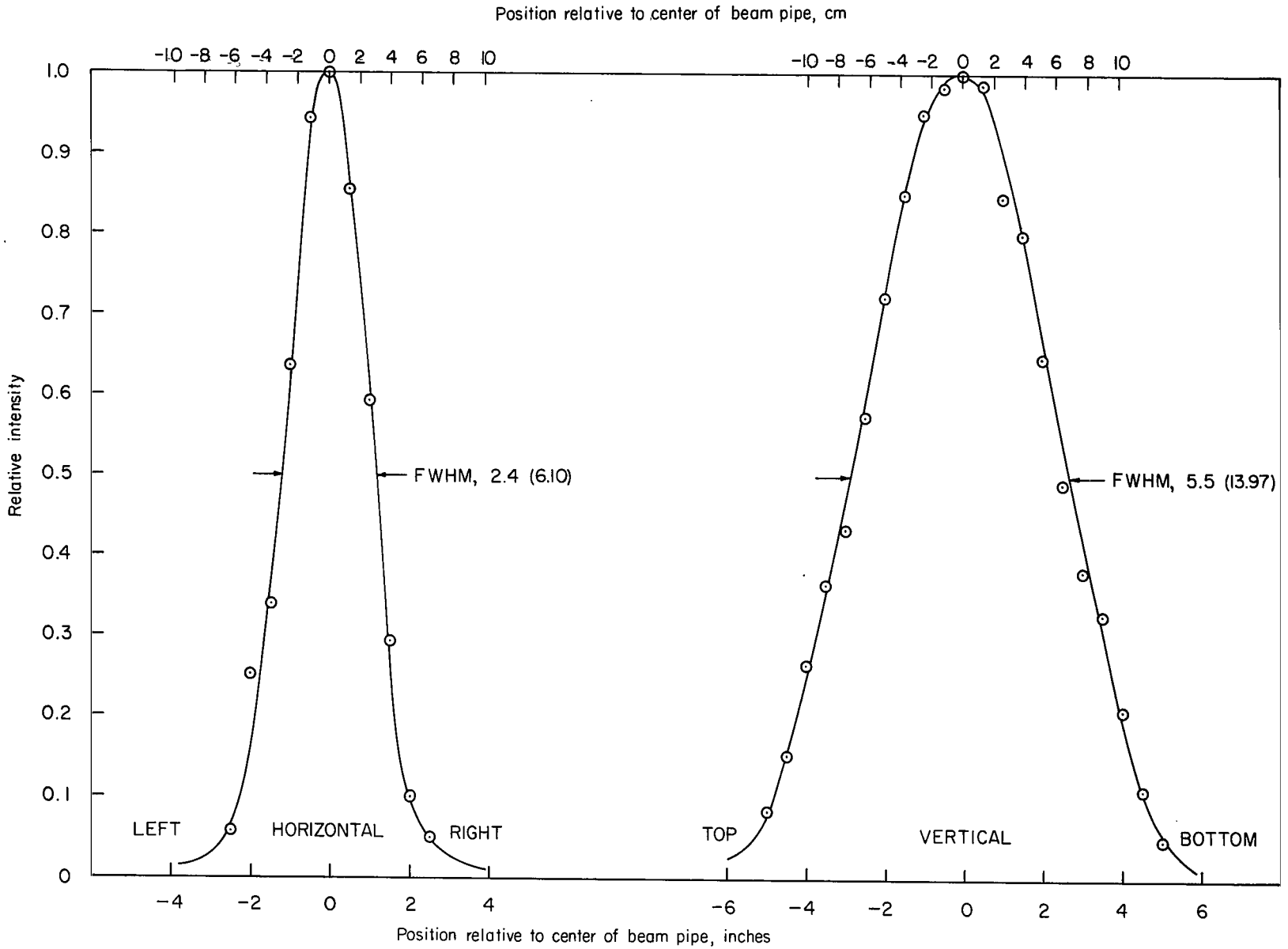

Figure 43.- Horizontal and vertical relative profiles of 155-MeV beam. Full width at half maximum is given in inches (centimeters).

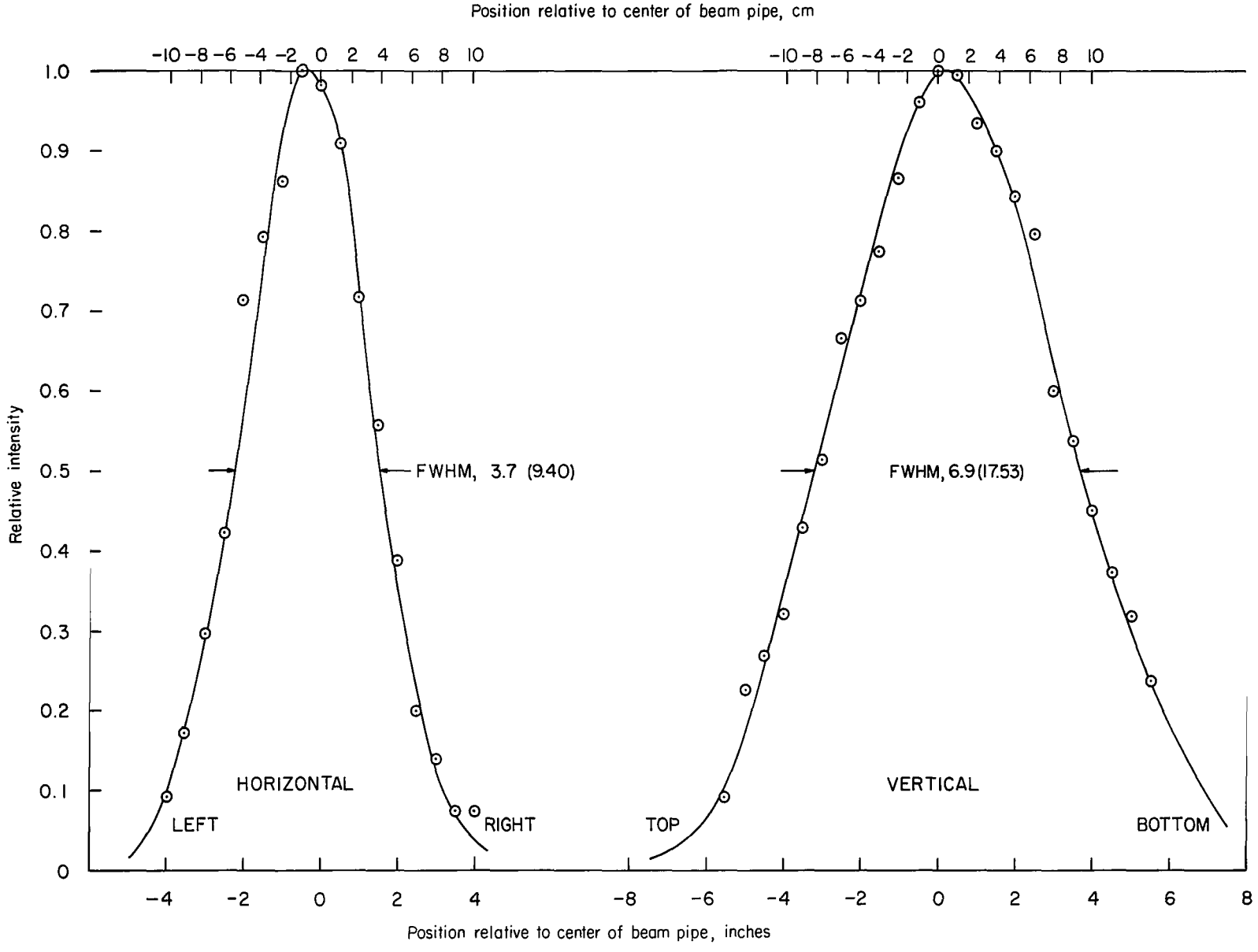

Figure 44.- Horizontal and vertical relative profiles of 95-MeV beam. Full width at half maximum is given in inches (centimeters).

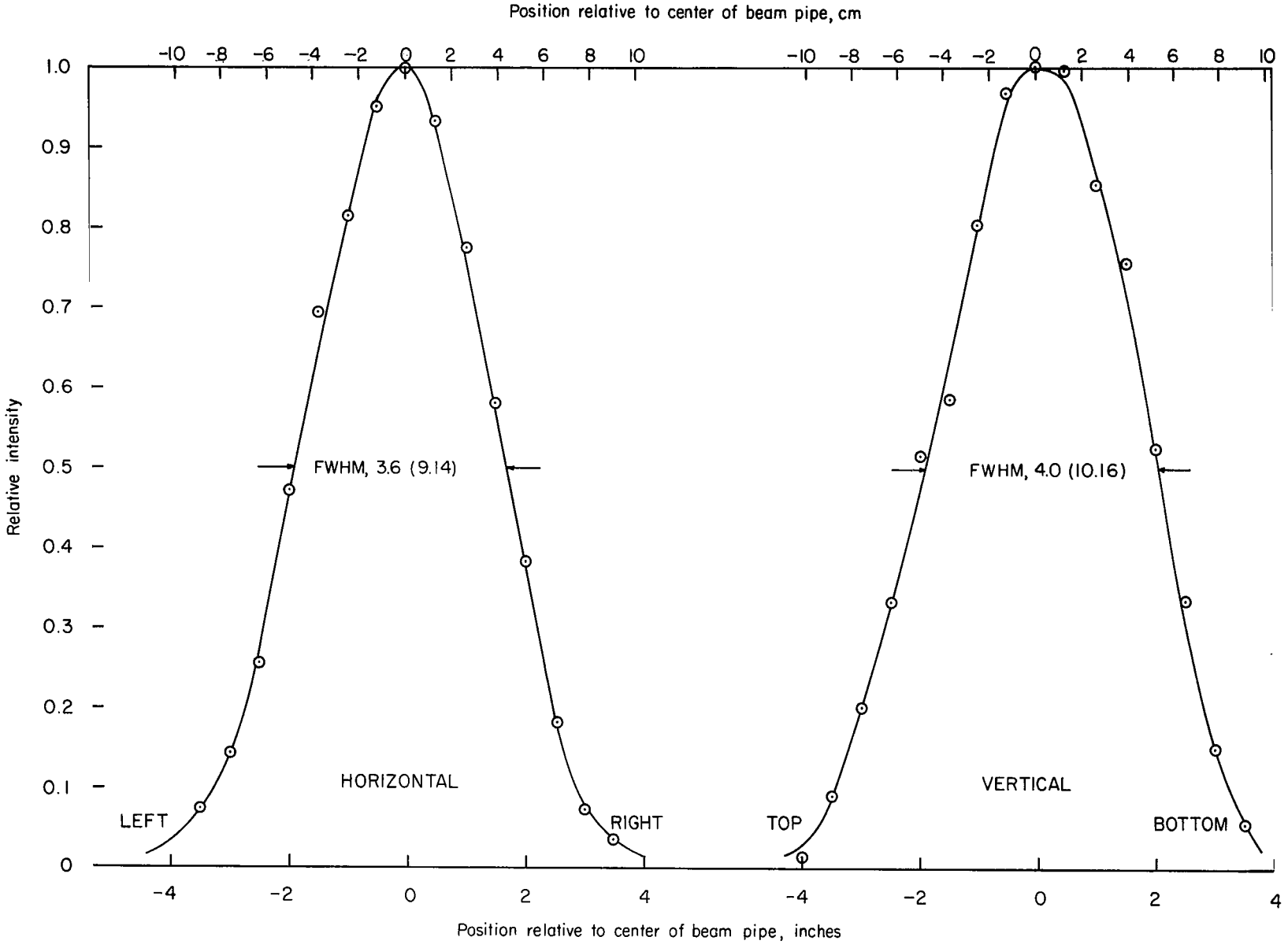

Figure 45.- Horizontal and vertical relative profiles of 75-MeV beam. Full width at half maximum is given in inches (centimeters).

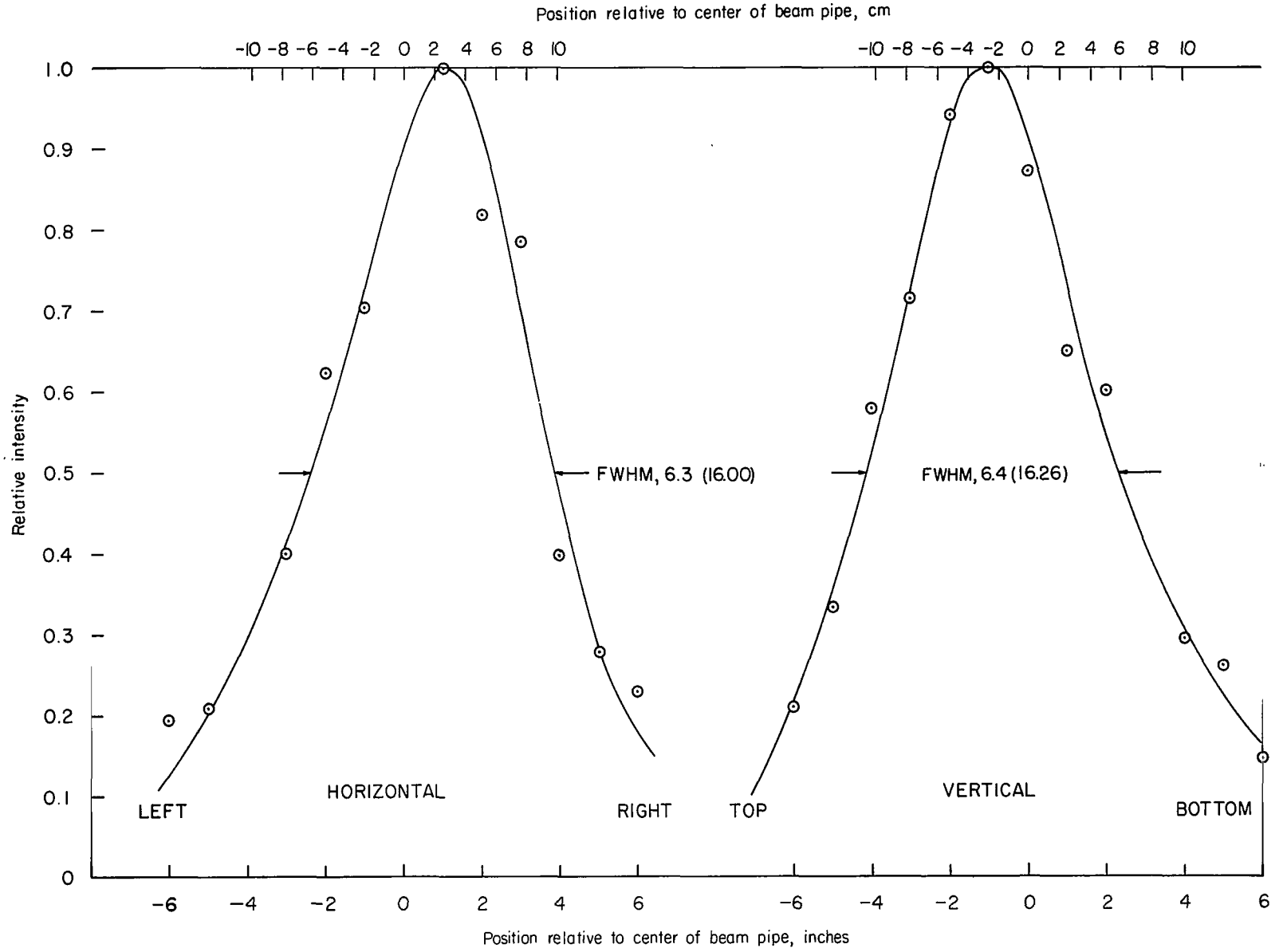

Figure 46.- Horizontal and vertical relative profiles of 50-MeV beam. Full width at half maximum is given in inches (centimeters).

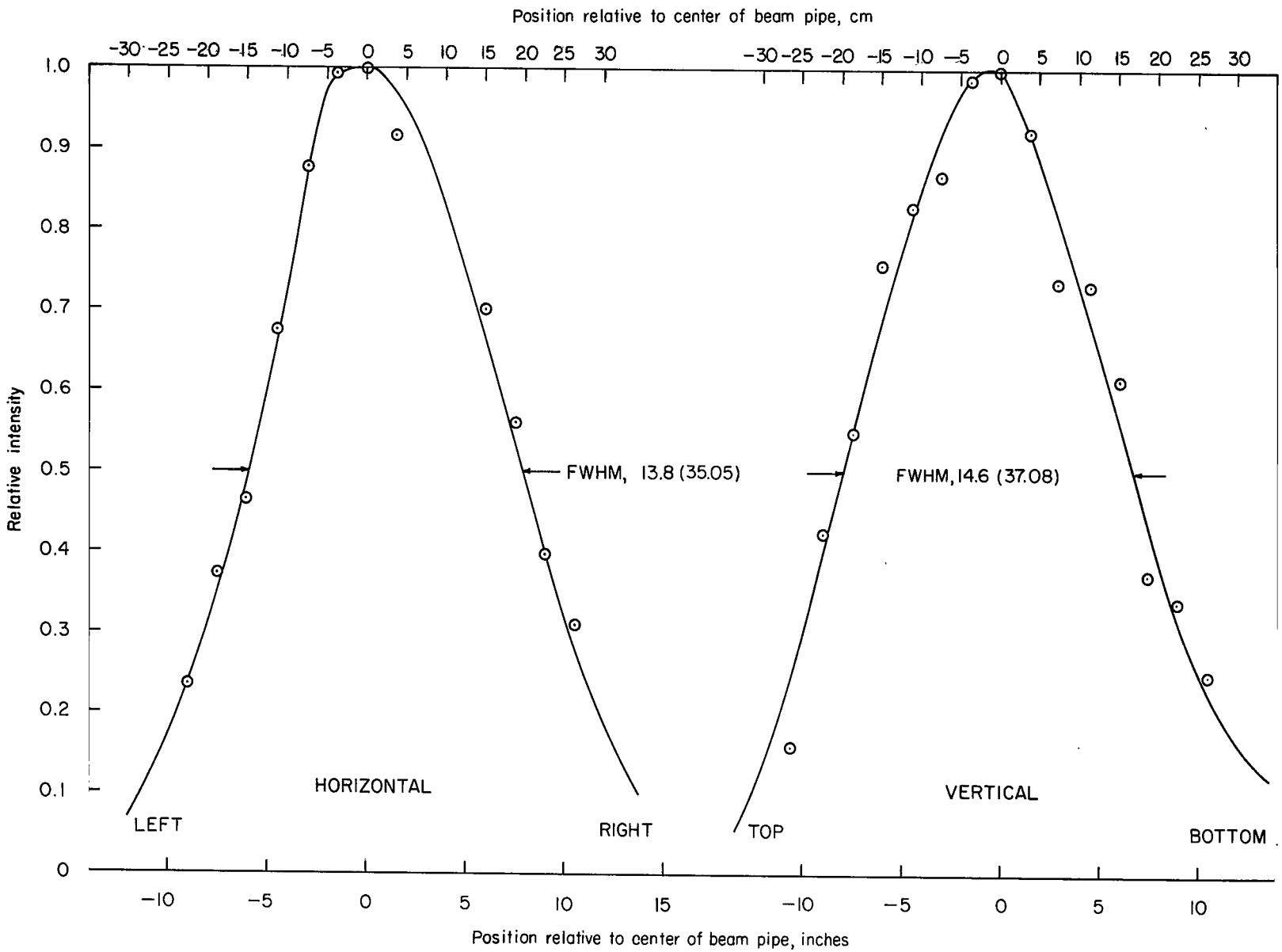

Figure 47.- Horizontal and vertical relative profiles of 40-MeV beam. Full width at half maximum is given in inches (centimeters).

NATIONAL AERONAUTICS AND SPACE ADMINISTRATION
WASHINGTON, D.C. 20546

OFFICIAL BUSINESS

FIRST CLASS MAIL

POSTAGE AND FEES PAID
NATIONAL AERONAUTICS AND
SPACE ADMINISTRATION

"The aeronautical and space activities of the United States shall be conducted so as to contribute . . . to the expansion of human knowledge of phenomena in the atmosphere and space. The Administration shall provide for the widest practicable and appropriate dissemination of information concerning its activities and the results thereof."

—NATIONAL AERONAUTICS AND SPACE ACT OF 1958

NASA SCIENTIFIC AND TECHNICAL PUBLICATIONS

TECHNICAL REPORTS: Scientific and technical information considered important, complete, and a lasting contribution to existing knowledge.

TECHNICAL NOTES: Information less broad in scope but nevertheless of importance as a contribution to existing knowledge.

TECHNICAL MEMORANDUMS: Information receiving limited distribution because of preliminary data, security classification, or other reasons.

CONTRACTOR REPORTS: Scientific and technical information generated under a NASA contract or grant and considered an important contribution to existing knowledge.

TECHNICAL TRANSLATIONS: Information published in a foreign language considered to merit NASA distribution in English.

SPECIAL PUBLICATIONS: Information derived from or of value to NASA activities. Publications include conference proceedings, monographs, data compilations, handbooks, sourcebooks, and special bibliographies.

TECHNOLOGY UTILIZATION PUBLICATIONS: Information on technology used by NASA that may be of particular interest in commercial and other non-aerospace applications. Publications include Tech Briefs, Technology Utilization Reports and Notes, and Technology Surveys.

Details on the availability of these publications may be obtained from:

SCIENTIFIC AND TECHNICAL INFORMATION DIVISION

NATIONAL AERONAUTICS AND SPACE ADMINISTRATION

Washington, D.C. 20546